INSIGHTS INTO THE MOLECULAR LEVEL COMPOSITION, SOURCES, AND FORMATION MECHANISMS OF DISSOLVED ORGANIC MATTER IN AEROSOLS AND PRECIPITATION

by

KATYE ELISABETH ALTIERI

A Dissertation submitted to the

Graduate School-New Brunswick

Rutgers, The State University of New Jersey

in partial fulfillment of the requirements

for the degree of

Doctor of Philosophy

Graduate Program in Oceanography

written under the direction of

Dr. Sybil P. Seitzinger

and approved by

_____

_____

_____

_____

_____

New Brunswick, New Jersey

May, 2009

ABSTRACT OF THE DISSERTATION

INSIGHTS INTO THE MOLECULAR LEVEL COMPOSITION, SOURCES, AND FORMATION MECHANISMS OF DISSOLVED ORGANIC MATTER IN AEROSOLS AND PRECIPITATION

By KATYE ELISABETH ALTIERI

Dissertation Director:
Dr. Sybil P. Seitzinger

Atmospheric aerosols scatter and absorb light influencing the global radiation budget and climate, and are associated with adverse effects on human health. Precipitation is an important removal mechanism for atmospheric dissolved organic matter (DOM), and a potentially important input for receiving ecosystems. However, the sources, formation, and composition of atmospheric DOM in aerosols and precipitation are not well understood. This dissertation investigates the composition and formation mechanisms of secondary organic aerosol (SOA) formed through cloud processing reactions, elucidates the composition and sources of DOM in rainwater, and provides links connecting the two.

Photochemical batch aqueous-phase reactions of organics with both biogenic and anthropogenic sources (i.e., methylglyoxal, pyruvic acid) and OH radical were performed to simulate cloud processing. The composition of products formed through cloud processing experiments and rainwater collected in New Jersey, USA was investigated

using a combination of electrospray ionization mass spectrometry techniques, including ultra-high resolution Fourier transform ion cyclotron resonance mass spectrometry.

This dissertation has resulted in the first evidence that oligomers form through cloud processing reactions, the first detailed chemical mechanism of aqueous phase oligomerization, the first identification of oligomers, organosulfates, and nitrooxy organosulfates in precipitation, and the first molecular level chemical characterization of organic nitrogen in precipitation. The formation of oligomers in SOA helps to explain the presence of large multifunctional compounds and humic like substances (HULIS) that dominate particulate organic mass. Oligomers have low vapor pressures and remain in the particle phase after cloud evaporation, enhancing SOA. The chemical properties of the oligomers suggest that they are less hygroscopic than the monomeric reaction products (i.e., organic acids). Their elemental ratios are consistent with the hypothesis that oligomers are a large contributor to aged organic aerosol mass. The majority of the compounds identified in rainwater samples by advanced mass spectrometry appear to be products of atmospheric reactions, including known contributors to SOA formed from gas phase, aerosol phase, and in-cloud reactions in the atmosphere. The similarities between the complex organic matter in rainwater and SOA suggest that the large uncharacterized component of SOA is the main contributor to the large uncharacterized component of rainwater DOM.

ACKNOWLEDGEMENTS

There are many people I would like to thank for supporting my endeavors in life and science to this point. Most importantly I thank my parents, Joseph and Donna Altieri, for always supporting and encouraging me in everything I pursued. Marybeth, no words could express or truly acknowledge my thanks for your love and support the past five years. While in graduate school I was very fortunate to cross paths with Dr. Annmarie Carlton. I learned a lot about science and graduate school from her, and I am happy to have her as a friend. I have had excellent officemates at IMCS: Rachel Sipler, Steve Litvin, and Joe Jurisa. Coming back to an office completely covered in aluminum foil was one of the high points of my graduate education. Rachel, I especially thank you for your friendship over the past five years. I want to thank Dr. Mark Perri for great scientific conversations and for becoming a good friend. To all of the IMCS graduate students, thank you for your comradeship and support. I want to especially thank all of the members of the Seitzinger and Turpin lab groups, past and present. I thank my committee, Drs. Paul Falkowski, Tim Jickells, and John Reinfelder for their useful insights and comments as I have moved towards completing my dissertation.

When I was a senior in college Sybil Seitzinger took a chance and let me come into her lab once a week for an internship. I had no idea at the time how fortunate I was for that chance, and how much that experience would shape my future. I want to express the most heartfelt thanks to Drs. Sybil Seitzinger and Barbara Turpin for being wonderful mentors and excellent examples of how to be a successful woman in science.

TABLE OF CONTENTS

LIST OF TABLES

LIST OF FIGURES

Chapter 1. Introduction

1.1 Atmospheric Organic Matter

The chemistry of the atmosphere impacts climate, human health, and all ecosystems on Earth. The chemical composition of the atmosphere is controlled by the emissions, transport, chemistry, and deposition of elements within the Earth system. For organic matter, the atmosphere is an efficient transportation system allowing emissions from one environment to be transported and deposited over long distances. However, during transportation, the chemistry of the atmosphere can fundamentally alter the composition of organic matter. Thus, the chemical composition of what is deposited might be very different from what was emitted.

The sources of organic compounds to the atmosphere are numerous and varied including, but not limited to, biomass burning, biological activity, fossil fuel combustion, and industrial and agricultural practices (Graedel et al., 1986;Saxena and Hildemann, 1996). Organic compounds can be emitted to the atmosphere in the gas or particle phase, and a complex set of chemical and physical factors control their cycling and fate. Water soluble organic carbon is a significant and variable component of total organic carbon and its concentration depends on a variety of factors including, for example, location, time of year, and length of time in the atmosphere (Anderson et al., 2008). While in the atmosphere organic matter exists in cloud droplets, rainwater, fog water, and the gas and particle phases. Due to the complexity of the sources and chemical reactions involving organic matter in the atmosphere, fundamental questions about these processes and their contributions to global biogeochemical cycles remain unanswered. This dissertation aims

to improve our understanding of the sources and composition of water soluble organic matter as it cycles through aerosols, cloud droplets, and rainwater.

1.1.1 Organic Aerosol

Aerosols scatter and absorb light affecting the global radiation budget, visibility and climate (IPCC, 2007). They are also associated with adverse health effects including myocardial infarctions and cancer (EPA, 2004;Claxton et al., 2004). Aerosol organic carbon can be a substantial portion (20-90%) of fine particulate matter in the lower troposphere (Kanakidou et al., 2005;Saxena and Hildemann, 1996). The dominant sources of particulate organic carbon include biomass burning, fossil fuel combustion, and atmospheric oxidation of volatile organic compounds (VOCs). Organic particulate matter (PM) can be both primary and secondary; primary aerosol refers to PM emitted to the atmosphere in the particle phase whereas secondary organic aerosol (SOA) refers to organic PM formed in the atmosphere from oxidation of gas phase precursors (i.e., VOCs). SOA can be the main contributor to continental organic particulate matter (20-80%; (Turpin and Huntzicker, 1995;Heald et al., 2006;de Gouw et al., 2005)), even in regions with high primary particulate matter sources (e.g., Atlanta; (Lim and Turpin, 2002)).

The composition of organic particulate matter is poorly understood. It is likely a mixture of thousands of compounds with a variety of sources, and chemical and optical properties (Saxena and Hildemann, 1996). An improved understanding of the composition of SOA formed through gas phase photochemical reactions and subsequent aerosol phase reactions is developing, as this process has been well studied in smog chamber experiments (Seinfeld and Pankow, 2003). Products include mono- and di-

carboxylic acids, oxygenated aromatic hydrocarbons, organic nitrates, phenols, oligomers and humic like substances (HULIS) (Dommen et al., 2006;Kalberer et al., 2004;Reinhardt et al., 2007;Tolocka et al., 2004;Hoffer et al., 2006).

In addition to gas-phase and aerosol-phase reactions, it has been proposed that, like sulfate, SOA can form through cloud processing (Blando and Turpin, 2000;Gelencser and Varga, 2005). SOA formation through cloud processing has been proposed to occur when gas phase organic emissions are oxidized by the hydroxyl radical in the interstitial spaces of clouds. The water soluble oxidation products (e.g., aldehydes) can then partition into cloud droplets and be oxidized further to form less volatile organics (e.g., oxalic acid). When the cloud droplets evaporate the low volatility organics remain, in part, in the particle phase, yielding SOA.

There are multiple lines of evidence that support the hypothesis that SOA can form through cloud processing. Oxalic acid is the most abundant particulate dicarboxylic acid in the atmosphere (Rogge et al., 1993;Kawamura et al., 1996), and it is now believed that the high concentrations of organic acids, including oxalic acid, found in aerosols and atmospheric waters are due to cloud processing (Chebbi and Carlier, 1996; Yu et al., 2005;Sorooshian et al., 2007;Crahan et al., 2004). This is supported by the temporal and concentration dynamics of organic acids measured in the atmosphere including, for example, correlations in *in situ* oxalate and sulfate measurements (Yu et al., 2005;Sorooshian et al., 2007). A variety of laboratory experiments have verified that aqueous reactions of precursor organics and the hydroxyl radical can form low volatility organics, including oxalic acid, that would contribute to SOA upon cloud droplet evaporation (Carlton et al., 2007;Carlton et al., 2006). The cloud chemistry experiments

conducted by Carlton et al. (2006, 2007) were designed to investigate the hypothesis that oxalic acid forms through cloud processing of biogenic precursors. Samples from the Carlton et al. (2006, 2007) cloud chemistry experiments were provided for analysis by electrospray ionization mass spectrometry in this work. This led to the identification of additional products including oligomers, which will also contribute to SOA upon cloud droplet evaporation due to their high molecular weight and thus low volatility (described in Chapters 2, 3). This previously unrecognized atmospheric oligomer formation pathway via aqueous OH oxidation could be an important source of HULIS in aerosols and clouds.

Most global and regional atmospheric models under-predict particulate organic carbon concentrations, especially in the free troposphere (Heald et al., 2006;Kanakidou et al., 2004). This poor performance is believed to result from missing SOA formation processes. Recently, in-cloud SOA production has been modeled using a chemical box model (Lim et al., 2005), a cloud parcel model (Ervens et al., 2004;Ervens et al., 2008), a regional air quality model (Carlton et al., 2008;Chen et al., 2007), and a global chemical transport model (Fu et al., 2008). The improved mechanistic understanding of SOA formation through cloud processing, including oligomer formation, developed during this dissertation will ultimately improve this currently very simple modeling. Results from this dissertation are currently being used to develop a detailed cloud chemistry model. The inclusion of cloud-produced SOA improved agreement between modeled and measured organic carbon in the free troposphere (Carlton et al., 2008;Chen et al., 2007).

1.1.2 Rainwater Organic Matter

Rainwater is an important removal mechanism for all atmospheric constituents. Aerosols can be removed from the atmosphere by acting as cloud condensation nuclei that grow into cloud droplets which precipitate out as rain, or through scavenging by falling raindrops. Understanding the composition of rainwater can thus provide insights into the composition of cloud droplets, aerosols, and cloud condensation nuclei. Rainwater can also be an important source of contaminants and/or nutrients to receiving ecosystems (Lamb and Bowersox, 2000). Rainwater has been sampled and studied in the USA since the late 1970's to monitor the deposition of acidic species (SO_x, NO_x, H^+), mercury, and other inorganic ions (Lamb and Bowersox, 2000). Despite the large and successful effort to monitor the impacts of anthropogenic activities on precipitation and the impacts of precipitation on ecosystems, measurements of organic matter are usually not included at these monitoring sites. Dissolved organic matter (DOM) in rainwater is a complex mixture of compounds that can have a variety of anthropogenic and natural sources (Seitzinger et al., 2003), and many of these compounds have the potential to influence climate, air quality, and health, though not necessarily with the same sign. Due to the lack of sampling and monitoring, the role rainwater plays in removing atmospheric organic matter and the potential impacts of deposited DOM on ecosystems remains largely unknown. This dissertation provides the first evidence that the complexity in the composition of SOA can provide insights into the complexity of rainwater DOM.

Rainwater plays an important role in regional and global carbon cycles. It has been estimated that the flux of DOC to the surface ocean through wet deposition is equal in magnitude to the riverine input of DOC to the ocean, though there are large uncertainties in these flux calculations (Willey et al., 2000). The concentration of DOC in

rainwater is usually greater than the concentration of the frequently monitored acids (e.g., nitric and sulfuric acids) combined (Avery et al., 2003;Kieber et al., 2002;Willey et al., 2000). Organic acids are also known to contribute to rainwater acidity and can be 15-35% of the total DOC (Kieber et al., 2002;Avery et al., 2005;Avery et al., 2006;Avery et al., 2001;Avery et al., 1991).

In rainwater collected in the continental USA, there is evidence that significant fractions of the DOC can have marine sources if a storm originates over the ocean (Raymond, 2005). This indicates that there is potentially a significant transfer of marine DOC to the continents, and that a significant fraction of marine rain may contain recycled marine DOC. There are not enough measurements to determine whether the net transfer of DOC in rainwater is from marine DOC to the continents or from continental DOC to the ocean. There is a significant fraction of DOC with fossil fuel sources in continental rainwater that could potentially be deposited on both terrestrial and marine systems (Raymond, 2005). Continental rainwater samples chemically characterized in this dissertation provide insights into the sources of DOC that are needed to assess the transfers of marine, terrestrial, and fossil fuel carbon through wet deposition (described in Chapters 4, 5).

1.1.3 HULIS

The chemical composition of DOM in all natural systems, including the atmosphere, is largely uncharacterized due to analytical constraints, with either bulk elemental ratios reported or small detailed fractions quantified (e.g., organic acids, dissolved free amino acids, neutral sugars) (Gors et al., 2007;Kawahata and Ishizuka, 2000;Pettine et al., 1999). However, there are similarities in the chemical composition of

DOM across environments. For example, fulvic and humic acids are a large component of the DOM in natural systems, aquatic and terrestrial. Humic substances are ubiquitous macromolecules. They are generally considered to be naturally occurring substances, biogenically derived, and of high molecular weight. Their true definition is an operational one, the fulvic acid fraction is water soluble at any pH (most relevant in this dissertation), and humic acids are the base soluble fraction. Similarly, there is a class of organic molecules extracted from atmospheric waters (aerosols, fogs, clouds) that are macromolecular and have been termed humic-like substances (HULIS) because they have properties similar to terrestrial and aquatic humic and fulvic acids (Graber and Rudich, 2006). The common characteristic of humic and fulvic substances in terrestrial and aquatic systems, and HULIS in atmospheric samples, is that they remain without a molecular definition or chemical speciation despite the application of numerous analytical techniques.

There are a large number of studies reporting macromolecular or high molecular weight species in atmospheric aerosols. Some studies compare the macromolecular species to humic and fulvic acids and use the HULIS classification (Zappoli et al., 1999;Gelencser et al., 2000a;Gelencser et al., 2000b;Decesari et al., 2000;Kiss et al., 2002), while others compare the macromolecular species to small polymers, and use the oligomer classification (Kalberer et al., 2004;Gao et al., 2004a;Gao et al., 2004b;Tolocka et al., 2004;Surratt et al., 2007;Altieri et al., 2006;Altieri et al., 2008). In this dissertation the contribution of oligomers formed through cloud processing to the HULIS measured in atmospheric aerosols is discussed for the first time (Chapters 2, 3). The presence of HULIS can influence many aerosol properties, including hygroscopicity, cloud

condensation nuclei activity, surface tension and optical properties (Hoffer et al., 2006;Kiss et al., 2005;Dinar et al., 2008;Dinar et al., 2006).

The actual distinctions between these loosely defined groups of material including oligomers, HULIS, and macromolecular material have rarely been discussed. The HULIS fraction is frequently described in relation to ambient samples, and is considered to be a complex mixture of polyacidic compounds with both aliphatic and aromatic structures, multiple functional groups, and high molecular weights (150-500 Da; Graber and Rudich, 2007). Oligomers are usually described as products of laboratory experiments, and are defined by both high molecular weights (100-1000 Da) and regular mass patterns. The HULIS group is more comprehensive than the oligomer classification, and it is likely that all oligomers fall into the HULIS fraction, with multifunctional compounds such as organosulfates, nitrooxy organosulfates, and organonitrates also contributing to HULIS.

The majority of progress in characterizing oligomers, HULIS, and complex organic matter has come from the application of advanced analytical techniques, including high resolution mass spectrometry. The coupling of electrospray ionization (ESI) inlet systems to mass spectrometers of various resolutions has greatly improved our ability to chemically characterize polar dissolved organic compounds at the molecular level in aqueous environmental samples (Altieri et al., 2006;Feng and Moller, 2004;Hoffer et al., 2006;Kim, 2006;Kujawinski, 2002;Kujawinski et al., 2002;Poulain, 2006;Seitzinger et al., 2003). In this dissertation, ESI coupled with a quadrupole mass selective detector (ESI-MS), a Fourier transform ion cyclotron resonance mass spectrometer (FT-ICR MS), and an ion trap mass spectrometer (ESI-MS-MS) were used

to analyze samples from cloud chemistry experiments designed to simulate cloud processing, and ambient wet deposition samples.

ESI is a "soft" ionization technique that does not fragment compounds. Therefore, intact compounds are transferred to the mass spectrometer providing molecular weight information for each ionizable compound (in the form of a mass-to-charge ratio, *m/z*). Compounds with primarily acidic functional groups (e.g., organic acids) are transferred to the detector as negative ions and those with primarily basic functional groups (e.g., alcohols, aldehydes) as positive ions. The ESI inlet system can be combined with different mass spectrometers to obtain different degrees of mass resolution and compound characterization. The most significant advances have been made with ultra-high resolution ESI Fourier transform ion cyclotron resonance mass spectrometry (FT-ICR MS). The FT-ICR MS has ultra-high resolution ($m/\Delta m_{50\%}$ >100,000, in which $\Delta m_{50\%}$ is mass spectral peak full width at half-maximum peak height) allowing separation of individual compounds, and mass accuracy < 1ppm allowing exact molecular formula assignments for each compound (Marshall et al., 1998). This ultra-high resolution allows for the separation and identification of thousands of organic compounds in a sample making it an ideal technique for characterizing complex dissolved organic matter in natural samples.

1.2 Atmospheric Organic Nitrogen

The global nitrogen cycle has been greatly perturbed by anthropogenic activities since the industrial revolution. The amount of reactive nitrogen has increased due to biological nitrogen fixation associated with agricultural activities, combustion of fossil fuels, and the use of the Haber-Bosch process for fertilizer production (Galloway et al.,

2003). The atmospheric emission, transportation, and deposition of reactive nitrogen are significant components of this perturbed global nitrogen cycle. The emission and subsequent deposition of the anthropogenic component of reactive nitrogen to the atmosphere has increased by a factor of 10 since preindustrial times (Galloway et al., 2004). The cycling of this anthropogenic reactive nitrogen in the atmosphere is usually measured in terms of inorganic nitrogen species (reduced NH_3, NH_4^+, oxidized NO_x, HNO_3, N_2O, NO_3^-). The impacts of this increased anthropogenic reactive nitrogen deposition are well documented and include, for example, acidification and loss of biodiversity in lakes and streams (Vitousek et al., 1997), and eutrophication and hypoxia in coastal systems (Howarth et al., 2000). The potential impact of the increased anthropogenic reactive nitrogen deposition to the oceans has also recently been discussed (Duce et al., 2008).

It is now recognized that organic nitrogen is an important contributor to the atmospheric cycling of reactive nitrogen, especially atmospheric nitrogen deposition (Cornell et al., 2003). The cycling of this organic component of reactive nitrogen is considered less frequently because the source and speciation of the organic nitrogen is not well understood (Cornell et al., 2001;Cornell et al., 1995;Cornell et al., 2003;Cornell et al., 1998;Mace et al., 2003a;Mace et al., 2003b;Jickells, 2006). The impacts of reactive organic nitrogen in the atmosphere are thus difficult to identify and quantify. Because of the role atmospheric dissolved organic nitrogen (DON) plays in the global nitrogen cycle and its role as a potential nutrient to receiving ecosystems, it is especially important to understand its sources and composition. This dissertation provides the first

molecular level chemical characterization of DON in continental precipitation and links compounds to distinct anthropogenic and biogenic sources.

Atmospheric water soluble organic nitrogen (WSON) is a subset of the complex dissolved organic carbon measured in atmospheric aerosols and rainwater and, as such, it impacts cloud condensation processes and aerosol chemical and optical properties. There are some known contributors to atmospheric WSON. For example, organic nitrates exist in polluted and remote regions of the atmosphere and form during gas phase photochemical reactions involving NO_x and VOCs (Kroll et al., 2006;Jang and Kamens, 2001). SOA formation through gas phase and subsequent aerosol phase reactions has been studied extensively and identified products include organic nitro- and nitrate compounds (Hung et al., 2005;Alfarra et al., 2006;Dommen et al., 2006;Kroll et al., 2006). However, their estimated total contribution to nitrogen deposition, including peroxyacetyl nitrates (PAN), is ~ 9 Tg N/yr (Neff et al., 2002). Reduced forms of nitrogen exist in the atmosphere including urea and amino acids, and their sources are most likely primary emissions from biomass burning and agricultural areas (Chan et al., 2005;Matsumoto and Uematsu, 2005;Mopper and Zimmermann, 1987). Their contribution to nitrogen deposition is estimated at < 1 Tg N/yr (Neff et al., 2002). When all of the known and measured species are summed > 50% of the WSON in atmospheric waters remains uncharacterized. The rainwater DON compounds characterized for the first time in this dissertation are complex, multifunctional and highly oxygenated, and they likely contribute to the HULIS fraction measured in atmospheric waters (described in Chapter 5). The large number of compounds and their complexity are likely the

reasons traditional analytical techniques have failed to completely characterize atmospheric WSON.

1.3 Objectives of Dissertation

This dissertation seeks to address the following questions:

1) Does aqueous in-cloud processing of biogenic VOCs (i.e., isoprene) lead to complex organic matter that will contribute to SOA?
2) What are the aqueous chemical mechanisms that lead to complex organic matter formation in the atmosphere?
3) Does aqueous in-cloud chemistry impact the composition of organic matter removed from the atmosphere via wet deposition?
4) What are the sources and composition of dissolved organic nitrogen in continental precipitation?

1.3.1 Dissertation Overview

This dissertation documents an investigation of the composition and formation mechanisms of SOA formed through cloud processing reactions of isoprene oxidation products, elucidates the composition and sources of DOM in New Jersey rainwater, and provides links connecting the two. Chapter 2 describes the composition of products formed through photochemical batch aqueous-phase reactions of pyruvic acid and OH radical that were performed to simulate cloud processing. Pyruvic acid is an important aqueous phase intermediate of many reactive organics including isoprene and methylglyoxal. Initially there was disagreement as to whether aqueous OH oxidation of pyruvic acid yielded acetaldehyde (Ervens et al., 2004) or organic acids (Lim et al., 2005). The measurement of organic acids in aqueous photooxidation experiments

conducted with pyruvic acid in the presence of OH resolved this discrepancy (Carlton et al., 2007;Carlton et al., 2006). In addition, analyses of these experimental samples by electrospray ionization mass spectrometry (ESI-MS) led to the identification of complex organic matter in the time series experimental samples as described in Chapter 2. This complex organic matter was identified as an oligomer system. Chapter 2 provides the first evidence that oligomers (i.e., small polymers) can form through in-cloud reactions. When cloud droplets evaporate, these oligomers are expected to be retained in the particle phase, thus producing new SOA.

Chapter 3 describes the results of photochemical batch aqueous-phase reactions of methylglyoxal and OH radical. Methylglyoxal is a product of gas phase biogenic (e.g., isoprene) and anthropogenic hydrocarbon oxidation and can produce pyruvic acid through aqueous phase reactions. It was found that the oligomer system formed through methylglyoxal photooxidation was almost identical to that formed from pyruvic acid photooxidation. In chapter 3 ultra-high resolution Fourier transform ion cyclotron resonance mass spectrometry (FT-ICR MS) was used to investigate the oligomer system formed through in-cloud processing of pyruvic acid and methylglyoxal. The chemical properties of the oligomers were investigated at the compound level, and the elemental formula information was used to hypothesize an aqueous phase chemical mechanism for oligomer formation.

Chapters 4 and 5 describe the composition of DOM in rainwater collected in New Jersey, USA. Chapter 4 focuses on the compounds detected in the rainwater by negative ion FT-ICR MS, including known SOA contributors such as organic acids, oligomers, organosulfates, and nitrooxy organosulfates identified in rainwater for the first time.

Chapter 5 describes the chemical characterization of nitrogen containing organic compounds in rainwater using both positive and negative ion FT-ICR MS. This is the first use of advanced mass spectrometry to elucidate the number of nitrogen containing organic compounds in rainwater and describe the nitrogen functionality of organic nitrogen compounds in rainwater.

1.4 Implications

The generally poor understanding of the formation of secondary organic particulate matter continues to be a major source of uncertainty in predictions of aerosol concentrations and properties that affect health, visibility and climate (Kanakidou et al., 2004). This dissertation has led to a better understanding of in-cloud SOA formation in multiple ways. The formation of oligomers in cloud processing reactions was identified for the first time. The chemical properties suggest that the oligomers are less hygroscopic than the simple organic acid products, and that the quickly forming oligomers may contribute to SOA upon cloud droplet evaporation. Further work investigating the oligomer system led to the first aqueous phase chemical mechanism that describes the complexity in the composition of cloud processed SOA. The oligomerization mechanism hypothesized in this work is similar to mechanisms reported in aerosol phase reactions (Gao et al., 2004a;Gao et al., 2004b). This similarity in the formation mechanisms of oligomers may help to explain the large quantity of oligomers, or macromolecular material, found in atmospheric particles. In addition, the oligomers likely contribute to the HULIS fraction found in atmospheric particles.

As discussed in a recent review article (Hallquist, 2009), due in part to a lack of knowledge about the sources, composition, properties and formation mechanisms of

SOA, there are still significant uncertainties as to the true impact of atmospheric aerosols on both climate and human and ecosystem health. It is especially important to understand the sources of high molecular weight products including oligomers and HULIS in atmospheric aerosols because the increase in carbon number of the products causes a decrease in the vapor pressure, potentially leading to increased SOA. The results of this dissertation have improved our understanding of in-cloud SOA formation and have assisted in moving the field towards addressing these uncertainties. This is demonstrated in part by the 20 citations of Chapter 2 since it was published in 2006 and the 11 citations of Chapter 3 since it was published in 2008.

The improved understanding of in-cloud SOA formation described in this dissertation will allow for a more accurate prediction of organic particulate matter formation from biogenic and anthropogenic emissions. Current air quality models are only now beginning to include multiphase SOA formation pathways. Without this they severely under-predict ambient organic particulate matter concentrations, especially in the free troposphere (Heald et al., 2006). There is growing evidence that the gap between measured and modeled organic particulate matter arises, at least in part, from multi-phase atmospheric processes including in-cloud SOA formation (Carlton et al., 2008).

In addition to impacting air quality, aerosols and precipitation impact climate in multiple and sometimes opposite ways. The role of aerosols, particularly sulfate aerosols, in “masking” the regional warming from greenhouse gases by reflecting sunlight back to space has been recognized since the 1970’s (IPCC, 2007). Aerosols can impact radiative forcing through both the direct and indirect effects. The direct effect is when aerosols scatter and/or absorb radiation altering Earth's radiative balance. The

direct radiative forcing of an aerosol is controlled, in part, by aerosol optical properties, which can be influenced by the aerosol composition. The indirect aerosol effect is the process by which aerosols modify the microphysical properties of clouds influencing the amount, lifetime, and fate of clouds in the atmosphere. The ability of an aerosol to act as cloud condensation nuclei is largely controlled by the chemical composition of the aerosol. Because of the large complexity in the number of organic compounds in the atmosphere, modeling the direct and indirect effects is extremely challenging (McFiggans et al., 2006). Currently, global models highly parameterize atmospheric organic carbon, which is typically represented in a simplistic manner by one or two tracers (e.g., water soluble and water insoluble fractions; (IPCC, 2007)). This dissertation has improved our understanding of how the composition, including the hygroscopicity and chemical properties, of atmospheric organic matter changes as it is aged and processed through clouds. Ideally this information, along with continued work, could one day be used to improve the treatment of organic aerosols in global climate models that are attempting to discern the direct and indirect aerosol effects on the global radiation balance.

The best estimates of the global rainwater dissolved organic carbon flux suggest it is 430 Tg C yr^{-1}, which is much greater than the rainwater flux of dissolved inorganic carbon (i.e., 80 Tg C yr^{-1}). Despite this large contribution of rainwater DOC to the global carbon cycle, the sources, temporal and spatial patterns, potential variations in these patterns, and resulting impact on climate and the environment are largely unknown. It was suggested that rainwater organic matter is a complex mixture of potentially hundreds of compounds (Seitzinger et al., 2003), but the actual number and type of compounds that might constitute rainwater DOM was previously unknown. This dissertation presents, for

the first time, specific information on the large number of multifunctional organic compounds that are present in continental rainwater. It provides evidence suggesting the majority of these compounds are from secondary processing in the atmosphere, and that they have anthropogenic precursors. These secondary compounds could be used as anthropogenic tracers in precipitation collected in remote locations to assess the potential for transport of terrestrial organic carbon. Many of the compounds identified in the rainwater are known contributors to SOA. This is the first evidence that the complexity in SOA is a large contributor to the complexity in rainwater DOM. This allows the extensive work on SOA formation mechanisms and product identification to be used as a tool for identifying anthropogenic and biogenic compounds in rainwater DOM.

Atmospheric WSON is an important subset of the atmospheric dissolved organic carbon (DOC) that cycles through cloud water, fog water, aerosols, and rainwater, and it has additional ecosystem implications because of the nitrogen content of the molecules. It is now recognized that organic nitrogen is an important contributor to atmospheric nitrogen (Cornell et al., 2003), but its sources, composition, reactivity, and fate are largely unknown. Some nitrogen containing organic compounds in the atmosphere can be toxic and carcinogenic, e.g., nitro PAH's (Talaska et al., 1996), and some WSON compounds can act as nutrients stimulating productivity in the open ocean or as nutrients contributing to coastal eutrophication (Paerl et al., 1999;Peierls and Paerl, 1997). Without information on the sources of WSON it is very difficult to propose control or remediation strategies. However, due to the lack of compositional information, it is not clear whether control or remediation strategies are needed for WSON in precipitation.

This dissertation provides the first chemical characterization of DON in rainwater using ultra-high resolution mass spectrometry. This dissertation provides evidence that there are nitrogen containing compounds with distinctly anthropogenic sources including nitrooxy organosulfates and compounds that contain only carbon, hydrogen, and nitrogen. The majority of the nitrogen containing compounds detected are likely secondary oxidation products including oxidation products of amino acids that have predominantly biogenic sources. The rainwater DON is dominated by compounds with reduced nitrogen functionality which indicates that a large percentage of the DON could be bioavailable. The WSON compounds formed through secondary reactions in the atmosphere could have both biogenic and anthropogenic VOC precursors, though they should still be considered anthropogenic because of the large anthropogenic sources of oxidants such as nitrate, NO_x, and OH. This dissertation has provided the first molecular level characterization of dissolved organic carbon and nitrogen in rainwater. The majority of the products identified are multifunctional and some are highly oxygenated. Thus, these compounds, much like the oligomers formed in the cloud processing laboratory experiments, likely contribute to the HULIS fraction of atmospheric organic matter.

An increase in aerosol concentrations is generally thought to cause a suppression of rainfall (IPCC, 2007). Increased aerosol loading in the atmosphere can produce brighter clouds that are less efficient at releasing precipitation. This can lead to less efficient pollutant removal from the atmosphere. The radiative and microphysical effects of aerosols lead to a weakened hydrological cycle and a general drying of the planet. However, the amount of precipitation is also impacted by other climatic factors.

Increased tropospheric temperatures associated with increased greenhouse gas concentrations can lead to an intensifying of the hydrological cycle and more rainfall. This increase in the hydrological cycle is balanced by the reduction in solar radiation at the surface from absorbing aerosols which makes the planet drier. According to the IPCC (2007), very heavy precipitation events may become more frequent with the anticipated changes in the hydrological cycle. The regions that will be impacted by heavy rainfall are the same regions where the mean rainfall is projected to decrease. This could lead to a decrease in the removal of pollutants from the atmosphere. The heavy rain events lead to increased flood risk, which could then potentially impact water quality. The improved understanding of the composition of precipitation described in this dissertation, especially the large contribution of secondary compounds with anthropogenic precursors, may be relevant to understanding the potential ecosystem and health impacts of a changing hydrological cycle associated with a changing climate.

Chapter 2. Evidence for Oligomer Formation in Clouds: Reactions of Isoprene Oxidation Products

Material in this chapter has been published previously as:

Altieri, K.E., Carlton, A.G., Turpin, B.J., Seitzinger, S.P., Evidence for oligomer formation in clouds: Reactions of isoprene oxidation products. *Environmental Science and Technology*, 2006, 40(16), 4956-4960

2.1 Abstract

Electrospray ionization mass spectrometry (ESI-MS) was used to investigate product formation in laboratory experiments designed to study secondary organic aerosol (SOA) formation in clouds. It has been proposed that water soluble aldehydes derived from aromatics and alkenes, including isoprene, oxidize further in cloud droplets forming organic acids and, upon droplet evaporation, SOA. Pyruvic acid is an important aqueous-phase intermediate. Time series samples from photochemical batch aqueous phase reactions of pyruvic acid and hydroxyl radical were analyzed for product formation. In addition to the monomers predicted by the reaction scheme, products consistent with an oligomer system were found when pyruvic acid and OH radical were both present. No evidence of oligomer formation was found in a standard mix composed of pyruvic, glyoxylic and oxalic acids prepared in the same matrix as the samples analyzed using the same instrument conditions. The distribution of high molecular weight products is consistent with oligomers composed of the mono-, oxo- and di-carboxylic acids expected from the proposed reaction scheme.

2.2 Introduction

Atmospheric particulate matter (PM) scatters and absorbs light, affecting the global radiation budget and climate (IPCC, 2001). Additionally, exposure to PM is associated with adverse health effects in humans (EPA, 2004). A fraction of organic PM, secondary organic aerosol (SOA), is formed by oxidation of reactive organic gases and the subsequent partitioning of low to semi volatile products into the particle phase (Seinfeld and Pankow, 2003). On an annual basis SOA contributes roughly 10-50% of total organic PM in urban areas and as much as 80% during the afternoon hours of ozone episodes (Turpin and Huntzicker, 1995;Polidori et al., 2005;Turpin et al., 2000). The vast majority of SOA research has been devoted to elucidating pathways and yields for homogeneous gas-phase reactions that produce SOA. SOA and oligomer formation through acid-catalyzed aerosol phase reactions has also been documented in smog chamber experiments (Jang et al., 2002;Kalberer et al., 2004;Tolocka et al., 2004;Gao et al., 2004b;Gao et al., 2004a;Kanakidou et al., 2004). Oligomer formation might explain the presence of large multifunctional compounds that have long been known to dominate particulate organic mass (e.g., organics not eluted from the GC column; (Rogge et al., 1993)).

In addition to homogeneous reactions and aerosol-phase reactions, it has been proposed that, like sulfate, SOA can form through cloud processing (Blando and Turpin, 2000;Ervens et al., 2004;Lim et al., 2005). Briefly, high hydroxyl radical concentrations in the interstitial spaces of clouds oxidize reactive organics to form highly water soluble compounds (e.g., aldehydes). These compounds partition into cloud droplets where they oxidize further to form less volatile organics (e.g., oxalic acid). When the cloud droplets evaporate the low volatility organics remain, in part, in the particle phase, yielding SOA.

To our knowledge, oligomerization reactions have not previously been observed or shown to form through cloud processing. Should they form, they could substantially enhance in-cloud SOA yields.

In-cloud SOA production from alkenes and aldehydes, including isoprene, has been modeled by Ervens et al. (2004) and Lim et al. (2005). In the chemical mechanism used by Lim et al. (2005), gas phase isoprene oxidation produces water-soluble compounds, glycolaldehyde, glyoxal, and methylglyoxal. These products dissolve into cloud water and react with OH radicals to form oxalic, glycolic, and glyoxylic acids via pyruvic and acetic acids (solid arrows, Figure 2-1).

Methylglyoxal and pyruvic acid are important intermediates in in-cloud reactions of many reactive organics. To ascertain the fate of pyruvic acid, photochemical batch aqueous phase reactions of pyruvic acid and OH radical were performed. Identified products were consistent with those suggested by Stefan and Bolton (1999) and used by Lim et al. (2005) as reported in detail by Carlton et al. (2006). This work will show that oligomer formation may be an important step omitted in the Lim pathway (Lim et al., 2005). If reactions that lead to oligomer products are included in the Lim pathway it could add substantially to the SOA formed.

2.3 Methods

2.3.1 Experimental Setup

Photochemical batch aqueous-phase reactions of pyruvic acid and hydrogen peroxide (H_2O_2) were conducted in 1 liter borosilicate vessels with quartz immersion wells under conditions encountered by cloud water (pH 2.7-3.1) for 202 minutes. The reaction vessels were wrapped in aluminum foil to minimize the influence of ambient

UV. Low pressure UV lamps with spectral irradiance at 254 nm were used in the experiments to produce hydroxyl radical from hydrogen peroxide for pyruvic acid oxidation. Three types of control experiments were conducted: 1) a UV control (i.e., pyruvic acid and H_2O_2), 2) a H_2O_2 control (i.e., pyruvic acid and UV), and 3) an organic control (i.e., UV and H_2O_2). Three experiments were conducted, two with pyruvic acid concentrations of 10 mM and H_2O_2 concentrations of 20 mM, and one with the concentrations halved. A 0.5% catalase solution was added to all experimental and control samples right after sampling to prevent further reaction with H_2O_2. Samples were stored frozen until analysis. More details on experimental setup, sampling and HPLC procedures can be found in Carlton et al. (2006).

2.3.2 Analytical Determinations

The electrospray ionization mass spectrometry (ESI-MS) analysis was conducted using an HP-Agilent 1100 Liquid Chromatograph/Mass Spectrometer consisting of an autosampler and quadrupole mass-selective detector equipped with an atmospheric pressure electrospray ionization source. The autosampler injects samples and standard solutions (20 μL) from individual vials into the LC system. The instrument was run with no column attached, a mobile phase, 60:40 v/v 100% methanol and 0.05% formic acid in deionized water, with a flow rate of 0.220 ml min^{-1}. The ESI-MS measurements were made in the negative ion mode over the mass range 50 to 1000 Da with a fragmentor voltage of 40 V unless otherwise noted. Nitrogen was the drying gas (350°C, 10 L min^{-1}, 25 psig). The capillary voltage was 3 kV. The electrospray ionization full-scan mass spectra (*m/z* 50-1000) with unit mass resolution was recorded on Agilent software

(Chemstation version A.07.01) and exported to Excel and Access (Microsoft, Inc.) for statistical analysis and interpretation.

Authentic individual and mixed standards of pyruvic, glyoxylic, acetic, formic, and oxalic acids, all expected precursors or products (Lim et al., 2005) (Figure 2-1), were analyzed using the same instrument conditions as the sample analysis described above. The standard mix used for calculating concentrations in the samples was composed of pyruvic, glyoxylic, and oxalic acids in the same matrix as the samples in the reaction vessels (H_2O_2 at a 1:2 ratio and 1 μL of catalase). The standard mix was analyzed over the range of concentrations (0.025-1.5 mM) typical of the samples and a standard curve was created for each compound (Table 2-1). Acetic acid was not included in the standard mix because the ESI-MS did not detect it in either the monomer or dimer form. Previous analysis of samples including acetic acid in the standard mix did not result in the detection of any new ions, nor did it significantly affect the ion abundances of the other compounds in the standard mix. Formic acid has a molecular weight (48 Da) below the detection limit of the instrument (*m/z* 50) and was not detected in either positive or negative mode ESI-MS analysis.

The standard and sample data from the ESI-MS were analyzed using a previously established method (Seitzinger et al., 2005). For each standard and time series sample, six replicate injections were made. The mean ion abundance (+/- SD) for each *m/z* in each sample was calculated for the standards and samples. Each mass to charge (*m/z*) with an abundance statistically different from zero at the 0.05 level (t-test; (Sokal, 1981)) was retained. The samples and standards were corrected for deionized blanks by

subtracting the ion abundance of any *m/z* found in the deionized water from the same *m/z* in standards and samples.

ESI-MS is a soft ionization method that does not fragment ions. The technique can be applied to any species that can be protonated or deprotonated. Large compounds that would be fragile to fragmentation in other mass spectrometers are analyzed intact by the ESI-MS, including peptides and proteins (Marshall, 2000). ESI-MS provides molecular weight information as mass to charge ratios (*m/z*) with unit mass resolution. In the negative mode acidic functional groups lose an H^+ and appear at an *m/z* of the molecular weight minus one $[M-H]^-$.

The fragmentor voltage on the instrument is usually set at 40 V to keep compounds intact. However, for analysis of a subset of samples, the fragmentor voltage was varied. First, the standard mixture of monomers was analyzed with varying fragmentor voltages (40-100 V). Then the time series samples, diluted (1:10) with deionized water, were analyzed at fragmentor voltages (40-100 V) to fragment the oligomers that had been formed in the aqueous batch reactions.

2.4 Results and Discussion

2.4.1 Standard Analysis

Pyruvic acid was detected in the negative ion mode as both the monomer (*m/z* 87) and homogeneous dimer (*m/z* 175) forms in authentic standards ($[M-H]^-$, $[2M-H]^-$). Glyoxylic (*m/z* 73) and oxalic (*m/z* 89) acids were detected in the monomer form only ($[M-H]^-$, Figure 2-2), which is consistent with other carboxylic acids in single and mixed standards. The response in the ion abundance of oxalic, glyoxylic, and pyruvic acids to increasing concentrations was linear up to approximately 1.5 mM (Table 2-1, Figure 2-3).

However, the slopes for each organic acid differ due to the relationship of ion abundance to concentration being compound dependent.

2.4.2 Sample Analysis

The ion abundance representing pyruvic acid decreased while glyoxylic and oxalic acids increased during the experiment as predicted by Lim et al. (2005) and discussed by Carlton et al. (2006) (Figure 2-4). The ion abundance of the reactant pyruvic acid (*m/z* 87, *m/z* 175) decreased from 44 seconds to 10 minutes, and then remained relatively constant throughout the remainder of the experiment. The intermediate glyoxylic acid (*m/z* 73) increased in ion abundance slightly from 10 to 27 minutes (3,971 to 4,678 units) and then steadily decreased in ion abundance for the remainder of the reaction to a final ion abundance of 758 units. The expected product oxalic acid (*m/z* 89) increased in ion abundance throughout the experiment (Figure 2-4) and became the dominant peak in the spectrum after 202 minutes showing good agreement with the proposed mechanism (Lim et al., 2005).

2.4.3 Oligomer Formation

If the time series samples were composed only of the monomers predicted by Lim et al. (2005), the ESI-MS spectrum should resemble the spectrum of the standard mix of reaction components (Figure 2-2). However, after ten minutes of photochemical oxidation, ions higher in molecular weight than the monomers appear in the time series spectrum (Figure 2-4a), in addition to the monomers predicted by Lim et al. (2005). The distribution of these higher molecular weight ions in the spectrum at ten minutes is not completely regular, but appears to be consistent with the development of an oligomer system (Figure 2-4a). The two peaks with the highest ion abundance in the spectrum are

m/z 147 and *m/z* 217. The most dominant mass species (*m/z* 147) has tentatively been identified (based on the molecular weight combinations) as a pyruvic and acetic acid dimer.

The spectral complexity increases with time in samples from the photochemical oxidation of pyruvic acid. There are six peaks that dominate the spectrum after 202 minutes of oxidation (Figure 2-4b). The most dominant peak is *m/z* 89, oxalic acid monomer. The following five ions with the next highest abundances after *m/z* 89 are 103, 133, 147, 177, and 217. The six peaks differ by 14, 30, 14, 30, and 40 Da, respectively. These six ions represent almost half of the total ion abundance of the entire sample. The other half of the total ion abundance in the sample is present in a pattern that is consistent with an oligomer system (Figure 2-4b). The oligomer haystacks show a highly regular pattern of mass differences of *m/z* 12, 14 and 16 in the mass range 80-500 Da and the peaks within the haystacks are separated by 2 Da (Figure 2-4b). If the mixed acid oligomers in the sample spectra were artifacts of the ESI-MS, they should also appear in the mixed standard spectra (Figure 2-2) where all of the reaction components are present; however, they do not. They also do not appear in the control spectra (see below), implying that the formation of oligomers in the samples requires the presence of both pyruvic acid and OH radical.

The main peaks in the haystacks can be accounted for by linear combinations of known monomer units, formic, acetic, pyruvic, glyoxylic, and oxalic acids. For example, the gain of 14 Da could be attributed to the addition of a glyoxylic acid (74 Da) instead of an acetic acid (60 Da), or the addition of a pyruvic acid (88 Da) instead of a glyoxylic acid. The mass difference of 16 Da could be attributed to adding an oxalic acid (90 Da)

instead of a glyoxylic acid. The regular distribution of the 6 dominant ions, the regularity of the lower abundance peaks, and the linear combinations of monomer units support the presence of an oligomer system (Nielen, 1999;Zoller and Johnston, 2000;Cox et al., 2004). This evidence is also consistent with a polydisperse copolymer system (Cox et al., 2004). An important next step is to identify the exact composition of each of the oligomers in the system. The experiments were conducted in the aqueous phase at pH values typical of clouds to simulate cloud chemistry and thus provide evidence that oligomer formation could be occurring under conditions encountered in clouds.

2.4.4 Control Experiments

The formation of the oligomer system requiring the presence of pyruvic acid and the OH radical is supported by the mixed standards (as discussed above) and the two control experiments. When pyruvic acid is exposed in the controls to UV alone or H_2O_2 alone there are additional peaks in the spectra that are not present in the mixed standard (Figure 2-5). However, the peaks in the control spectra are not as regular or dense as those in the time series reaction spectra. It is known that pyruvic acid will react to some degree with UV alone (e.g., formic and acetic acids (Carlton et al., 2006)). However, the extent of reaction in the control with UV alone is much less than when the pyruvic acid is exposed to UV plus H_2O_2 (i.e., OH). The pyruvic acid (*m/z* 87, 175) (after approximately 161 minutes of exposure to UV) is 42% of the total ion abundance, as compared to ~2% of the total ion abundance when oxidized by the OH radical. The lack of regularity and density in the control spectra supports the conclusion that pyruvic acid and the OH radical are required for the regularly distributed oligomer system to form. However,

compounds formed from the reaction of pyruvic acid and UV alone may be atmospherically relevant and warrant further investigation.

2.4.5 Oligomer Quantification

The goal of changing the fragmentor voltage when analyzing standards and samples was to see if the potential monomer constituents increased in abundance as the larger molecular weight compounds were broken apart. This would provide additional evidence that these high molecular weight compounds are oligomers. In the mixed monomer standards as the fragmentor voltage increased, the monomer ion abundances $[M-H]^-$ decreased as expected as the compounds were fragmented (Table 2-2, Figure 2-6, Appendices A1, A2, A3). The fragmented components smaller than *m/z* 50, which is the lower mass detection limit of the instrument, are not detected.

For the sample analysis, the percent of initial monomer abundance that should be lost by increasing the fragmentor voltage was known from the standard analysis. In contrast to the standards decreasing in ion abundance, the monomers (pyruvic and glyoxylic acid) in the samples initially increased in abundance as fragmentor voltage increased (Figure 2-6, Appendices A1, A2). This *increase* in abundance implies that a larger molecular weight compound was breaking apart and contributing to the monomer abundance. The oxalic acid monomer decreased in ion abundance with increased fragmentor voltage in the samples but this decrease was 20% less than the standard decrease (Appendix A3). The decrease in ion abundance from fragmentation seen in the standards was overwhelmed in the samples by an increase in abundance from fragmentation of higher molecular weight species. This is consistent with the decrease in abundance in the higher molecular weight compounds as the fragmentor voltage was

increased. Thus, the larger molecular weight oligomers are at least partially composed of the known monomers, pyruvic acid, glyoxylic acid, and oxalic acid.

The increased monomer abundance in the samples with increased fragmentor voltage, in contrast to the decrease in the standard monomer abundance, was used to estimate the concentration of monomer present in the oligomers. The percent of monomer lost with increased fragmentor voltage for the standards is concentration independent (Table 2-2). For example, the 0.5 mM mixed standard was used to determine the percent loss of glyoxylic acid (*m/z* 73) in ion abundance (67%) as the fragmentor voltage was increased from 40 to 80 V (Table 2-2). In sample t_{g1} (sample from a replicate experiment due to insufficient sample volume) glyoxylic acid (*m/z* 73) had an abundance of 7,284 units (Appendix A2). After increasing the fragmentor voltage to 80 V, fragmentation alone would have decreased the glyoxylic acid (*m/z* 73) ion abundance by 67% to 2,404 units. In sample t_{g1}, the glyoxylic acid (*m/z* 73) actually increased in ion abundance to 11,755 units (Appendix A2). Thus 9,351 units of glyoxylic acid were generated by fragmentation of oligomers. This increase in ion abundance, the glyoxylic acid response factor (Table 2-1) and the dilution factor (1:10) were used to calculate that at least 0.49 mM of glyoxylic acid was present in the oligomers in the t_{g1} sample, and 0.85 mM in the t_{g2} sample.

The concentration of monomers from oligomer breakup was calculated as described above for pyruvic and oxalic acids. The pyruvic acid calculated to be in oligomers is 0.29 mM in sample t_3. The oxalic acid calculated to be in oligomers is 0.06 mM for sample t_3 and 0.09 mM in sample t_6. For sample t_3, there is approximately the same amount of oxalic acid present as a monomer (0.04 mM; Appendix A4) as there is

present in oligomers (0.06 mM). As the reaction proceeds, sample t_6 has more oxalic acid present in its monomer form (0.30 mM; Appendix A4) than it does in oligomers (0.09 mM). The concentration of oxalic acid monomer increases with time (Figure 2-4, Appendix A4) but the concentration of oxalic acid in oligomers increases very little in comparison to the monomer increase from sample t_3 to t_6.

This work is the first time that evidence for oligomer formation in cloud processing reactions has been reported. The presence of the reaction components as oligomers instead of only monomers is likely to have important implications to in-cloud SOA formation. The oligomer forms will have lower vapor pressures and will remain to a much larger extent in the particle phase after cloud evaporation than the monomers. Also, oligomer formation from reaction products may enhance the effective Henry's law constants for precursor aldehydes, further enhancing SOA. It is possible that the absorptive and scattering properties of clouds and particles could be altered by the presence of oligomers since large multifunctional compounds believed to be formed in the atmosphere have some associated absorption (Gelencser et al., 2003). Thus, in-cloud oligomer formation could affect radiative forcing.

There remain many unanswered questions about the potential impacts of oligomers formed through cloud processing. These experiments are consistent with oligomers forming through irreversible reactions. However, the laboratory experiments are conducted in a closed system while the atmosphere is an open system which allows partitioning. The behavior of oligomers upon droplet evaporation is yet unknown. Oligomers formed through in-cloud aqueous-phase reactions could contribute to the concentration of surfactants observed in cloud droplets (Decesari et al., 2003); however,

it is not clear whether surfactant formation through this pathway will be great enough to substantially alter surface coverage, droplet surface tension, and gas exchange. An important next step is to parameterize oligomer formation for SOA modeling.

Table 2-1 Mixed Standard Response in ESI-MS

Response of ESI-MS to compounds in the standard mix composed of the same matrix as the samples in units of ion abundance per mM compound. The r^2 values and equations are calculated from linear regression analysis based on the ion abundance of the mixed standards as a function of concentrations 0.025 mM to 1.5 mM.

Compound	Molecular Formula	Molecular Weight	a	y_0	r^2
Pyruvic acid[a]	$CH_3COCOOH$	88.1	472,400	25,630	0.9753
Pyruvic acid[b]	$2(CH_3COCOOH)$	176.2	95,130	3,032*	0.9847
Glyoxylic acid	OCHCOOH	74.0	47,960	6,999	0.8083
Oxalic acid	HOOCCOOH	90.0	647,820	-690*	0.9997

[a]$[M-H]^-$ [b]$[2M-H]^-$

a=slope of the line and y_0=y intercept

*not significantly different than zero $t_{0.05, 3}$

Table 2-2 Effect of Changing Fragmentor Voltage on Ion Abundance
Comparison of the percent change in ion abundance of standards as fragmentor voltages increased (40-80 V) to the percent change in ion abundance of the samples as fragmentor voltages increased (40-80 V).

	% change 0.5 mM standard	% change 1.0 mM standard	% change $t_{3\ 27\ min}$	% change $t_{6\ 86\ min}$
Pyruvic acid	-88	-87	557	825
Glyoxylic acid	-67	-65	61**	179**
Oxalic acid	-98	-97	-77	-81

** t_{g1}=21 and t_{g2}=59 min sample from replicate experiment due to insufficient sample volume

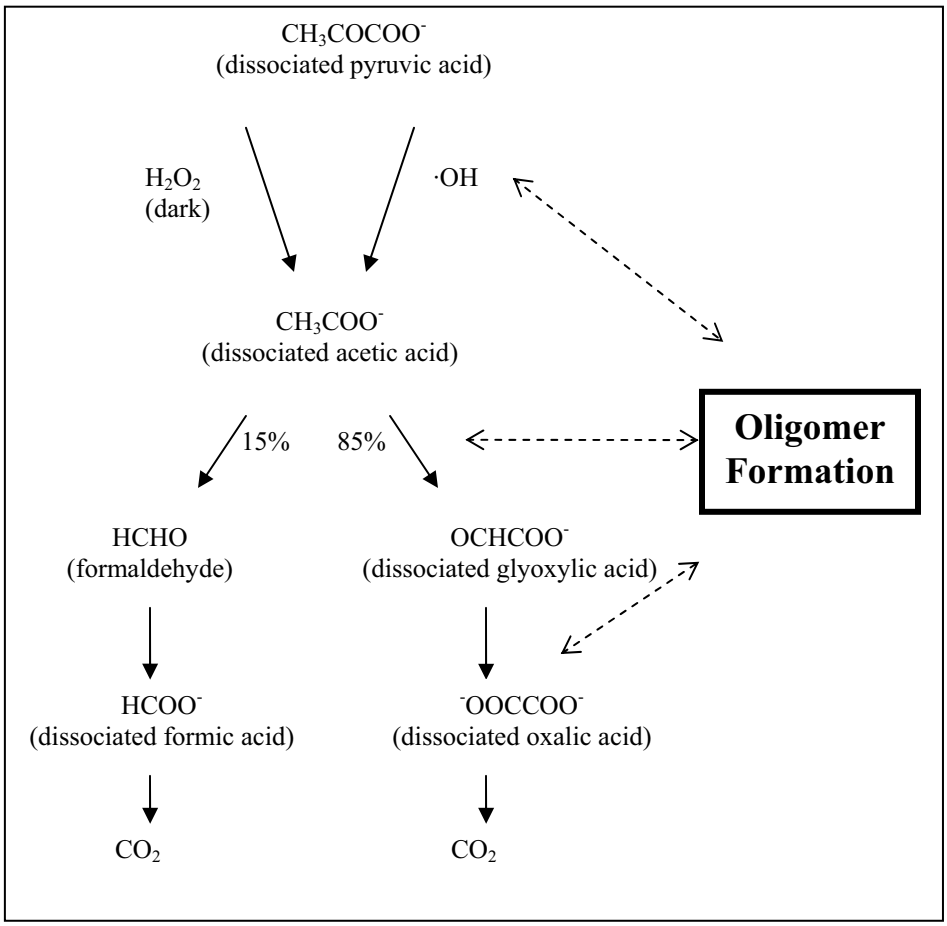

Figure 2-1 Mechanism of Pyruvic Acid Photooxidation
Mechanism of oxalic acid formation through isoprene cloud processing. Modified from Lim et al. (2005) and Carlton et al. (2006) to focus on the pyruvic acid pathway and to include oligomer formation.

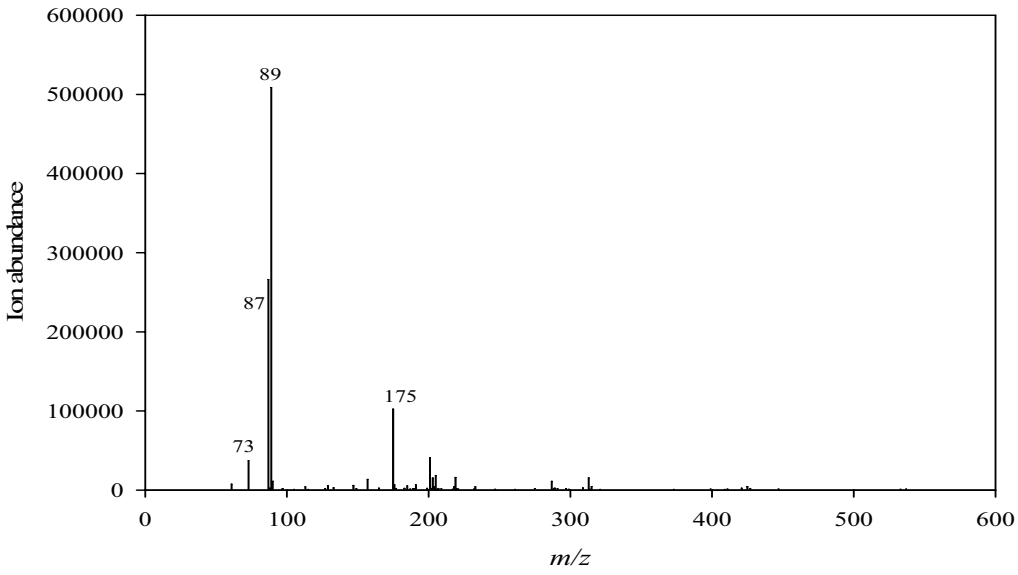

Figure 2-2 Mixed Standard in Negative Mode ESI-MS
Abundance of pyruvic acid monomer (*m/z* 87) and dimer (*m/z* 175), glyoxylic acid (*m/z* 73), and oxalic acid (*m/z* 89) in a 1.5 mM per compound mixed standard in the same matrix as the samples, detected by negative ionization mode ESI-MS.

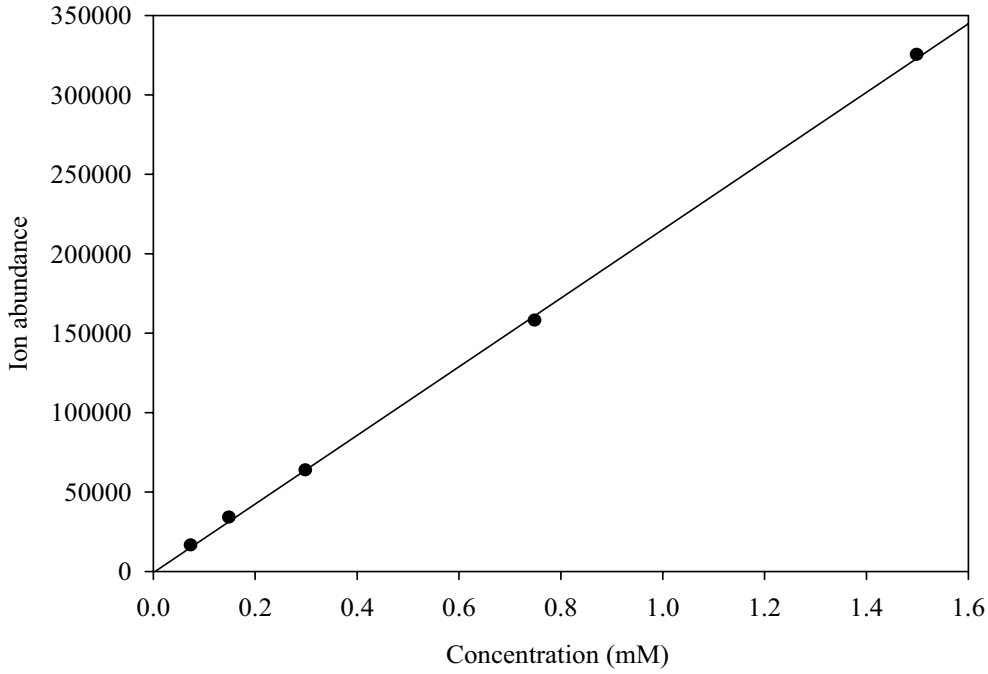

Figure 2-3 Oxalic Acid Ion Abundance in Mixed Standard
ESI-MS response (ion abundance) to oxalic acid (*m/z* 89) in a mixed standard that included pyruvic and glyoxylic acids in the same matrix as the samples across a range of concentrations (0.075-1.5 mM compound; r^2=0.9997 y=647,820x-690).

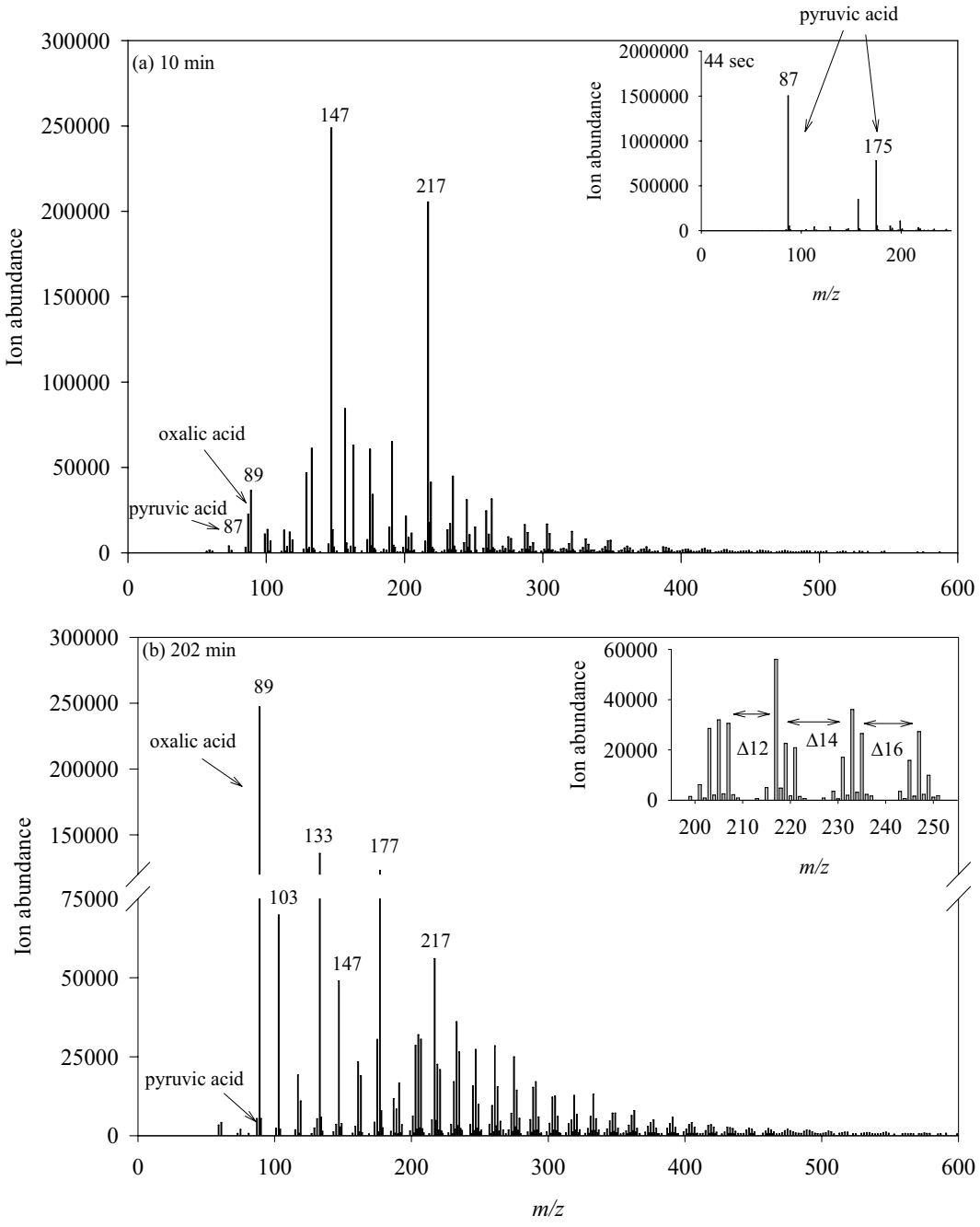

Figure 2-4 Time Series Samples of Pyruvic Acid Photooxidation
ESI-MS spectra of time series samples from pyruvic acid UV/H_2O_2 oxidation after (a) 10 minutes and (b) 202 minutes. Pyruvic acid (*m/z* 87, 175) is the main compound present in a 44 second time series sample from a replicate experiment (inset a). The regular distribution of *m/z* 12, 14, 16 indicating the oligomeric system is shown for an enlarged portion of (b) in the inset. Note break in y-axis scale.

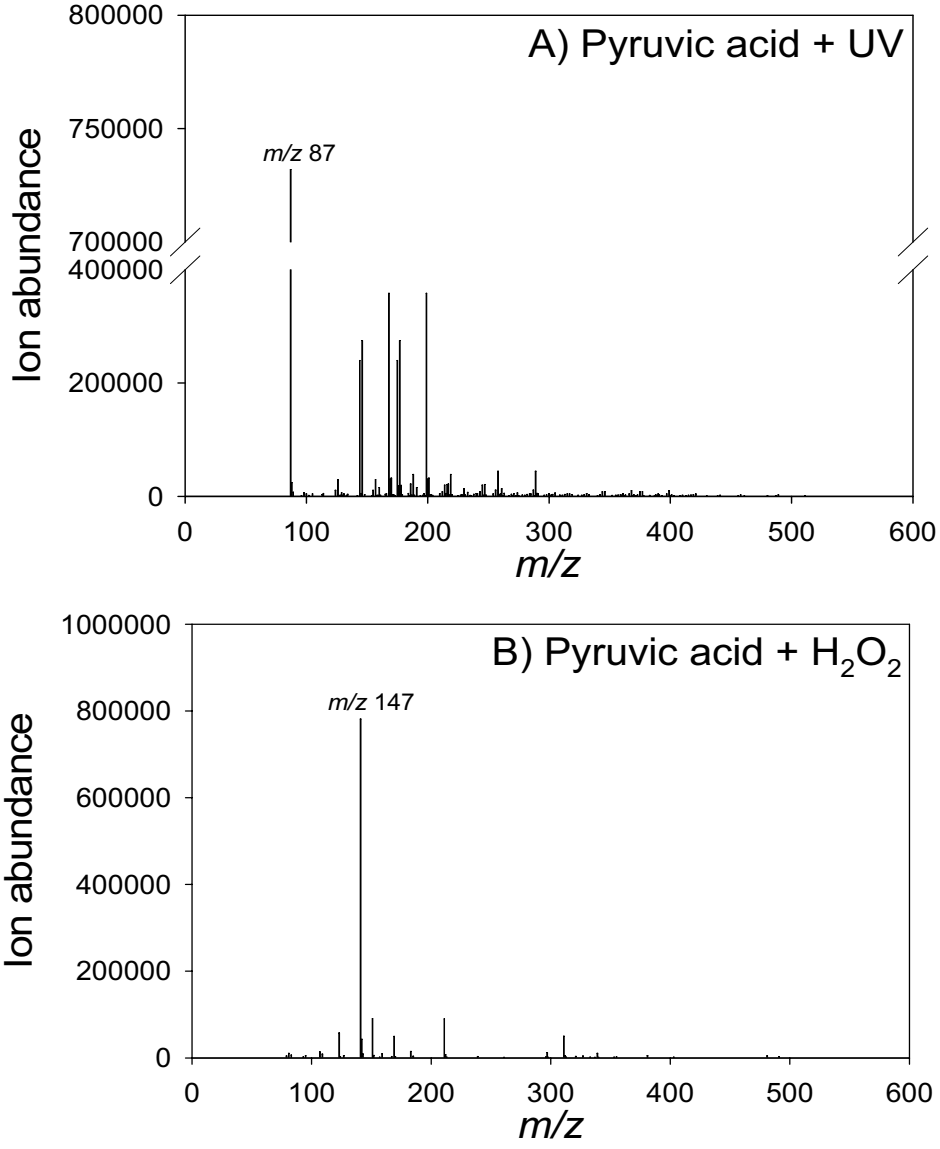

Figure 2-5 Pyruvic Acid H_2O_2 and UV Controls
ESI-MS spectrum of the A) UV degradation of pyruvic acid (no H_2O_2 added) after 161 minutes. Pyruvic acid (*m/z* 87) is present as the most abundant compound and there is a higher molecular weight cluster that is not representative of an oligomer system. ESI-MS spectrum of the B) degradation of pyruvic acid in the presence of H_2O_2 (no UV added) after 174 minutes.

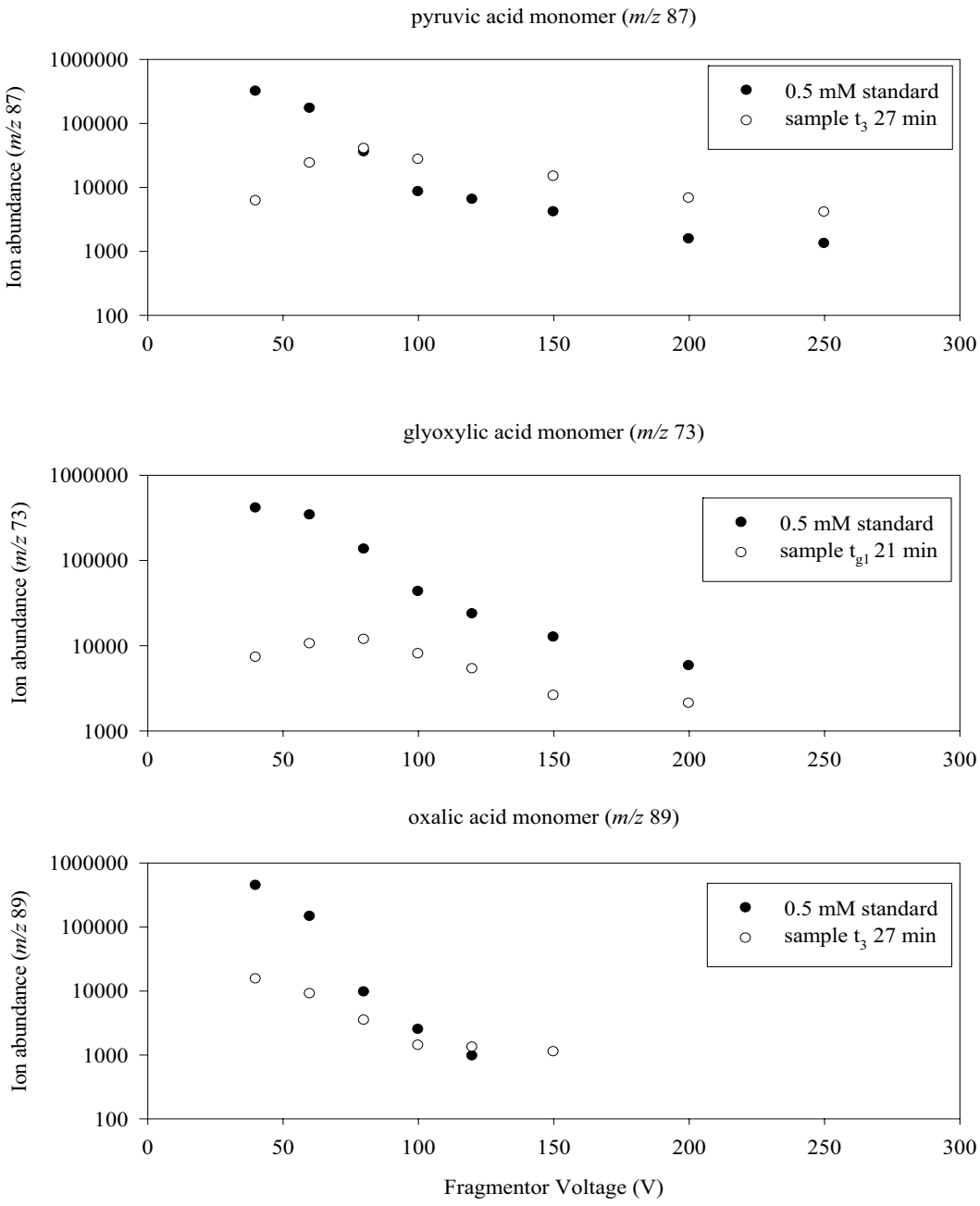

Figure 2-6 Response of Organic Acids to Varying Fragmentor Voltage
Response (ion abundance) of pyruvic acid (*m/z* 87), glyoxylic acid (*m/z* 73), and oxalic acid (*m/z* 89) to varying fragmentor voltages in a 0.5 mM mixed standard (filled circles) and time series samples (empty circles).

Chapter 3. Oligomers Formed Through In-Cloud Methylglyoxal Reactions: Chemical Composition, Properties, and Mechanisms Investigated by Ultra-High Resolution FT-ICR Mass Spectrometry

Material in this chapter has been published previously as:

Altieri, K.E., Seitzinger, S.P., Carlton, A.G., Turpin, B.J., Klein, G.C., Marshall, A.G., Oligomers formed through in-cloud methylglyoxal reactions: Chemical composition, properties, and mechanisms investigated by ultra-high resolution FT-ICR Mass Spectrometry, *Atmospheric Environment*, 2008, vol. 42, 1476-1490

3.1 Abstract

Secondary organic aerosol (SOA) is a substantial component of total atmospheric organic particulate matter, but little is known about the composition of SOA formed through cloud processing. We conducted aqueous phase photooxidation experiments of methylglyoxal and hydroxyl radical to simulate cloud processing. In addition to predicted organic acid monomers, oligomer formation from methylglyoxal-hydroxyl radical reactions was detected by electrospray ionization mass spectrometry (ESI-MS). The chemical composition of the oligomers and the mechanism of their formation were investigated by ultra-high resolution Fourier transform ion cyclotron resonance mass spectrometry (FT-ICR MS) and LCQ DUO ion trap mass spectrometry (ESI-MS-MS). Reaction products included 415 compounds detected in the mass range 245-800 Da and the elemental composition of all 415 compounds were determined by ultra-high resolution FT-ICR MS. The ratio of total organic molecular weight per organic carbon weight (OM:OC) of the oligomers (1.0-2.5) was lower than the OM:OC of the organic acid monomers (2.3-3.8) formed, suggesting that the oligomers are less hygroscopic than

the organic acid monomers formed from methylglyoxal-hydroxyl radical reaction. The OM:OC of the oligomers (average = 2.0) is consistent with that of aged atmospheric aerosols and atmospheric humic like substances (HULIS). A mechanism is proposed in which the organic acid monomers formed through hydroxyl radical reactions oligomerize through esterification. The mechanism is supported by the existence of series of oligomers identified by elemental composition from FT-ICR MS and ion fragmentation patterns from ESI-MS-MS. Each oligomer series starts with an organic acid monomer formed from hydroxyl radical oxidation, and increases in molecular weight and total oxygen content through esterification with a hydroxy acid ($C_3H_6O_3$) resulting in multiple additions of 72.02113 Da ($C_3H_4O_2$) to the parent organic acid monomer. Methylglyoxal is a water soluble product of both gas phase biogenic (i.e., isoprene) and anthropogenic (i.e., aromatics, alkenes) hydrocarbon oxidation. The varied and multiple sources of methylglyoxal increase the potential for these low volatility cloud processing products (e.g., oxalic acid and oligomers) to significantly contribute to SOA. Aqueous phase oligomer formation investigated here and aerosol phase oligomer formation appear to be more similar than previously realized, which may simplify the incorporation of oligomers into atmospheric SOA models.

3.2 Introduction

Atmospheric aerosols scatter and absorb light influencing the global radiation budget and climate (IPCC, 2001), and are associated with adverse effects on human health (EPA, 2004). Secondary organic aerosol (SOA), a fraction of total organic aerosol, is formed through gas-to-particle conversion processes involving products of reactive organic gases (Seinfeld and Pankow, 2003;Jang et al., 2002). SOA formation

through condensation/sorption of gas phase reaction products and subsequent aerosol phase reactions has been studied extensively and SOA constituents include oligomers and humic like substances (HULIS) (Gao et al., 2004;Graber and Rudich, 2006;Kalberer et al., 2004;Tolocka et al., 2004;Reinhardt et al., 2007;Surratt et al., 2006). Ultra-high resolution Fourier transform ion cyclotron resonance mass spectrometry (FT-ICR MS) has been used to investigate SOA oligomers formed through smog chamber experiments (Tolocka et al., 2004;Kalberer et al., 2004;Reinhardt et al., 2007), and to analyze ambient aerosols (Reemtsma et al., 2006;Denkenberger et al., 2007). There is growing evidence that, just as sulfate is formed through aqueous phase reactions, secondary organic aerosol is also formed through aqueous phase reactions in clouds, fogs and aerosols (Blando and Turpin, 2000;Ervens et al., 2004;Gelencser and Varga, 2005;Altieri et al., 2006;Carlton et al., 2006;Lim et al., 2005;Carlton et al., 2007;Heald et al., 2006;Sorooshian et al., 2007;Ervens et al., 2003).

Methylglyoxal is found widely in urban, rural, and remote environments (Kawamura et al., 1996;Kawamura and Yasui, 2005). Methylglyoxal is a secondary product formed from the oxidation and ozonolysis of anthropogenic hydrocarbons (e.g., aromatics, toluene, xylene) making it a potentially important contributor to SOA on urban and regional scales (Smith et al., 1999;Ham et al., 2006;Atkinson and Arey, 2003). It is also a secondary product from the oxidation of biogenic hydrocarbons (e.g., isoprene) (Atkinson, 2000;Atkinson and Arey, 2003). Because isoprene has a large world-wide emission flux, even small SOA yields from isoprene would have significant climate implications (Henze and Seinfeld, 2006). Recent smog chamber and aqueous

photochemistry experiments suggest that isoprene is an SOA precursor (Altieri et al., 2006;Carlton et al., 2006;Carlton et al., 2007;Kroll et al., 2006;Surratt et al., 2006).

There is experimental evidence that oligomeric products form through cloud processing: aqueous phase self-polymerization of methylglyoxal (Loeffler et al., 2006;Hastings et al., 2005), photoinduced self-oligomerization of aqueous pyruvic acid (Guzman et al., 2006), acid catalyzed aqueous phase reactions of levoglucosan (Holmes and Petrucci, 2006), and aqueous reaction of hydroxyl radical and pyruvic acid (Altieri et al., 2006;Carlton et al., 2006). The properties of oligomers formed through atmospheric aqueous phase photochemistry, the reaction mechanisms leading to oligomer formation and the resulting atmospheric implications for SOA produced through cloud processing, however, have not been elucidated.

The mechanism of oligomer formation and the properties of the oligomers formed through aqueous-phase photooxidation of methylglyoxal were investigated in this study. Oligomers were detected by ESI-MS analysis of time series samples. Their chemical composition and formation mechanism were investigated by ultra-high resolution FT-ICR MS (Marshall et al., 1998). Evidence for the proposed structures of the oligomers and the proposed mechanism of formation was provided by ESI-MS-MS. Implications for SOA produced through cloud processing are discussed. To our knowledge this is the first description of the chemical composition and formation mechanism of oligomers formed through aqueous phase reactions relevant to atmospheric waters.

3.3 Experimental

Batch photochemical aqueous phase reactions of methylglyoxal (2 mM) and hydrogen peroxide (10 mM) were conducted in triplicate in 1 L borosilicate vessels under

conditions encountered by cloud water (pH 4.2-4.5). The concentrations in the experiment are higher than those in cloud and fog droplets (Matsumoto et al., 2005), but lower than those in aerosol water (Munger et al., 1995). The UV irradiation of hydrogen peroxide was the source of hydroxyl radicals in the reaction vessel. The UV source was a low pressure monochromatic (254 nm) mercury lamp placed in a quartz immersion well. The details of the experimental setup are described elsewhere (Altieri et al., 2006;Carlton et al., 2006;Carlton et al., 2007). Briefly, a t=0 min sample was taken from the volumetric flask used to prepare the solution, and then samples were taken from the reaction vessel every 20-30 minutes for the duration of the experiment (~6.5 hours). A 0.5% aqueous catalase solution was used to destroy the hydrogen peroxide (0.25 μL/1mL sample) (Stefan et al., 1996). The samples were stored in the dark in the freezer until analysis. For each experiment there were two control experiments: 1) UV control (methylglyoxal plus H_2O_2 with no UV) and 2) H_2O_2 control (methylglyoxal plus UV with no H_2O_2 added).

3.3.1 ESI-MS

All experimental samples discussed below were analyzed with an HP-Agilent 1100 atmospheric pressure electrospray ionization mass spectrometer with a quadrupole mass-selective detector. A liquid chromatograph (LC) autosampler was used to inject sample solutions (6 replicate injections, 20 μL each) from individual vials into the LC system; no column was used in these analyses. The mobile phase was 60:40 v/v 100% methanol and 0.05% formic acid in deionized water with a flow rate of 0.220 mL min^{-1}. Experimental samples, controls, and standards were analyzed as negative and positive ions (mass range 50-1000 Da, fragmentor voltage 40 V, capillary voltage 3 kV). The ion

abundance of any *m/z* detected in the deionized water blank was subtracted from the spectra of all experimental samples, controls, and standards. Nitrogen was the drying gas (350 °C, 24 psig, 10 L min^{-1}). The unit mass resolution spectra were recorded with Agilent software (Chemstation version A.07.01) and exported to Access and Excel (Microsoft, Inc.) for statistical analysis and interpretation as described previously (Altieri et al., 2006). A mixed standard of methylglyoxal, pyruvic acid, acetic acid, glyoxylic acid, and oxalic acid (precursor and expected monomeric products) in the same matrix as samples (H_2O_2 1:5 ratio, 1 μL catalase) was analyzed under the same instrument conditions as experimental time series samples. Methylglyoxal was detected as a proton-bound positive-ion dimer $[2M+H]^+$. Pyruvic, glyoxylic, and oxalic acids were detected as negative ions $[M-H]^-$. Acetic acid is not detected by ESI-MS as discussed previously (Altieri et al., 2006), but its presence was verified by HPLC (Carlton, 2006).

3.3.2 Ultra-High Resolution Electrospray Ionization FT-ICR MS

Analyses were performed on a 69 minute experimental time series sample with a 9.4-T Fourier transform ion cyclotron resonance mass spectrometer equipped with an ESI source at the National High Magnetic Field Laboratory (NHMFL) (Senko et al., 1997;Senko et al., 1996;Marshall and Guan, 1996). The needle voltage was +/- 2000 V, the heated capillary current was ~3.5 A, and the tube lens was +/- 350 V. Ions were accumulated external to the magnet in a linear octopole ion trap (25.1 cm long) equipped with axial electric field (Wilcox et al., 2002) and transferred through rf-only multipoles to a 10 cm diameter, 30 cm long open cylindrical Penning ion trap. Multipoles were operated at: 1.6 MHz/0.5 V_{p-p}, 1.7 MHz/0.5 V_{p-p}, 1.8 MHz/1.4 V_{p-p}. The data were zero-filled, Hamming apodized, and then processed by Fourier transform and magnitude

computation. The spectra were mass calibrated with standard ions with an internal calibrant (G2421A Agilent "tuning mix") and MIDAS Analyzer software. The residual root-mean-square mass error after internal calibration was 0.42 ppm.

MIDAS Formula Calculator Software (v1.1) was used to calculate all mathematically possible formulas for all ions detected with a mass tolerance of ±1 ppm. An unlimited number of ^{12}C, ^{1}H, ^{16}O and one ^{13}C were allowed in the molecular formula calculations. There were 446 ions where only one chemical formula containing ^{12}C, ^{1}H, and ^{16}O was possible, within ±1 ppm of the measured mass. Elemental formulas with a ^{13}C were checked for the ^{12}C counterpart; if it was not present the ^{13}C formula was deleted. This process eliminated 31 formulas, including all four compounds that had multiple assigned molecular formulas. The average mass error for all assignments was 0.67 ppm for the 446 ions identified. Ions were also characterized by the number of rings plus double bonds (i.e., double bond equivalents (DBE)), calculated from equation 3-1 (McLafferty, 1993)

$$DBE = c - \frac{1}{2}h + 1 \qquad \text{for elemental composition, } C_cH_hO_o \tag{3-1}$$

3.3.3 Comparison of ESI-MS and FT-ICR MS Spectra

The ESI-MS was used to analyze a mass range of 50-1000 Da and the FT-ICR MS was used to analyze a mass range of 245-1200 Da. The overlap range of *m/z* 300-500 was arbitrarily chosen and used to compare the output from the two mass spectrometers for the same sample (t=69 min). There is excellent agreement in the masses detected when the sample is analyzed by both ESI-MS and FT-ICR MS (Appendix B1). At unit

mass resolution 45% of the ions detected have two compounds in the unit mass bin detected by FT-ICR MS, and 13% of the ions detected have more than two compounds present in the unit mass bin. The relative ion abundance pattern is also conserved for the masses in the overlapping section in both mass spectrometers.

3.3.4 ESI-MS-MS

The Finnigan LCQ Duo quadrupole ion trap mass spectrometer (San Jose, CA) (ESI-MS-MS) was used to obtain further structural information for ions of a select number of masses. The samples were infused directly into the mass spectrometer at 0.033 mL min^{-1}. The spray voltage was -4 kV with a capillary temperature of 150 °C. The capillary voltage was -13 V with the sheath gas flow rate (arbitrary units) set at 96 and the auxiliary gas flow rate at 5. The ion optics were set as follows: octopole 1 offset 6.5 V, octopole 2 offset 9 V, inter-octopole lens 32 V, and the tube lens 10 V. Collision induced dissociation (CID) negative ion spectra were obtained with normalized collision energies of 20-30%.

3.4 Results and Discussion

3.4.1 Organic Acid Monomer Formation

The appearance of organic acids in the ESI mass spectrum is consistent with the methylglyoxal photooxidation mechanism used by Lim, (Lim et al., 2005) and the results of pyruvic acid photooxidation experiments (Altieri et al., 2006;Carlton et al., 2006) (Figure 3-1, solid arrows). The precursor methylglyoxal reacts almost immediately with little remaining in the first time series sample (t=0 min; positive ion data not shown). Pyruvic acid (*m/z* 87) and glyoxylic acid (*m/z* 73), two of the originally hypothesized intermediates to oxalic acid formation, are low in ion abundance (< 1000 abundance

units) throughout the experiment. Oxalic acid (*m/z* 89) forms over time and is the dominant peak in the last time series sample (Figure 3-2). This result is similar to previous pyruvic acid photooxidation experiments wherein the pyruvic acid reacted quickly, the glyoxylic acid ion abundance remained low throughout the experiment, and oxalic acid was an end product (Altieri et al., 2006;Carlton et al., 2006).

3.4.2 OligomerFormation

In addition to the organic acid monomers, after ~35 minutes of photooxidation we observe a large number of compounds (Figure 3-2) that are of a higher molecular weight than the precursor and products in the reaction scheme used by Lim (Lim et al., 2005) (Figure 3-1). The complexity of the ESI-MS spectra increases with time (until t=69 min) and there is a regular pattern of mass differences (12, 14, 16 Da) in the higher molecular weight products (Figures 3-2, 3-3) indicating an oligomer system (Tolocka et al., 2004;Kalberer et al., 2004;Reinhardt et al., 2007). The oligomer system develops over time, reaching maximum ion abundances for most peaks at ~69 minutes and then decreasing in ion abundance as other products form (e.g., *m/z* 89 oxalic acid, *m/z* 103, 133, 177). The complexity of the experimental time series spectra and the simplicity of the mixed standard spectra (Figure 3-4) reaffirm that oligomer formation is not an artifact of the ESI process. The oligomers and oxalic acid/oxalate (Martinelango et al., 2007) are both low volatility products that will contribute to SOA upon cloud droplet evaporation.

The oligomer pattern in the aqueous methylglyoxal-hydroxyl radical reaction time series sample spectra is almost identical to that for oligomers seen in aqueous pyruvic acid-hydroxyl radical experiments previously described (Altieri et al., 2006). At maximal oligomer formation the methylglyoxal experimental sample exhibited 296 ions

whereas the pyruvic acid experimental sample showed 249 ions, with 230 ions present in both spectra (mass range 50-500 Da, ESI-MS). This result is consistent with the mechanism used by Lim (Lim et al., 2005) (Figure 3-1) in which pyruvic acid is produced from aqueous methylglyoxal oxidation. Initiating reactions with methylglyoxal rather than pyruvic acid caused almost no change in the oligomer distribution, indicating that oligomer formation does not require the presence of methylglyoxal, only its reaction products (e.g., pyruvic acid, acetic acid, formic acid). Although hydration of aldehydes and subsequent self-polymerization have been hypothesized as an aqueous phase SOA formation pathway (Hastings et al., 2005), we found no evidence that this mechanism contributes to oligomer formation from methylglyoxal when hydroxyl radicals are present, either because the concentrations used in these experiments are too low for self-polymerization, or the oligomer formation mechanism that occurs when hydroxyl radical is present is the dominant oligomer formation mechanism.

3.4.3 Control Samples

In the H_2O_2 control experiment (methylglyoxal plus UV, no H_2O_2), and the UV control experiment (methylglyoxal plus H_2O_2, no UV) no significant product formation was observed by ESI-MS (Appendix B2) indicating that the oligomer formation is due to the reaction of methylglyoxal with the hydroxyl radical, and not hydrogen peroxide or UV light alone. This is consistent with previously reported in-cloud oligomer formation through pyruvic acid photooxidation (Altieri et al., 2006).

3.4.4 Oligomer Properties

The 69 minute experimental time series sample was chosen for negative ion FT-ICR MS analysis because at this time the oligomer formation was at a maximum in ion

abundance (Figure 3-2). The FT-ICR MS (9.4 T magnet) has ultra-high resolution ($m/\Delta m_{50\%}$ >100,000, in which $\Delta m_{50\%}$ is mass spectral peak full width at half-maximum peak height) allowing separation of individual compounds, and mass accuracy < 1ppm allowing exact molecular formula assignments for each compound (Marshall et al., 1998). The molecular formulas were used to calculate the organic matter to organic carbon (OM:OC) ratio of each compound in the sample, to construct a van Krevelen diagram, and to analyze series of compounds related by regular elemental differences.

The OM:OC ratios of masses detected from *m/z* 245-800 ranged from 1.0-2.5 with an average ratio (arithmetic mean) of 2.0 (Figure 3-5) --comparable to the OM:OC ratio of the precursor methylglyoxal (2.0), and lower than that of the organic acid monomer products (2.3-3.8) in the proposed reaction scheme (Figure 3-1, solid arrows). OM:OC is primarily driven by the oxygen content of the compound (Pang et al., 2006); therefore, we expect the oligomers to be less hygroscopic than the organic acid monomers. The ratios for the compounds in this simulated cloud water sample are consistent with bulk ratios reported in aged atmospheric aerosols (Kiss et al., 2002;El-Zanan et al., 2005) and similar to several classes of atmospherically relevant aerosol species including aliphatic dicarboxylic acids, ketocarboxylic acids, polyols (Turpin and Lim, 2001), and smog chamber generated oligomers (Kalberer et al., 2004). These similarities at the bulk level suggest that the oligomers formed in this study are similar to oligomers formed through cloud processing and aerosol phase reactions in the atmosphere.

The ultra-high resolution of FT-ICR MS allows a further level of analysis than bulk ratios because the elemental composition, and thus OM:OC, may be calculated for *each compound*. The elemental ratios were used to construct a van Krevelen plot (Wu et

al., 2004), in which the hydrogen to carbon (H:C) ratio is plotted as a function of the oxygen to carbon (O:C) ratio (Figure 3-6). The average (arithmetic mean) O:C ratio was 0.69 and the average H:C ratio was 1.10 which is slightly higher than the average O:C ratios (0.4-0.6) and slightly lower than average H:C ratios (1.4-1.7) reported for particle phase oligomers formed in smog chamber experiments of α-pinene ozonolysis (Reinhardt et al., 2007). The average H:C (1.1) of the oligomers formed in these experiments is lower than the H:C of the precursor methylglyoxal (1.3) indicating that oxidation reactions occurred.

3.4.5 Oligomer Series

The van Krevelen plot serves to identify a set of compounds related by regular mass differences. There are nine series that converge on a particular point in the van Krevelen diagram (Table 3-1, Figure 3-6, Appendix B4). This convergence point has an O:C of 0.66 and an H:C of 1.3. The difference in mass between compounds in any given series is 72.02113 which is the exact mass of a subunit ($C_3H_4O_2$) (determined by the Midas Formula Calculator Software v1.1) that repeatedly adds to the parent organic acid monomer in each of the nine series and has an O:C of 0.66 and an H:C of 1.33.

There are sixty-five measured compounds in the nine series. Each of the nine series (Table 3-1, Appendix B4) consists of a parent peak (e.g., oxalic acid), and then the following *m/z* value represents the addition of $C_3H_4O_2$ (5-8 times) resulting in an increase in molecular weight, total oxygen content and double bond equivalents (DBE). The linear increase in DBE with each additional compound is consistent with the addition of one ring or double bond (Pellegrin, 1983;McLafferty, 1993). Because of the consistency in detected masses between the ESI-MS and FT-ICR MS, elemental compositions

assigned to compounds of *m/z* > 300 in the nine series detected were extended to ions detected by ESI-MS for ions of *m/z* < 300. The molecular formula assignments were extended for the series by subtracting $C_3H_4O_2$ and verifying the presence of ions of the corresponding *m/z* in the ESI-MS spectra.

The compounds in the nine series identified (Table 3-1, Figure 3-6, Appendix B4) account for 71% of the total ion abundance in the 69 minute ESI-MS negative ion sample spectrum. In seven of the series the parent compound has been identified as an organic acid monomer (Table 3-2). Four of the series begin with organic acids included in the reaction scheme used by Lim (Lim et al., 2005) and verified by HPLC (Carlton, 2006). These are pyruvic acid (*m/z* 87), glyoxylic acid (*m/z* 73), oxalic acid (*m/z* 89), acetic acid (Figure 3-1 solid arrows, Table 3-2). In the series that begins with *m/z* 131 ($C_5H_7O_4$) the subtraction of one subunit ($C_3H_4O_2$) leaves a compound consistent with acetic acid as the parent compound ($C_2H_3O_2$). To verify the structure of *m/z* 131 the ESI-MS-MS was used to isolate and fragment the ion. The ESI-MS-MS of *m/z* 131 produces fragments consistent with carboxylic acid (-44, -62, -18) and a fragment (-72) consistent with the loss of one subunit ($C_3H_4O_2$, 72 Da) leaving acetic acid as the parent molecule (Appendix B3).

Additional organic acid monomers (Figure 3-1, dashed arrows) were not included in the mechanism modeled by Lim (Lim et al., 2005). One series begins with glycolic acid (*m/z* 75; Table 3-2), a proposed intermediate in the hydroxyl radical oxidation of acetic acid to oxalic acid (Stefan et al., 1996). Another series begins with succinic acid (*m/z* 117 in Figure 3-2, Table 3-2), which was experimentally demonstrated to form from

acetyl radical recombination in a pulse radiolysis study of acetic acid-hydroxyl radical reactions (Wang et al., 2001).

In addition to oxalic acid, there are three parent monomers (*m/z* 103, 133, 177; Table 3-2) that persist until the last time series sample (Figure 3-2). We propose that the compound at *m/z* 133 $C_4H_6O_5$ (Table 3-2, Figure 3-2) is malic acid (MW 134), which we suggest is formed from the reaction of succinic acid and hydroxyl radical (Figure 3-7). Multiple compounds are consistent with *m/z* 103 (Figure 3-2) and an elemental composition $C_3H_4O_4$ (Table 3-2) (e.g., hydroxypyruvate, malonic acid, 2-hydroxy-3-oxopropanoate). Hydroxypyruvate has been hypothesized to form through the hydroxyl radical oxidation of pyruvic acid (Stefan and Bolton, 1999), but was not experimentally verified. ESI-MS-MS was used to isolate and fragment *m/z* 103 in order to assign a structure. However, the fragmentation pattern of *m/z* 103 in the ESI-MS-MS does not allow an exact structural assignment because the main loss is -44 (CO_2) (McLafferty, 1993) which is consistent with the carboxylic acid functionality of hydroxypyruvate, malonic acid, and 2-hydroxy-3-oxopropanoate. Two potential compounds could correspond to *m/z* 177, $C_6H_{10}O_6$, and $C_5H_6O_7$. The second is consistent with an oxalic acid-pyruvic acid dimer. Evidence for the formation of an oxalic acid-pyruvic acid dimer was presented previously (Altieri et al., 2006). ESI-MS-MS was used to isolate and fragment *m/z* 177 and the loss of fragments consistent with pyruvic and oxalic acids (-88, -90) supports the hypothesis that one of the compounds is an oxalic and pyruvic acid dimer.

3.4.6 Oligomerization Mechanism

We propose acid catalyzed esterification involving the addition of a hydroxy acid $C_3H_6O_3$ to each organic acid monomer parent (Figure 3-8). The hydroxy acid could be lactic acid, an α-hydroxy acid, or hydracrylic acid, a β-hydroxy acid. The addition of lactic acid to the standard mix did not cause an oligomer system to develop, which supports our previous assertion that the oligomers are not artifacts of the electrospray process. The addition of the hydroxy acid through esterification (5-8 times) results in the addition of $C_3H_4O_2$ to each parent molecule, increasing the molecular weight by 72.0213 and the DBE by one, resulting in the series of oligoesters (Table 3-1, Appendix B4) described above. Oligomerization might be limited to the addition of 5-8 subunits in the reaction vessel because precursors are not continuously supplied. However, the average molecular weight of HULIS in atmospheric aerosols is 200-300 Da suggesting atmospheric oligomer formation does not proceed further (Graber and Rudich, 2006).

The repeated addition of hydroxy acid through esterification is supported by the ESI-MS-MS fragmentation patterns of the oligomers in the series. The oligomers' fragmentation patterns result in losses of -72 and -88 from the first subunit fragmentation and losses of -144 and -160 consistent with the loss of the second subunit (e.g., *m/z* 231, Figure 3-9). Those products are consistent with cleavage of the ester bond on both sides (McLafferty, 1993). Structural information was obtained for 54 of the compounds in the oligomer series by isolating and fragmenting the ion by ESI-MS-MS. Of the 54 ions targeted for fragmentation, 50 had fragments consistent with the loss of one subunit (-72, -88), and 28 also had fragments consistent with the loss of the second subunit (-144, -160).

The formation of the hydroxy acid initiates esterification reactions. The difference in structure between lactic acid and hydracrylic acid is the positioning of the hydroxy group on the carbon α or β to the carboxylic acid functionality. We do not have a proposed pathway for lactic acid formation in these experiments. However, we do propose a mechanism in which the formation of hydracrylic acid, the β-hydroxy acid, is possible from the reaction of succinic acid with hydroxyl radical (Figure 3-7). The proposed mechanism is analogous to the reactions of carboxylic acids and hydroxyl radicals described by Stefan and Bolton (1996, 1999). Briefly, the degradation of succinic acid proceeds by a hydrogen abstraction and subsequent peroxyl radical formation through the addition of molecular oxygen (Alfassi, 1997). The second step involves the formation of a tetroxide which can undergo multiple degradation reactions including disproportionation to malic acid, and fragmentation to a radical species (Stefan and Bolton 1996). The radical undergoes disproportionation in the solvent cage to yield hydracrylic acid (Stefan and Bolton 1996, 1999 and references therein).

3.5 Conclusions and Implications

The formation of oxalic acid and higher molecular weight oligomer products from methylglyoxal photooxidation has been confirmed. This work adds to the growing body of literature (Altieri et al., 2006;Carlton et al., 2006;Warneck, 2003;Carlton et al., 2007;Yu et al., 2005;Crahan et al., 2004) supporting the hypothesis that cloud processing is a significant source of oxalic acid, the most abundant dicarboxylic acid in the atmosphere. Organic acids (especially oxalic, pyruvic, and succinic acids (Saxena and Hildemann, 1996)) and the low volatility oligomer products will contribute to SOA upon cloud droplet evaporation. The varied and multiple sources of methylglyoxal increase the

potential for this pathway to contribute significantly to SOA through cloud processing. The OM:OC ratios of the oligomers are comparable to aged atmospheric aerosols, and lower than those of prevalent organic acids suggesting that the oligomers are less hygroscopic than the organic acids and consistent with the growing belief that oligomers are a large contributor to aged organic aerosol mass.

Organic acid monomers form from aqueous reactions with hydroxyl radical. We propose that the oligomerization of these organic acid monomers proceeds through esterification with an α or β-hydroxy acid. This mechanism is supported by the high resolution elemental composition data and the ESI-MS-MS fragmentation data. The esterification causes the regular addition of $C_3H_4O_2$ to the organic acid monomers resulting in series of oligoesters related by regular differences in elemental composition and mass. The esterification mechanism proposed in this work is similar to mechanisms proposed for oligomers formed in the aerosol phase (Gao et al., 2004;Surratt et al., 2007;Surratt et al., 2006), which have been reported to be thermodynamically favorable (Barsanti and Pankow, 2006). In both aerosol phase and cloud processing reactions (aqueous phase), the oligomers formed are less hygroscopic and less volatile than the low molecular weight compounds that lead to their formation. Multiple precursor organics lead to oligomer products through similar mechanisms in both aerosol phase reactions (e.g., isoprene, α-pinene, trimethylbenzene) and cloud processing reactions (e.g., methylglyoxal, pyruvic acid). The similarities in properties and formation mechanisms of oligomers may help to explain the large quantity of oligomers found in atmospheric particles.

Table 3-1 Example Series of Oligomers
Two examples of series of compounds starting with the parent organic acid and differing in mass by 72.02113, which is equivalent to $C_3H_4O_2$, are grouped to show the regular increase in mass, DBE, and elemental composition within the series. The series of formulas starting with oxalic acid (*m/z* 89) and *m/z* 177 are distinguished by the labels numeral (1-9), and letter (a-h), respectively, here and in Figure 3-3.

Label	m/z (Measured)	Formula $[M-H]^-$	DBE[a]	Mass Error (ppm)
1	89	$C_2H_1O_4$	2	--
2	161	$C_5H_5O_6$	3	--
3	233	$C_8H_9O_8$	4	--
4	305.05163	$C_{11}H_{13}O_{10}$	5	0.7
5	377.07274	$C_{14}H_{17}O_{12}$	6	0.5
6	449.09398	$C_{17}H_{21}O_{14}$	7	0.7
7	521.11503	$C_{20}H_{25}O_{16}$	8	0.4
8	593.13631	$C_{23}H_{29}O_{18}$	9	0.6
a	177	$C_6H_9O_6$	2	--
b	249.06175	$C_9H_{13}O_8$	3	0.6
c	321.08295	$C_{12}H_{17}O_{10}$	4	0.7
d	393.10417	$C_{15}H_{21}O_{12}$	5	0.8
e	465.12534	$C_{18}H_{25}O_{14}$	6	0.8
f	537.14629	$C_{21}H_{29}O_{16}$	7	0.3
g	609.16781	$C_{24}H_{33}O_{18}$	8	0.9

-- indicates the mass was detected using the ESI-MS and the elemental formula was assigned based on the "subunit" series
[a] Double bond equivalents (number of rings plus double bonds) for neutral compound

Table 3-2 Parent Organic Acids
Parent organic acids formed through methylglyoxal-hydroxyl radical reaction. These organic acids then undergo oligomerization reactions with a hydroxy acid forming series of oligoesters (example series in Table 3-1, full series in Appendix B4). Oxalic acid (*m/z* 89) and *m/z* 177 are distinguished by the labels numeral (1-9), letter (a-h), respectively, here and in Figure 3-3.

Label	m/z (Measured)	Formula $[M-H]^-$	DBE[a]
1	89	$C_2H_1O_4$	2
a	177	$C_6H_9O_6$	2
nl	73	$C_2H_1O_3$	2
nl	87	$C_3H_3O_3$	2
nl	75	$C_2H_3O_3$	1
nl	103	$C_3H_3O_4$	2
nl	117	$C_4H_5O_4$	2
nl	133	$C_4H_5O_5$	2
nl	131	$C_5H_7O_4$	2

[a]Double bond equivalents (number of rings plus double bonds) for neutral compound

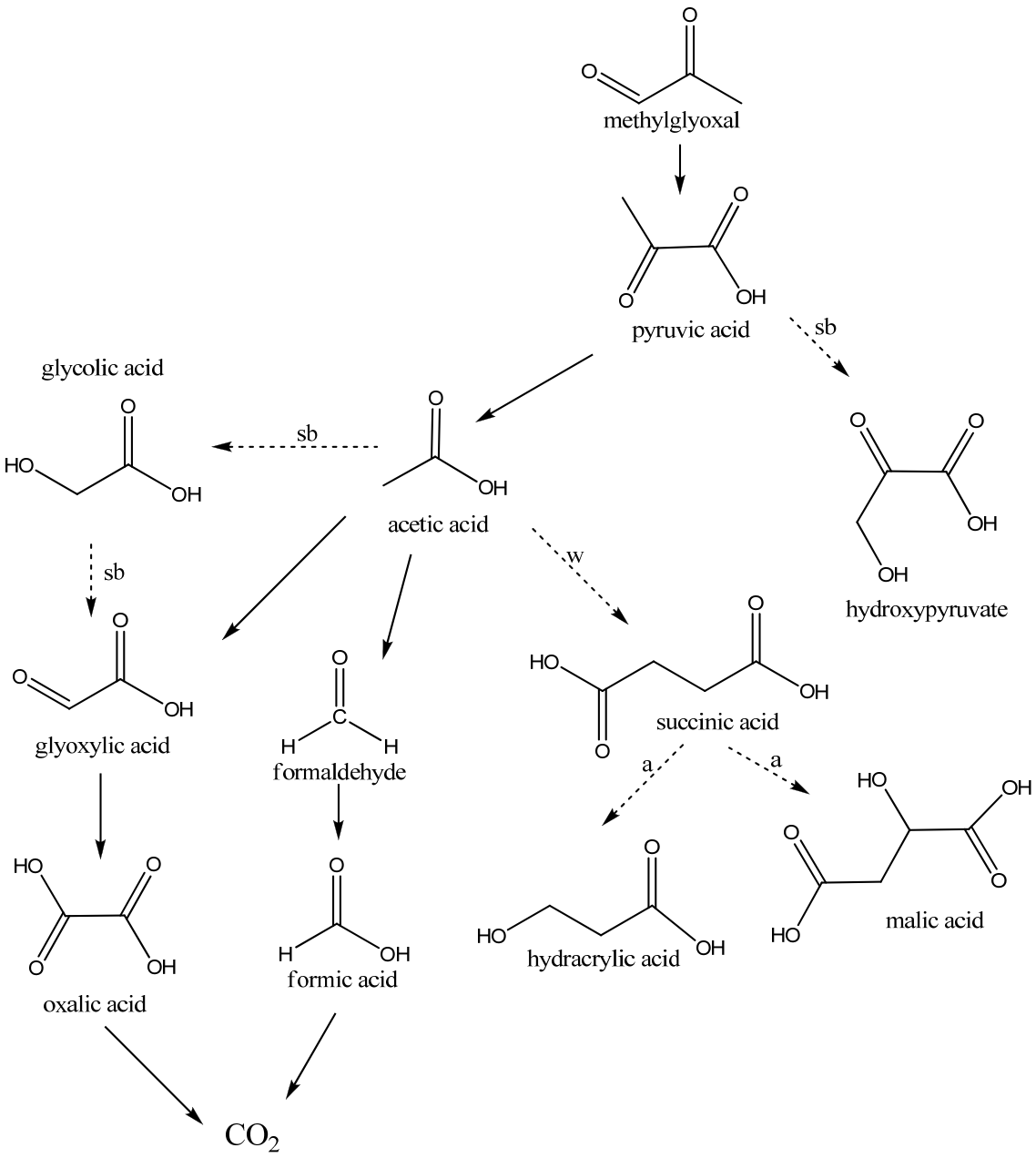

Figure 3-1 Mechanism of Methylglyoxal Photooxidation
Proposed mechanism of aqueous phase photooxidation of methylglyoxal and hydroxyl radical leading to organic acid monomers that then participate in oligomerization reactions. The dotted line labeled "a" is original to this work. The solid arrows represent the mechanism used by Lim et al. (2005) originally from Stefan et al. (1996) and Stefan and Bolton (1999) whereas the dashed lines labeled "sb" indicate reactions taken from Stefan et al. (1996) and Stefan and Bolton (1999) that were not outlined in Lim et al. (2005). The dashed line labeled "w" is a reaction taken from Wang et al. (2001). All reactions proceed via the hydroxyl radical.

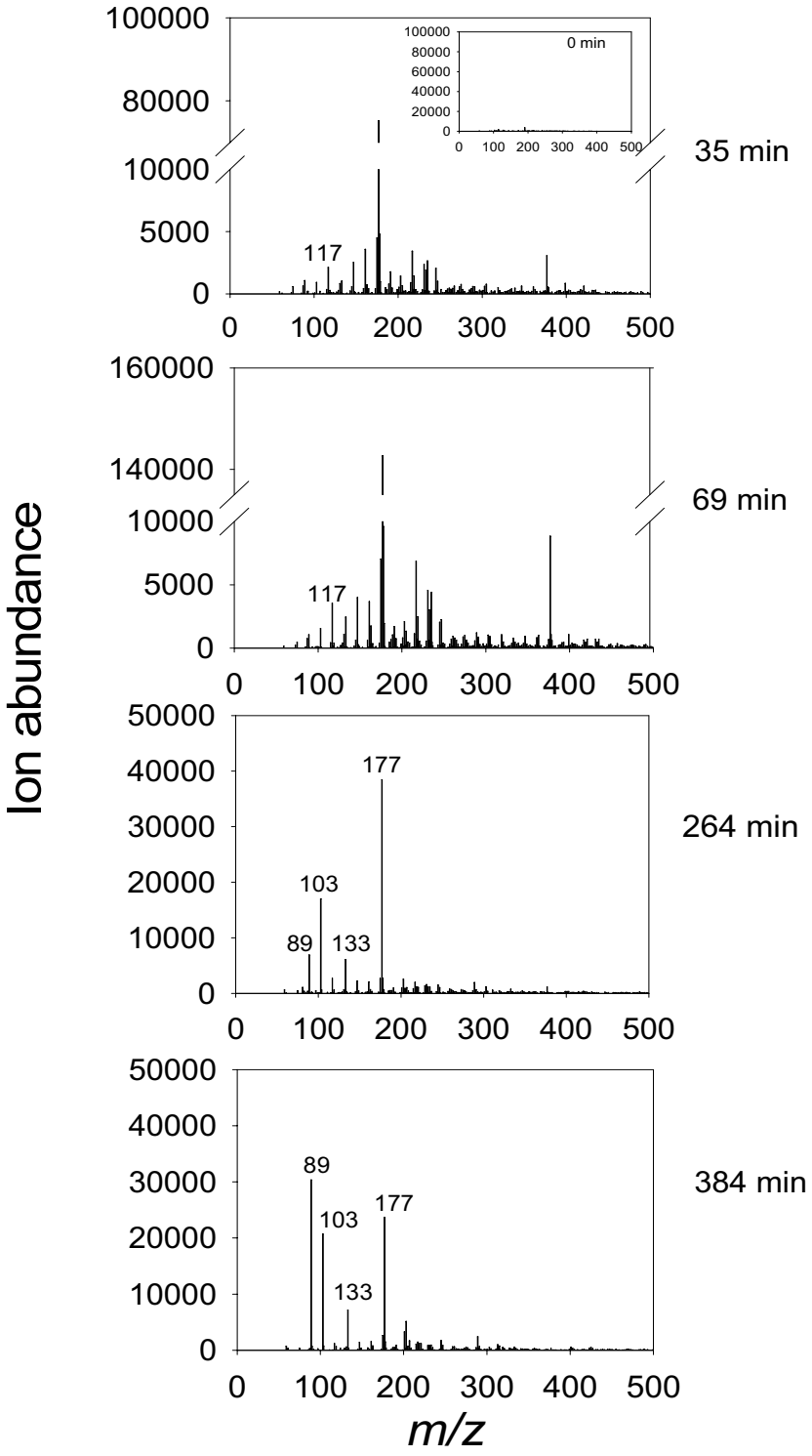

Figure 3-2 Time Series Samples of Methylglyoxal Photooxidation
ESI-MS negative ion spectra from methylglyoxal + OH radical oxidation experimental samples. Note the different y-axis scale. Inset is t=0 min sample.

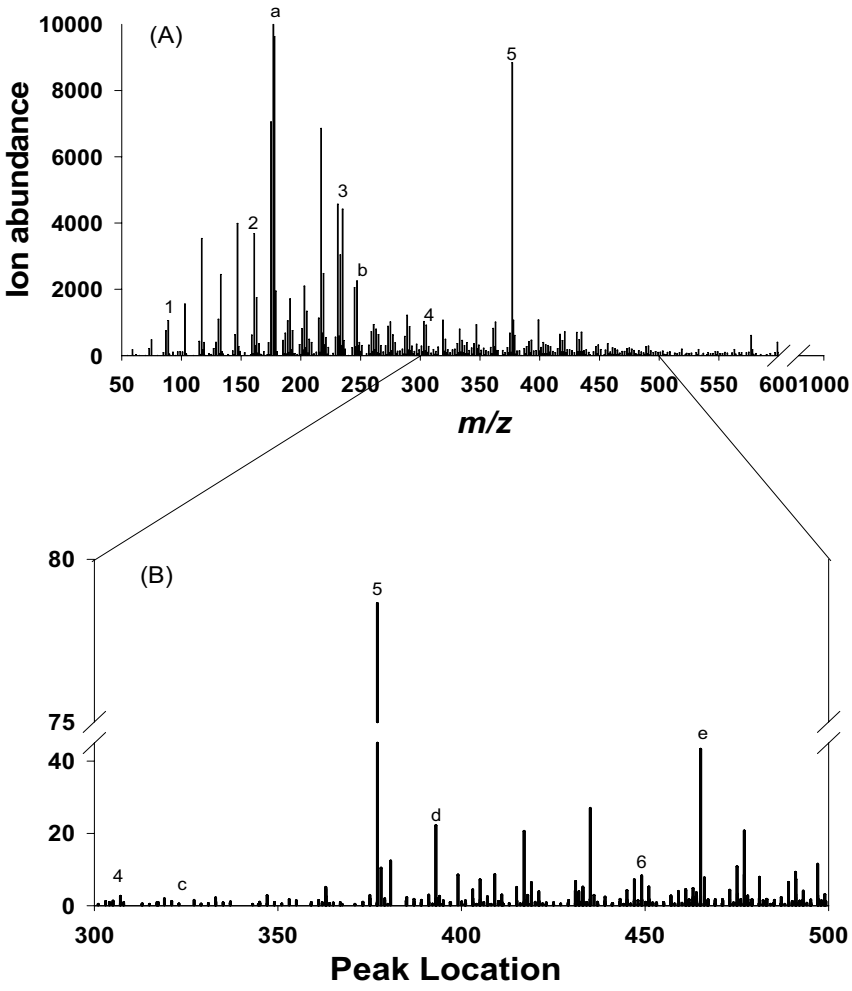

Figure 3-3 Comparison of Methylglyoxal Samples in ESI-MS and FT-ICR MS
The pattern of high molecular weight products from the methylglyoxal + OH radical oxidation experiment (t=69 min) analyzed by negative ion (A) ESI-MS and (B) ultra-high resolution FT-ICR MS. The ESI-MS spectrum of a mixed standard of the predicted reaction components (methylglyoxal, pyruvic acid (*m/z* 87), glyoxylic acid (*m/z* 73), oxalic acid (*m/z* 89), and acetic acid; Figure 3-4) is simple compared to the complex spectra from the photooxidation experimental samples. The labels 1-8 and a-e refer to the labeled compounds in Table 3-1. In (A) the ion abundance of *m/z* 177 (a), and in (B) the ion abundance of *m/z* 377 (5) are off scale.

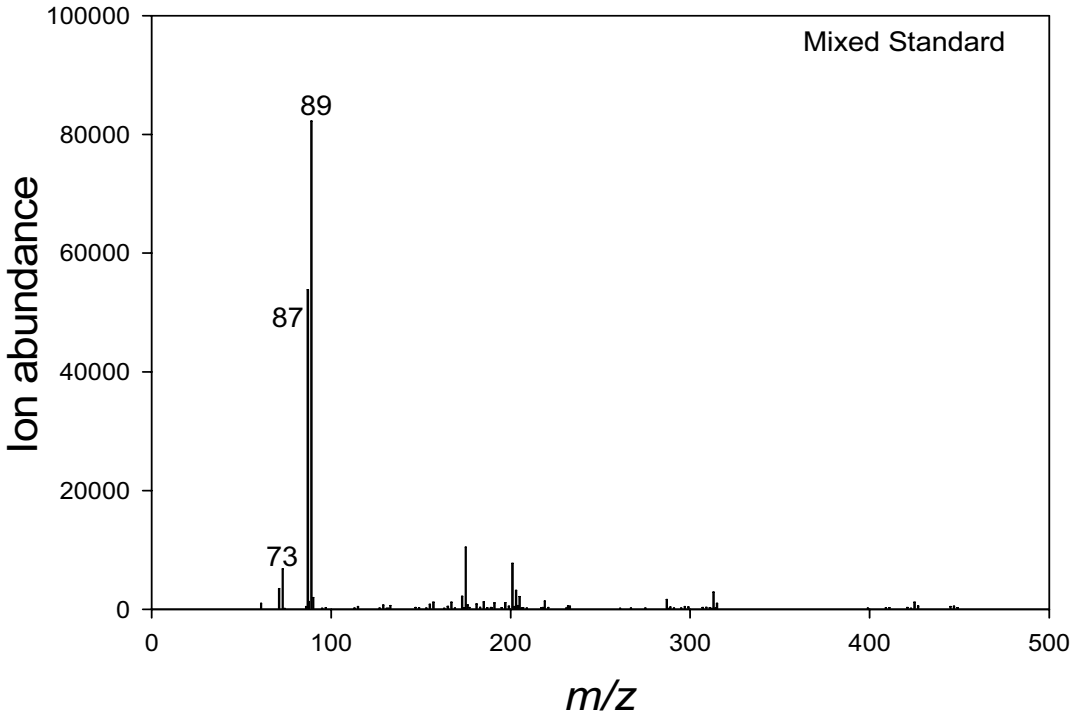

Figure 3-4 Methylglyoxal Mixed Standard in Negative Mode ESI-MS
ESI-MS negative ion spectrum of 0.5 mM (per compound) mixed standard of methylglyoxal (detected as positive ion), oxalic acid (*m/z* 89), pyruvic acid (*m/z* 87), glyoxylic acid (*m/z* 73), and acetic acid (not detected) in the same matrix as samples (H_2O_2 1:5 ratio, 1 μL catalase). These are the precursor and expected products in the mechanism used by (Lim et al., 2005).

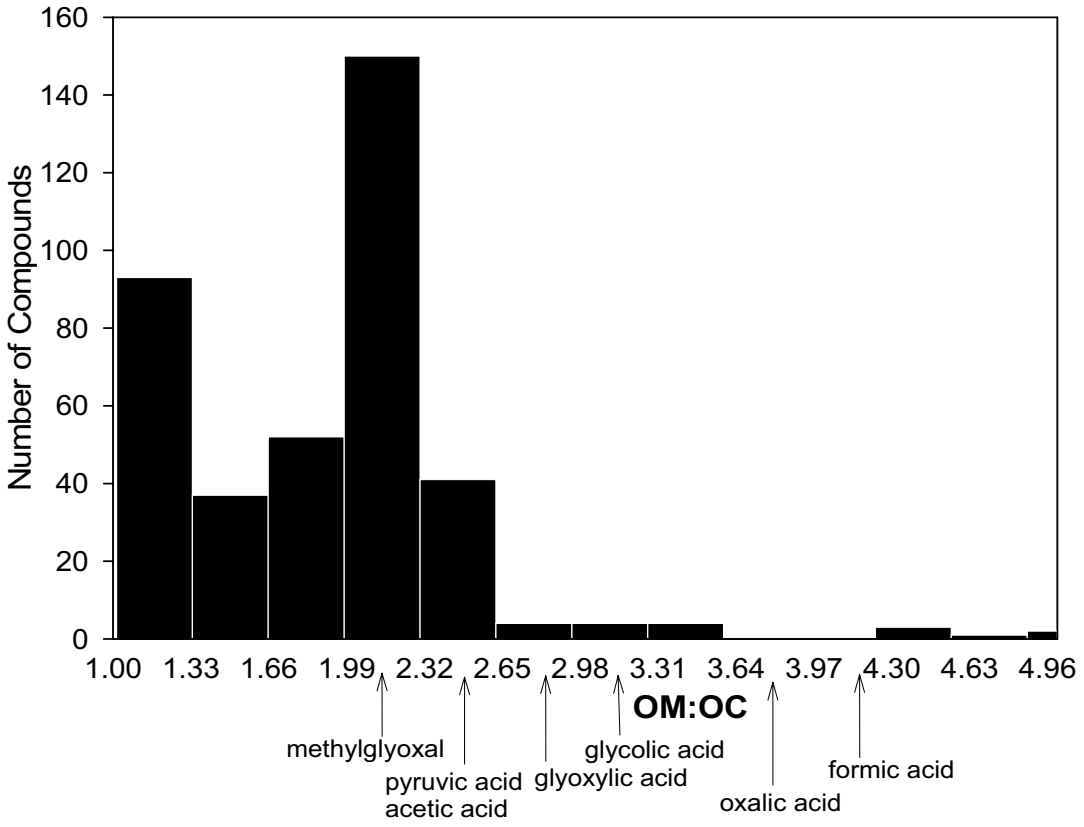

Figure 3-5 OM:OC Ratios of Oligomers and Organic Acids
Calculated OM:OC ratio (organic molecular weight per carbon weight) distribution for ions of each of the 415 *m/z*'s from the t=69 min methylglyoxal UV/H_2O_2 oxidation FT-ICR MS (*m/z* >300 only) negative ion spectrum. The OM:OC ratios of the precursor methylglyoxal and the predicted organic acid monomers (*m/z* < 300) are noted. Each y-value is the number of compounds that had an OM:OC ratio in the bin labeled on the x-axis.

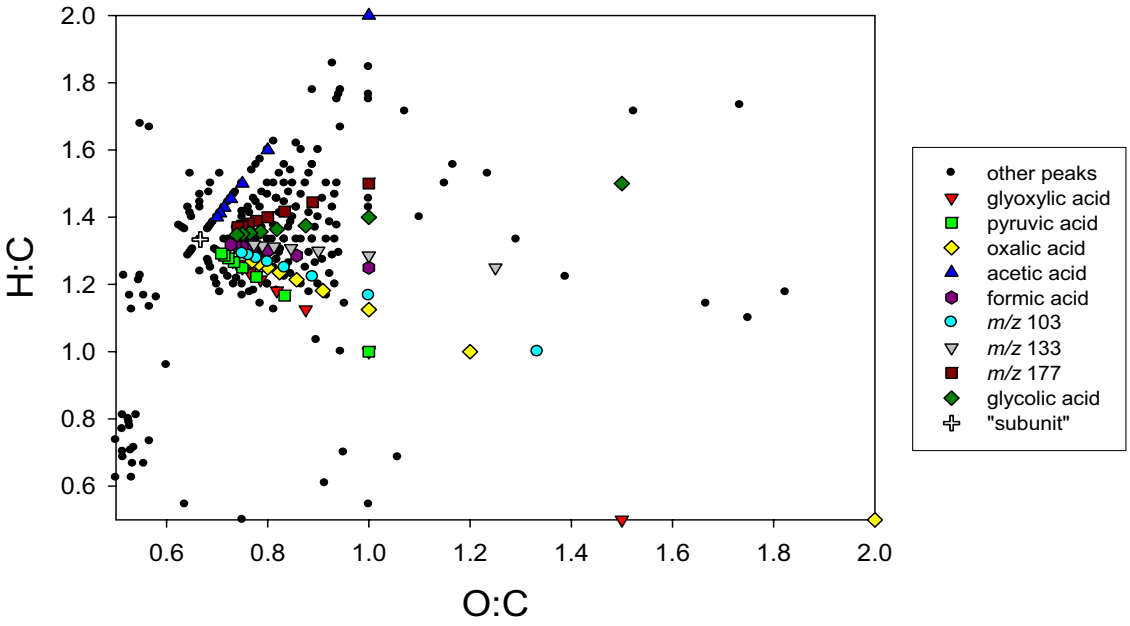

Figure 3-6 Methylglyoxal Time Series Sample van Krevelen
Van Krevelen plot for the methylglyoxal + OH radical oxidation experiment (t=69 min) FT-ICR MS negative ion data. All of the peaks with molecular formulas assigned (*m/z* > 300) are represented by black circles. Note that only compounds with O:C and H:C > 0.5 are visible. The nine oligomer series are denoted by different symbols labeled in the legend according to the parent compound of each series. The subunit is denoted by the white plus sign and is not a data point. The nine series include compounds detected by ESI-MS (*m/z* < 300) that were assigned an elemental composition based on the repeating pattern of subunit addition ($C_3H_4O_2$).

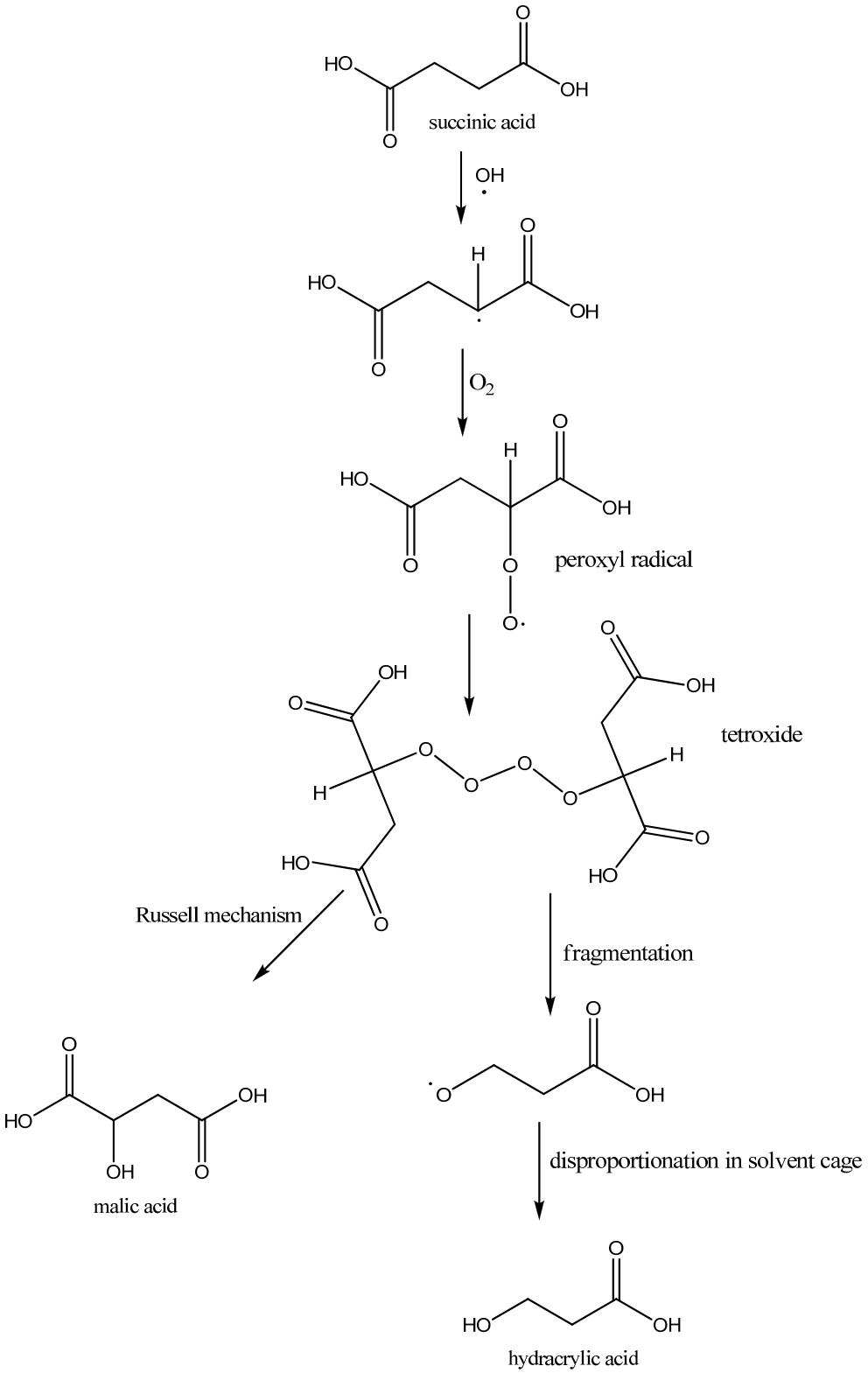

Figure 3-7 Mechanism of Succinic Acid Photooxidation
Proposed mechanism of hydracrylic acid and malic acid formation from succinic acid.

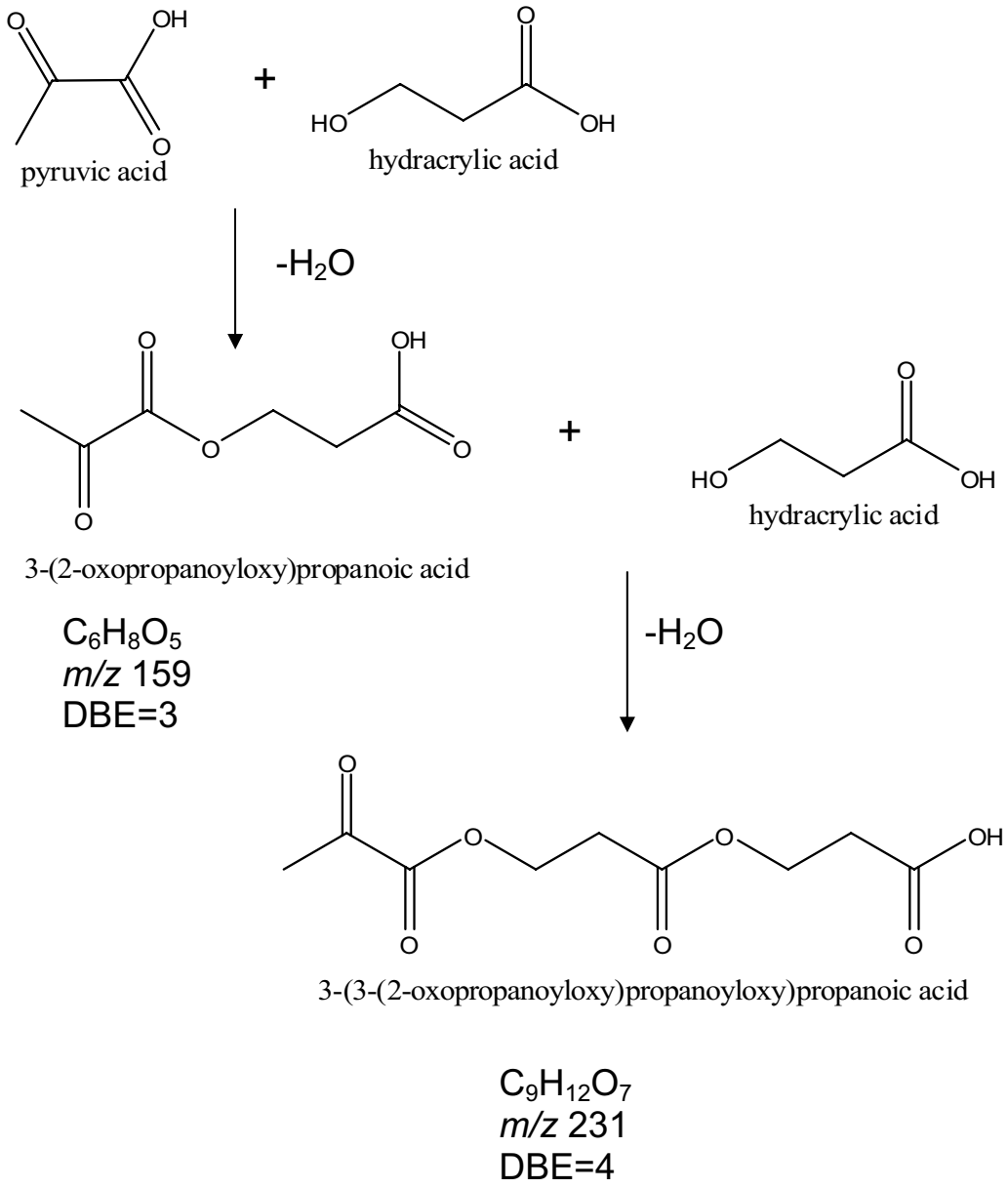

Figure 3-8 Mechanism of Aqueous Phase Oligomerization
Proposed non-radical esterification reactions that lead to oligomeric products. The loss of water at each step causes the higher molecular weight oligomers to have a lower OM:OC than the parent organic acid monomers. The repeating addition of hydracrylic acid creates the constant increase of $C_3H_4O_2$ in the series (Table 3-1, Appendix B4). The oligomer species were named using the ChemDraw Ultra 10.0 "structure to name" algorithm.

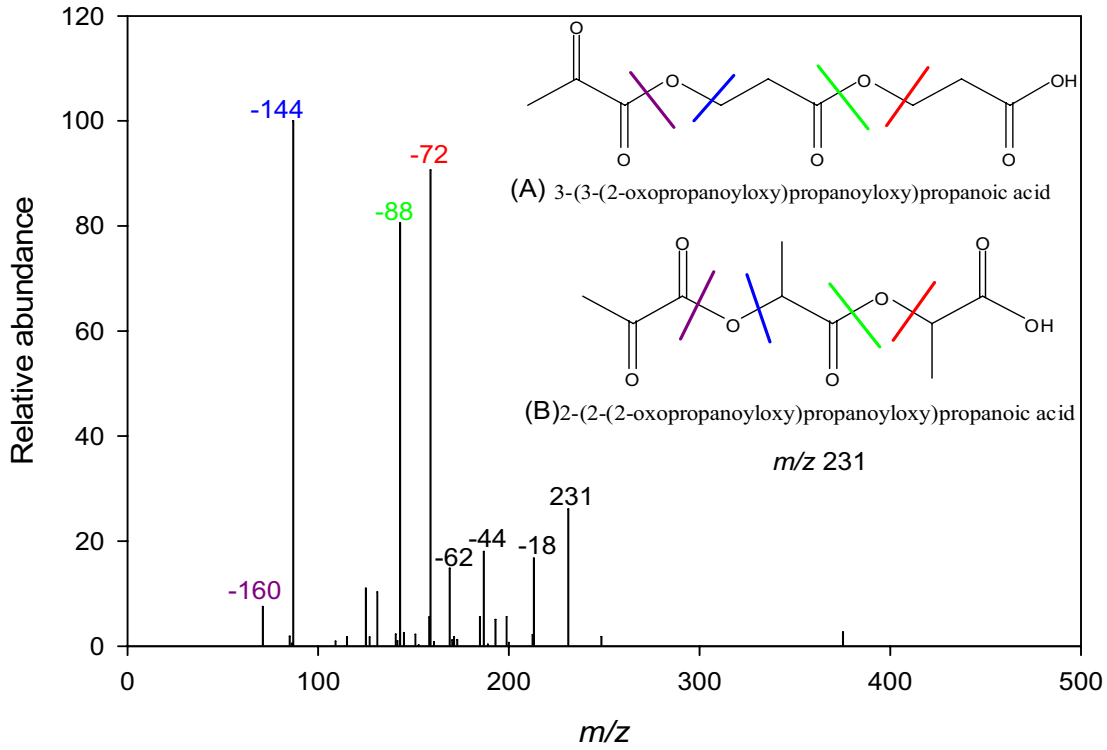

Figure 3-9 Ion Fragmentation Pattern of *m/z* 231
ESI-MS-MS (negative ion) of *m/z* 231 from t=129 minute methylglyoxal hydroxyl radical photooxidation experiments. The two hypothesized structures in the upper right hand corner are based on the esterification mechanism with (A) hydracrylic acid and (B) lactic acid, and the elemental composition assignments from the oligomer series (parent is pyruvic acid, (Table 3-2)). The colored lines on the structure indicate the bond that fragments to give ions of the *m/z* labeled (corresponding color) with the weight of the fragment lost.

Chapter 4. Oligomers, Organosulfates, and Nitrooxy Organosulfates in Rainwater Identified by Ultra-High Resolution Electrospray Ionization FT-ICR Mass Spectrometry

Material in this chapter has been published previously as:

Altieri, K.E., Turpin, B.J., Seitzinger, S.P., Oligomers, organosulfates, and nitrooxy organosulfates in rainwater identified by ultra-high resolution electrospray ionization FT-ICR mass spectrometry. *Atmospheric Chemistry and Physics*, 2009, vol. 9, 2533-2542

4.1 Abstract

Wet deposition is an important removal mechanism for atmospheric organic matter, and a potentially important input for receiving ecosystems, yet less than 50% of rainwater organic matter is considered chemically characterized. Precipitation samples collected in New Jersey, USA were analyzed by negative ion ultra-high resolution electrospray ionization Fourier transform ion cyclotron resonance mass spectrometry (FT-ICR MS). Elemental compositions of 552 unique molecular species were determined in the mass range 50-500 Da in the rainwater. Three main groups of organic compounds were identified: compounds containing carbon, hydrogen, and oxygen only (CHO), sulfur (S) containing CHOS compounds, and S- and nitrogen containing CHONS compounds. Organic acids commonly identified in precipitation were detected in the rainwater. Within the three main groups of compounds detected in the rainwater, oligomers, organosulfates, and nitrooxy-organosulfates were assigned based on elemental formula comparisons. The majority of the compounds identified are products of atmospheric reactions and are known contributors to secondary organic aerosol (SOA) formed from gas phase, aerosol phase, and in-cloud reactions in the atmosphere. It is

suggested that the large uncharacterized component of SOA is the main contributor to the large uncharacterized component of rainwater organic matter.

4.2 Introduction

Precipitation is an efficient removal mechanism for atmospheric organic matter which is a mixture of organic compounds that can influence climate, air quality, and ecosystem health. Dissolved organic carbon (DOC) is a ubiquitous component of rainwater and can be higher in concentration than inorganic species such as nitric and sulfuric acids (Willey et al., 2000). Organic acids contribute significantly to rainwater acidity in urban areas (Kawamura et al., 1996;Pena et al., 2002), and can be the main contributor to acidity (80-90%) in remote areas (Andreae et al., 1988). Thus, organic acids are frequently the focus of studies on rainwater DOC. However, the contribution of organic acids to total DOC ranges from only 14-36%, with other known compound classes (e.g., aldehydes, amino acids) contributing < 10% to the total DOC (Avery et al., 2006). Approximately 50% of rainwater dissolved organic matter (DOM) is considered uncharacterized at both the compound class and individual compound level (Willey et al., 2000). The complexity of rainwater DOM and the large percent considered uncharacterized has made it difficult to determine the role of rainwater DOM in regional and global carbon budgets (Raymond, 2005).

A large percentage of the uncharacterized rainwater DOM has been attributed to macromolecular organic matter like that found in atmospheric aerosols, fog water and cloud water (Zappoli et al., 1999;Krivacsy et al., 2000;Feng and Moller, 2004;Likens, 1983). Much of this macromolecular material has been termed humic like substances (HULIS) because of properties similar to terrestrial and aquatic humic and fulvic acids

(Graber and Rudich, 2006). It is largely unknown how the HULIS fraction of atmospheric organic matter may affect aerosol properties, including the ability to nucleate cloud droplets, and the ability to absorb light. The complexity of HULIS in atmospheric waters (aerosol water, rainwater, and cloud water) poses a significant analytical challenge, and thus the sources of HULIS to the atmosphere are not well understood. Possibilities include primary terrestrial and marine sources, biomass burning, and secondary organic aerosol (SOA) formation mechanisms such as oligomerization (Graber and Rudich, 2006).

Significant progress has been made in identifying the composition of complex DOM in organic aerosols. Advances have been made using mass spectrometric methods such as electrospray ionization mass spectrometry (ESI-MS), matrix assisted laser desorption/ionizaton mass spectrometry (MALDI-MS), and aerosol mass spectrometry (Kalberer et al., 2004;Tolocka et al., 2004;Iinuma et al., 2007;Gao et al., 2004a;Gao et al., 2004b;Gao et al., 2006;Liggio et al., 2005). The advances are possible because high resolution mass spectrometry allows assignments of elemental compositions to all compounds detected in a sample (Marshall, 1995, 1997). For example, Fourier transform ion cyclotron resonance mass spectrometry (FT-ICR MS) can have sub ppm accuracy and resolution > 100,000 (Senko et al., 1996). These advanced mass spectrometry techniques have allowed the identification of oligomers formed through smog chamber and cloud water experiments (Altieri et al., 2008;Gao et al., 2004a;Gao et al., 2004b;Gao et al., 2006;Kalberer et al., 2004), oligomers and fulvic acids in ambient aerosols (Reemtsma et al., 2006a;Reemtsma et al., 2006b), and organosulfates and nitrooxy organosulfates in smog chamber and ambient aerosols (Gomez-Gonzalez et al., 2008, Iinuma et al., 2007a,

Romero and Oehme, 2005, Surratt et al., 2007,2008). To our knowledge ultra-high resolution mass spectrometric techniques have not yet been applied to investigate the complex mixture of DOM in rainwater.

In this study ultra-high resolution electrospray ionization (ESI) FT-ICR MS is used to conduct a detailed analysis of the compound specific composition of precipitation in the mass range 50-500 Da collected in New Jersey, USA. Three main compound classes with both biogenic and anthropogenic sources were detected in the precipitation. Some compounds detected have distinct primary sources; however, the majority of these compounds are formed from secondary processes, and can be incorporated into rainwater either from cloud droplets directly, or from SOA formed through gas phase, aerosol phase, and in-cloud reactions.

4.3 Sample Collection and Analysis

4.3.1 Sample Collection

Rainwater was collected from two sites in the northeastern USA. The urban site Camden, NJ (Latitude 39° 56’ 57.45” N; Longitude 75° 7’ 16.60” W; elevation 11 m) is a city directly across the Delaware River from Philadelphia, PA and is in a heavily urbanized region. The rural site Pinelands, NJ is located 30 miles east of Camden in the Lebanon State Forest. Though the site is located in a forest it is impacted by urban airflow (Latitude 39° 56’43.61” N; Longitude 74° 37’1.52” W; elevation 1 m). Two samples were collected from the Camden, NJ site, one collected in spring and one collected in fall. One sample was collected from the Pinelands, NJ site in summer (Table 4-1). The samples were collected using wet-dry deposition collectors (Aerochem Metrics Model 301, Bushnell, FL). The rain collectors were fitted with stainless steel buckets and

opened only during wetfall events. The type of collector used and the placement of the collector at the site adhere to regulations outlined by the National Atmospheric Deposition Program (Bigelow et al., 2001). Samples were collected within 12 hours of each rain event to minimize microbial degradation of DOM and consumption of inorganic nutrients. Sample temperature and pH were measured immediately after collection and samples were filtered through pre-combusted glass fiber filters (Whatman GFF; baked for four hours at 500 °C; then rinsed with deionized water) ensuring analysis of the dissolved constituents only. Contamination due to field sampling and laboratory sample processing was minimal (field and filter blanks < 5% DOC). Rainwater was stored at -20 °C in polypropylene screw-capped tubes until analysis.

4.3.2 Chemical Analyses

Bulk inorganic nutrients (NO_3^- + NO_2^-, NH_4^+, PO_4^{3-}) were measured on the three rain samples with an automated nutrient analyzer and standard colorimetric methods (Lachat, Inc). DOC was measured by high-temperature catalytic oxidation with a Shimadzu Total Organic Carbon (TOC) 5000A analyzer (Sharp et al., 1993). Dissolved organic nitrogen was determined as the difference between total dissolved nitrogen measured with an Antek 7000 TN Analyzer (Seitzinger and Sanders, 1999) and dissolved inorganic nitrogen (NO_3^- + NO_2^-, and NH_4^+). Calibrations were performed using potassium hydrogen phthalate standards for DOC and urea and nitrate standards for TDN.

4.3.3 Ultra-High Resolution Electrospray Ionization FT-ICR MS

Analyses were performed on the three rainwater samples with a 7-T Fourier transform ion cyclotron resonance mass spectrometer equipped with an ESI source (FT-ICR MS) and operated in the negative ion mode. The sample was diluted with methanol

50:50 v/v immediately before injection to limit solvent interaction. The sample was introduced into the ESI source by direct infusion with a flow rate of 5 μL min^{-1}. The needle voltage was 3.02 kV, the capillary voltage was -9.44 V, the capillary temperature was 260 °C, and the tube lens was -57 V. The spectra were mass calibrated with standard ions using an external calibrant (G2421A Agilent "tuning mix") and the residual root mean square error after calibration was 1.1-1.6 ppm. The mass lists were processed and exported using Xcalibur v 2.0 SR2 (ThermoFisher Scientific).

Midas Formula Calculator Software (v1.1) was used to calculate all mathematically possible formulas for all ions with a signal to noise ratio ≥ 10 using a mass tolerance of ±1 ppm. An unlimited number of ^{12}C and ^{1}H, up to fifteen ^{14}N and ^{16}O, and one of each ^{32}S and ^{31}P were allowed in the molecular formula calculations. The average mass error for all assignments was 0.3 ppm. Boundary values for molecular elemental ratios were applied as a filtering tool (Koch et al., 2005). The O:C, H:C, and N:C ratios were limited to < 5, ≥ 0.3, and < 2 respectively. Ions were also characterized by the number of rings plus double bonds (i.e., double bond equivalents (DBE)), calculated from equation 4-1 (McLafferty, 1993):

$$DBE = c - \frac{1}{2}h + \frac{1}{2}(n + p) + 1 \qquad \text{for elemental composition, } C_cH_hO_oN_nP_pS_s \quad (4\text{-}1)$$

4.4 Sample Comparison

Though the three rainwater samples analyzed were from different locations and seasons, the storm trajectories and bulk properties of the samples are similar (Table 4-1) and fall within the ranges reported for continental precipitation (Seitzinger et al., 2003;Willey et al., 2000). The composition of the DOM in all three samples was also very similar, as discussed below. In the Camden spring sample, there were 161 masses

detected in the mass range of $^{-}m/z$ 50-300. However, only 13% of them were unique to that sample, i.e., 87% of the masses detected appeared in one or both of the other samples. Though the Pinelands sample was analyzed over a slightly smaller mass range ($^{-}m/z$ 50-400) than the fall Camden sample ($^{-}m/z$ 50-500), the samples are similar in the total number of masses detected, 388 and 383, respectively. Of the 388 masses detected in the Pinelands sample, 64% were detected in one of the other two samples (i.e., 36% are unique). For the fall Camden sample, 84% of the masses were detected in one of the other two samples (i.e., 16% are unique).

The masses detected fall into three main compound classes: carbon, hydrogen and oxygen only (CHO), sulfur (S) containing CHOS compounds, and S- and nitrogen (N) containing CHONS compounds. The number of compounds in each compound class was very similar in both the Camden fall and Pinelands summer samples (Figure 4-1). Approximately 50% of the compounds in the negative ion mode are composed only of CHO. Approximately 25-30% of the compounds are composed of CHOS, and ~ 5% are composed of CHONS. The remaining 10-25% of the elemental formulas includes CHON compounds and compounds with phosphorous (P) in the elemental formula; those compounds will be discussed in a later chapter. This analysis is based solely on negative ion FT-ICR MS, and as such focuses only on compounds that can be detected in the negative ion mode (e.g., carboxylic acids). It should be noted that for each elemental composition assigned based on the measured mass, multiple structural isomers are possible, and thus the reported total number of compounds is likely an underestimate. The van Krevelen diagrams, which plot the hydrogen to carbon (H:C) ratio as a function of the oxygen to carbon (O:C) ratio for each compound, can be used to display

compositional characteristics and to compare the elemental ratios of each compound in a sample (Wu et al., 2004). As evident in the van Krevelen diagrams, the elemental ratios of the compounds in each group (i.e., CHO, CHOS, CHONS) are also similar in both the Camden and Pinelands samples (Figure 4-2).

In the analysis that follows (e.g., Figure 4-3, Table 4-2), we have combined the elemental formulas for each of the three samples due to the high percentage of overlap in the types of elemental formulas (i.e., compound class; Figure 4-1) the similarities in number and type of elemental formulas (Figure 4-2), and the small number of samples. Thus we will consider this combined data representative of a precipitation sample collected from an urban impacted (i.e., downwind of a major city) location in New Jersey, USA.

4.5 Organic Acids and Oligomers

Eight organic acids identified in the rainwater based on their elemental formulas have been previously detected in precipitation samples: glyoxylic, glycolic, pyruvic, oxalic, lactic, malonic, and succinic acids (Kieber et al., 2002). Formic acid is commonly detected in precipitation, but has a molecular weight less than the lower mass detection limit of the FT-ICR MS *m/z* 50; therefore, although it is likely present in the samples, it is not detectable.

The potential sources of these eight organic acids include primary anthropogenic and biogenic emissions, as well as secondary formation from biogenic and anthropogenic precursors in the atmosphere (Kawamura et al., 2001, 2003; Sorooshian et al., 2007). Though there are primary emissions of organic acids, atmospheric aqueous phase reactions in clouds and aerosols have been hypothesized to be the predominant formation

pathway of these organic acids (Blando and Turpin, 2000). Similarly, the atmospheric concentrations of these organic acids can only be supported by a substantial secondary formation mechanism (Sorooshian et al., 2007). Thus, the organic acids detected in the rainwater are likely predominantly from secondary atmospheric processes and incorporated during in-cloud or below-cloud scavenging.

In addition to the eight identified organic acids, there were an additional 254 CHO compounds detected, representing 48% of the total compounds in the mass range 50-500 Da. The average (arithmetic mean) organic molecular weight to organic carbon weight (OM:OC) ratio for the CHO compounds in the mass range 50-500 Da was 2.1 ± 0.7, the average H:C and O:C ratios were 1.5 ± 0.4 and 0.7 ± 0.5, respectively (Table 4-2). The elemental ratios for the CHO compounds are lower than the ratios of measured atmospheric organic acids (OM:OC 2.5-3.8), and are more consistent with measured ratios for smog chamber generated oligomers, oligomers formed through cloud processing, aged atmospheric aerosol, and HULIS, all contributors to SOA (El-Zanan et al., 2005;Kiss et al., 2002;Kalberer et al., 2004;Altieri et al., 2008;Polidori et al., 2008).

The elemental formulas of the CHO compounds in the rainwater were compared to the elemental formulas of oligomers known to form through cloud processing reactions of methylglyoxal (Altieri et al., 2008); methylglyoxal is a water soluble compound with both biogenic and anthropogenic sources. The organic acids known to form through cloud processing of methylglyoxal were all detected in the rainwater, i.e., glyoxylic, glycolic, pyruvic, oxalic, succinic, malonic, and malic acids (Table 4-3). The methylglyoxal aqueous oligomerization scheme involves acid- or radical- catalyzed esterification of the organic acids with a hydroxy acid, e.g., lactic acid, leading to series

of oligomers related by regular mass differences of 72.02113 Da ($\Delta C_3H_4O_2$; Altieri et al., 2008). All nine oligomer series present in the methylglyoxal cloud processing scheme were detected in the rainwater based on elemental formula comparisons (Table 4-3). For each organic acid detected, compounds containing elemental formulas consistent with the addition of one and two hydroxy acids through esterification were detected. For example, moving from left to right in Table 4-3, glyoxylic acid ($C_2H_1O_3$), glyoxylic acid plus one addition of hydroxy acid through esterification ($C_5H_5O_5$), and glyoxylic acid plus two additions of hydroxy acid through esterification ($C_8H_9O_7$) were all detected. In addition to the elemental formulas being consistent with methylglyoxal oligomers, some of these elemental formulas are also consistent with compounds formed from photooxidation of other biogenic precursors such as α–pinene oxidation leading to hydroxy glutaric acids (Claeys et al., 2007), highlighting that multiple structural isomers of each elemental formula are possible. Without further liquid chromatography or MS-MS analysis, it is not possible to discern the exact structure of these higher molecular weight compounds. Compounds with the same elemental formulas and patterns as reported here in the rainwater were also detected in the high molecular weight fraction (≥ *m/z* 223) of aerosol derived water soluble organic carbon (Wozniak et al., 2008).

There are CHO compounds detected in the rainwater sample that are not part of the methylglyoxal oligomer series, but also have regular mass differences indicative of oligomers and/or HULIS (Figures 4-3, 4-4). In addition to the van Krevelen (Figure 4-3), another way to visualize compounds related by regular mass differences is an island plot (Reemtsma et al., 2006a), which plots the number of carbon atoms of each molecule against the molecular weight of the molecule. When the sum of the number of carbons

and oxygens for a set of compounds is the same, those compounds group as “islands” in the plot (denoted by different markers; Figure 4-4). There were 19 islands detected in the mass range 50-500 Da for the compounds containing only CHO, and the sum of carbon and oxygen ranged from 4-23.

In each island the elemental composition changes in a systematic way from one molecule to the next. Moving horizontally within an island increases the saturation of a molecule (+2 H). Moving horizontally from one island to another introduces additional oxygen (+1 O). Moving vertically within an island changes the composition by exchanging one oxygen atom for CH_4, hence the island number (#C + #O) remains unchanged. These clustered island patterns in the rainwater are typical of fulvic acid isolates from natural organic matter samples (Reemtsma et al., 2006a;Stenson et al., 2003), and fulvic acids and oligomers detected in water soluble aerosols (Reemtsma et al., 2006b), indicating the presence of oligomeric compounds and HULIS in the complex rainwater DOM.

4.6 Sulfur Compounds

4.6.1 Organosulfates

There were 139 CHOS compounds detected ($\bar{m/z}$ 50-500), representing 25% of the total compounds (Table 4-2). The average molecular weight and average OM:OC ratio of the CHOS compounds were higher than the CHO compounds, which is consistent with the addition of a sulfur atom onto the molecule. The number of double bond equivalents (DBE) calculated from the CHOS elemental formulas indicates that they are likely aliphatic compounds (average DBE < 3). The average H:C and O:C ratios for the CHOS compounds were also higher than the elemental ratios of the CHO compounds.

The CHOS compounds (red triangles, Figure 4-3) group to the right, and higher, on the van Krevelen diagram than the CHO compounds (black circles), indicating a higher degree of oxidation. This placement on the van Krevelen, and the higher H:C and O:C ratios, are consistent with the addition of the sulfur as a sulfate (SO_4^{2-}) group. Sulfate was detected in all of the samples at *m/z* 96.960103, and organosulfates, if present, are also expected to be seen in the negative ion mode (Surratt et al., 2008 and references within). There were 134 CHOS compounds with oxygen to sulfur (O:S) ratios of 4-11, which allows all 134 compounds to potentially have sulfate functionalities. The high O:S ratios and the high degree of oxidation in the molecular formulas indicates that the bulk of the negative ion CHOS compounds detected in the rainwater samples are likely organosulfates.

Of the 134 CHOS compounds detected with O:S ratios > 4, 28 have elemental formulas consistent with organosulfate esters detected in ambient SOA, and demonstrated to form in laboratory smog chamber experiments (Surratt et al., 2008;Romero and Oehme, 2005;Reemtsma et al., 2006b). These organosulfate esters are formed in the presence of high acidity sulfate seed aerosols during particle phase and aqueous phase reactions of biogenic VOCs and their oxidation products (Surratt et al., 2008). Organosulfates formed from the gas phase oxidation of isoprene, α-pinene, β-pinene, limonene, α-terpinene, and γ-terpinene were all detected in the rainwater (Table 4-4).

4.6.2 Nitrooxy-organosulfates

There were 28 CHONS compounds detected (*m/z* 50-500), representing 5% of the total compounds. The CHONS compounds had an average H:C ratio similar to the CHOS compounds, but slightly higher O:C and OM:OC ratios (Table 4-2). The CHONS

compounds have elemental formulas with higher oxygen content than the organosulfates and cluster even further to the right and above the CHO and CHOS compounds in the van Krevelen diagram (blue squares; Figure 4-3) indicating an even higher degree of oxidation. The location of the CHONS compounds on the van Krevelen diagram, and the higher O:C ratios indicate that the nitrogen on the molecule is most likely an organic nitrate (ONO_2) functionality.

Five of the CHONS compounds have elemental formulas consistent with nitrooxy organosulfates detected in ambient aerosols and formed during laboratory smog chamber experiments (Table 4-5) conducted with high acidity sulfate seed aerosols and high NO_x conditions (Surratt et al., 2007, 2008). Of the 23 remaining CHONS compounds, 18 have enough oxygen in their elemental formula for both a sulfate and nitrate functionality to be present (> 7 O) suggesting those compounds are also nitrooxy organosulfates formed from other biogenic and anthropogenic VOC precursors.

4.6.3 Sulfonates

Four of the CHOS compounds have an O:S ratio too low to be sulfate functionalities (< 3), a high C content, and differ only by CH_2 units ($C_{16}H_{25}O_3S$, $C_{17}H_{27}O_3S$, $C_{18}H_{29}O_3S$, and $C_{19}H_{31}O_3S$). The elemental formulas of these four compounds are consistent with a class of persistent pollutants known as linear alkylbenzene sulfonates (LAS). The LAS compounds are used as synthetic surfactants and are surface active ingredients in detergents, shampoos, other cleaning compounds, and personal care products (Debelius et al., 2008;Lara-Martín et al., 2006). LAS compounds are toxic to a variety of organisms (Debelius et al., 2008) and as such are targeted in wastewater treatment plants (Reemtsma, 2003). Due to their widespread use,

LAS compounds have been detected at various concentrations in river water, seawater and sediments (González-Mazo and Gómez-Parra, 1996;González-Mazo et al., 2002). To our knowledge, this is the first evidence that LAS compounds can occur in atmospheric samples of any kind, and their presence in the atmosphere is difficult to explain. If the LAS compounds were able to reach the atmosphere, the potential for negative impacts on receiving ecosystems would be extended due to the possibility of long transport times in the atmosphere before deposition.

4.7 Atmospheric Implications

A number of lines of evidence suggest that the majority of compounds detected in these rainwater samples are from secondary processing in the atmosphere, and not primary emissions. First, the similarity in the number and types of compounds detected in the three rainwater samples from different seasons and locations in New Jersey is consistent with the organic matter being primarily from secondary processing in the atmosphere, and not local primary emissions. Second, the organic acids detected in the rainwater are likely predominantly formed through secondary processing reactions in the atmosphere, including in-cloud processing. In contrast, the sulfonates are likely primary anthropogenic compounds, and are pollutants known to be toxic to aquatic ecosystems; though the sulfonates are only four compounds out of the 552 total compounds detected. The majority of the compounds detected by negative ion FT-ICR MS in the rainwater have secondary sources both anthropogenic (e.g., organosulfates and nitrooxy organosulfates) and biogenic (e.g., oligomers from cloud processing of methylglyoxal).

Organosulfates likely contribute to the large percentage of uncharacterized water soluble organic carbon in atmospheric organic matter and could have been missed until

recently because single derivatization protocols are likely to cause degradation or misinterpretation of these compounds (Surratt et al., 2007). Several organosulfates detected in the rainwater could be used as tracers for SOA that was formed under highly acidic conditions. Interestingly, in a study of DOM recovered from ice cores collected in Russia, 21% of the ions detected had organic S present in a sample from 1950, compared to 12% in a sample from 1300 AD (Grannas et al., 2006). This is consistent with an anthropogenic source of organic S capable of being transported long distances in the atmosphere before deposition, supporting the use of organosulfates as anthropogenic tracer compounds.

The nitrooxy organosulfates detected in the rainwater have been seen in nighttime ambient aerosol samples, highlighting the importance of NO_3 radical oxidation chemistry in their formation (Iinuma et al., 2007a, 2007b). In the Surratt et al. (2008) study, nitrooxy organosulfates were detected during both the nighttime oxidation and photooxidation experiments with acidic sulfate seed aerosol, and intermediate or high NO_x conditions (~1 ppm). The nitrooxy organosulfates detected in the precipitation samples could also be used as tracers for SOA that was formed under high acidity and high NO_x conditions.

The oligomers, organosulfates, and nitrooxy organosulfates detected in the rainwater could all contribute to the HULIS fraction of atmospheric organic matter (Graber and Rudich, 2006;Romero and Oehme, 2005). If the aqueous oligomerization of one water soluble organic compound (i.e., methylglyoxal) can account for 26 previously unidentified CHO compounds in the rainwater, it is possible that oligomerization of other known biogenic and anthropogenic precursor organic compounds through in-cloud or

aerosol-phase reactions may contribute substantially to the complex HULIS fraction measured in aqueous atmospheric organic matter, including rainwater. Previous studies have suggested that no one compound comprises more than a small percentage of the total DOC in rainwater. The large number of compounds detected (552 unique masses from *m/z* 50 to 500), and the large contribution of multifunctional compounds (e.g., oligoesters, organosulfates, nitrooxy organosulfates) detected in the rainwater supports this idea. Unfortunately, quantification is not possible using ESI FT-ICR MS unless an authentic standard is used for each identified compound. Due to the large number of masses detected, and the lack of commercial availability of standards for these compounds, we were not able to quantify the mass contribution of each identified compound to total DOC concentration. However, as is typical for HULIS, the majority of these multifunctional compounds would not be separated and detected by traditional analytical techniques, highlighting the important advances made capable by ultra-high resolution mass spectrometry. This work provides motivation to expand studies of complex atmospheric organic matter to include quantitation, chromatographic separation and tandem MS-MS.

Table 4-1 Rainwater Bulk Properties
Bulk properties of rainwater samples collected in New Jersey, USA.

Date Collected	Storm Trajectory	Rainfall Amount (cm)	Temp °C	pH	NO_3^- (μM)	NH_4^+ (μM)	DON (μM)	DOC (μM)	PO_4^{3-} (μM)
14 May 2002 Camden	SW	3.0	15	4.0	32	44	29	259	0.1
5 October 2002 Camden	W	0.4	21	4.1	44	94	33	263	0.5
20 July 2002 Pinelands	WNW	2.1	22	3.7	59	42	38	224	0.2

Table 4-2 Elemental Ratios of Compound Classes in Rainwater
The number of masses in each compound class and the average (arithmetic mean) elemental ratios for each compound class. The compounds contributing to the "other" category are listed below the darkened line.

Type	# of Compounds	% of Total	H:C	O:C	N:C	MW	OM:OC
CHO	262	48	1.5 ± 0.4	0.7 ± 0.5	--	193 ± 58	2.1 ± 0.7
CHOS	139	25	1.9 ± 0.5	1.3 ± 0.8	--	246 ± 54	3.4 ± 1.5
CHONS	28	5	1.8 ± 0.6	1.7 ±0.9	2.7 ± 1.9	271 ± 60	4.2 ± 1.5
CHON	74	13	1.9 ± 0.8	1.6 ± 1.4	2.6 ± 2.4	192 ± 68	3.7 ± 2.2
Other	49	9	1.5 ± 1	1.0 ± 1.1	5.4 ± 3.9	272 ± 80	3.4 ± 1.9
CHONP	29	5					
CHONSP	8	2					
CHOP	7	1					
CHOSP	5	1					

Table 4-3 Comparison of Oligomers in Rainwater and Methylglyoxal Experimental Samples

Organic acids and oligomers detected both in the methylglyoxal + OH radical experiments and in the rainwater by negative ion FT-ICR MS. Compound identification based on comparison with FT-ICR MS negative ion data from methylglyoxal + OH oligomer series as described in (Altieri et al., 2008). Compounds from all 9 methylglyoxal oligomer series are represented. n=1 and n=2 indicates the addition of one and two hydroxy acids (+$C_3H_4O_2$) through esterification, respectively.

Parent			Oligomers	n=1		n=2
	$\bar{m}/z$	Elemental Formula	$\bar{m}/z$	Elemental Formula	$\bar{m}/z$	Elemental Formula
Glyoxylic acid	72.9931	$C_2H_1O_3$	145.01426	$C_5H_5O_5$	217.03546	$C_8H_9O_7$
Glycolic acid	75.00875	$C_2H_3O_3$	147.02991	$C_5H_7O_5$	219.05107	$C_8H_{11}O_7$
Pyruvic acid	87.0087	$C_3H_3O_3$	159.0299	$C_6H_7O_5$	231.05109	$C_9H_{11}O_7$
Oxalic acid	88.98796	$C_2H_1O_4$	161.00922	$C_5H_5O_6$	233.03034	$C_8H_9O_8$
Succinic acid	117.01935	$C_4H_5O_4$	189.04032	$C_7H_9O_6$	261.06157	$C_{10}H_{13}O_8$
m/z 131	131.03501	$C_5H_7O_4$	203.0562	$C_8H_{11}O_6$	275.07719	$C_{11}H_{15}O_8$
Malonic acid	103.00358	$C_3H_3O_4$	175.02483	$C_6H_7O_6$	247.04596	$C_9H_{11}O_8$
Malic acid	133.01427	$C_4H_5O_5$	205.03546	$C_7H_9O_7$	277.05647	$C_{10}H_{13}O_9$
m/z 177	177.04047	$C_6H_9O_6$	249.0616	$C_9H_{13}O_8$		

Table 4-4 Rainwater Organosulfates
Organosulfate compounds detected in the rainwater by negative ion FT-ICR MS and reported in (Surratt et al., 2008) as organosulfates formed when biogenic precursor VOCs are oxidized with high acidity sulfate seed aerosols.

Isoprene		α-pinene		Limonene		α -terpinene	
m/z	Elemental Formula	*m/z*	Elemental Formula	*m/z*	Elemental Formula	*m/z*	Elemental Formula
138.97067	$C_2H_3O_5S$	223.02818	$C_7H_{11}O_6S$	239.0231	$C_7H_{11}O_7S$	253.0387	$C_8H_{13}O_7S$
152.98632	$C_3H_5O_5S$	226.98671	$C_5H_7O_8S$	251.05948	$C_9H_{15}O_6S$	279.0544	$C_{10}H_{15}O_7S$
154.96558	$C_2H_3O_6S$	237.04383	$C_8H_{13}O_6S$	267.0544	$C_9H_{15}O_7S$	281.0700	$C_{10}H_{17}O_7S$
168.98123	$C_3H_5O_6S$	279.0544	$C_{10}H_{15}O_7S$	279.0544	$C_{10}H_{15}O_7S$	283.0493	$C_9H_{15}O_8S$
210.9918	$C_5H_7O_7S$	281.07005	$C_{10}H_{17}O_7S$	281.0701	$C_{10}H_{17}O_7S$	283.0857	$C_{10}H_{19}O_7S$
213.00745	$C_5H_9O_7S$	297.06496	$C_{10}H_{17}O_8S$			297.065	$C_{10}H_{17}O_8S$
215.0231	$C_5H_{11}O_7S$						

Table 4-5 Rainwater Nitrooxy-organosulfates

Nitrooxy-organosulfate compounds detected in rainwater by negative ion FT-ICR MS and reported by (Surratt et al., 2008). They are formed when parent biogenic VOC's undergo reactions with high acidity sulfate seed aerosols with intermediate to high NO_x levels.

Isoprene		α-pinene[a]		Monoterpene	
m/z⁻	Elemental Formula	*m/z*⁻	Elemental Formula	*m/z*⁻	Elemental Formula
244.013261	$C_5H_{10}N_1O_8S_1$	294.065296	$C_{10}H_{16}N_1O_7S_1$	342.05004	$C_{10}H_{16}N_1O_{10}S_1$
260.008175	$C_5H_{10}N_1O_9S_1$				
304.993253	$C_5H_9N_2O_{11}S_1$				

[a] The same nitrooxy organosulfates are also formed during α-terpinene, γ-terpinene, and β–pinene oxidation (Surratt et al., 2008).

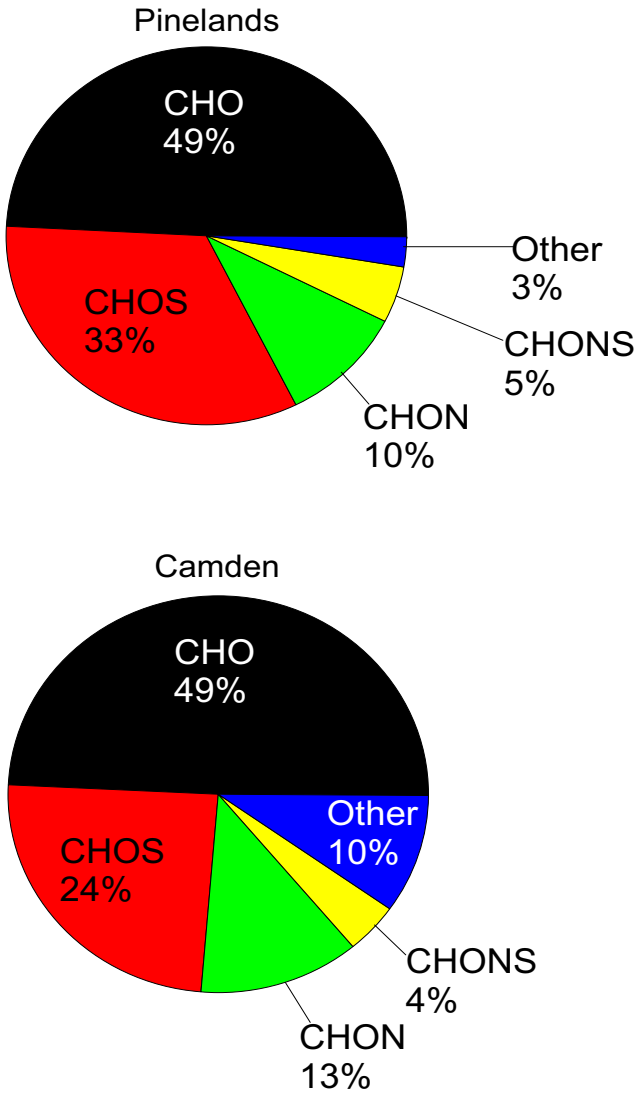

Figure 4-1 Comparison of the Number of Elemental Formulas in Compound Classes Comparison of the number of each type of elemental formula present (negative ion mode) in precipitation samples. There were 388 total masses detected in the Pinelands sample collected on the 20 July 2002 and 383 total masses detected in the Camden sample collected on the 5 October 2002.

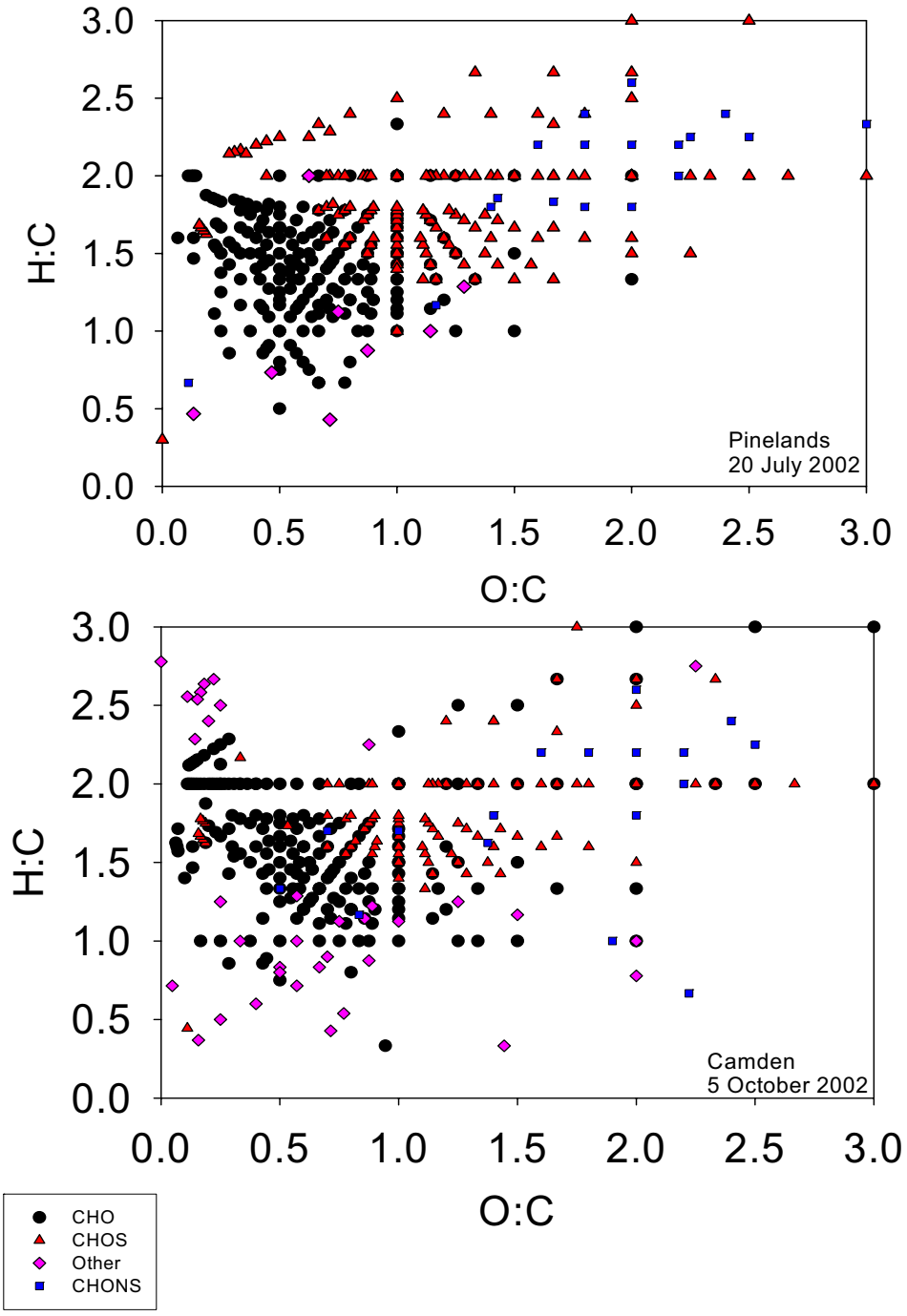

Figure 4-2 Comparison of the Elemental Ratios in Compound Classes
Comparison of the elemental ratios of negative ion mode compounds in precipitation samples collected in July and October 2002 in the Pinelands and Camden, NJ (USA), respectively.

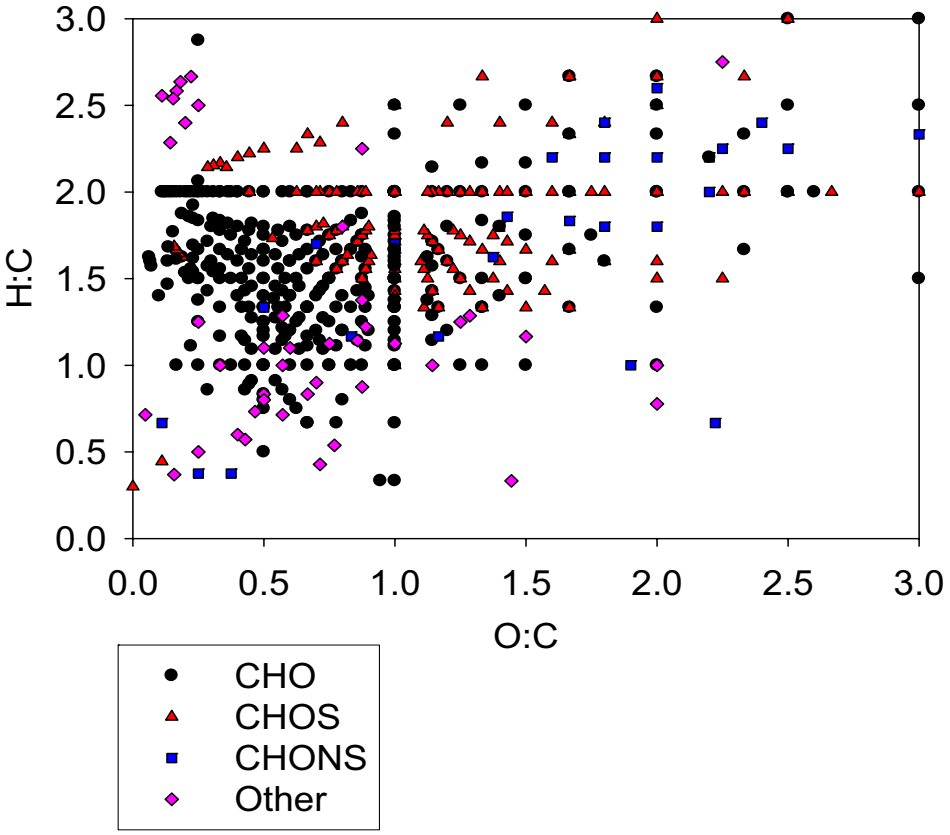

Figure 4-3 Negative Ion Rainwater van Krevelen
Van Krevelen plot of the combined precipitation samples FT-ICR MS negative ion mode *m/z* 50 to 500.

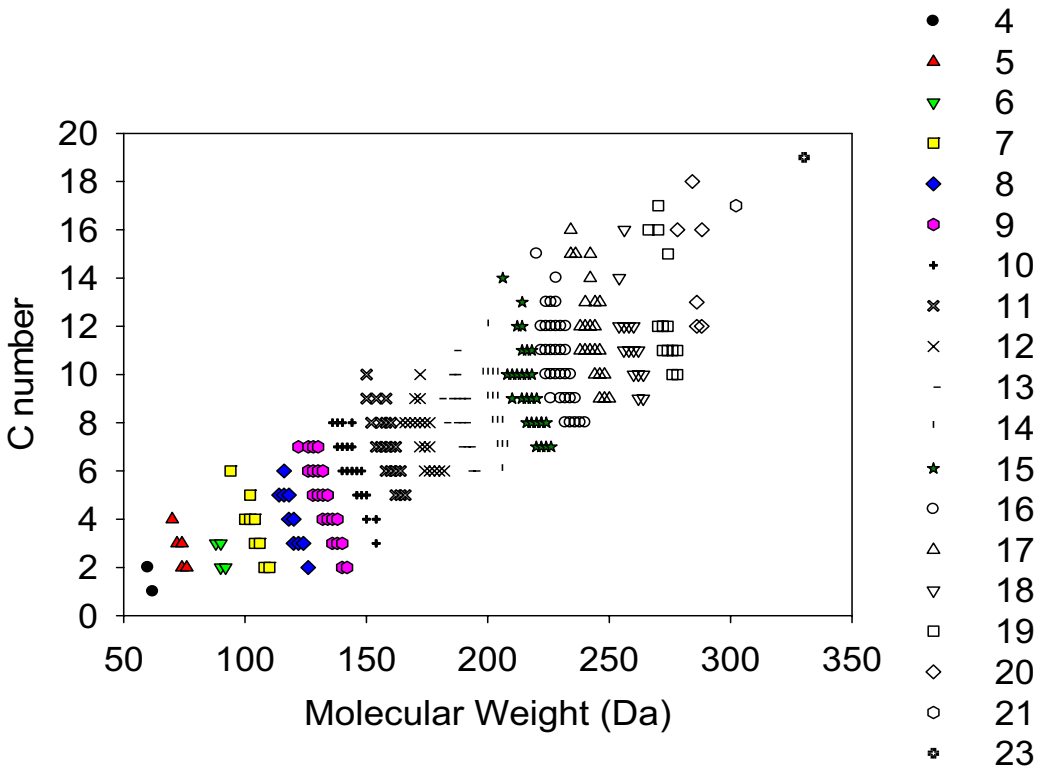

Figure 4-4 Island Plot of Negative Ion CHO Compounds
Number of carbons per molecule versus the molecular weight of the molecule for compounds containing only CHO detected in the negative ion mode. Molecules with the same number of carbon and oxygen are marked by the same symbol and denoted as one "island." The island number in the legend corresponds to the sum of carbon and oxygen.

Chapter 5. The Composition of Dissolved Organic Nitrogen in Continental Precipitation Investigated by Ultra-High Resolution FT-ICR Mass Spectrometry

Material in this chapter has been submitted to Environmental Science & Technology for publication as:

Altieri, K.E., Turpin, B.J., Seitzinger, S.P., The composition of dissolved organic nitrogen in continental precipitation investigated by ultra-high resolution FT-ICR mass spectrometry

5.1 Abstract

The atmospheric transport of fixed nitrogen (N) is a critical component of the global N cycle and, as with many other aspects of the global N cycle, it is heavily impacted by human activities. It has been shown that organic N is an important contributor to atmospheric N, but its sources, composition, reactivity, and fate are largely unknown. Rainwater samples collected in New Jersey, USA were analyzed by negative and positive ion ultra-high resolution electrospray ionization Fourier transform ion cyclotron resonance mass spectrometry (FT-ICR MS). Elemental compositions of 402 N containing compounds were determined in the mass ranges $^{-}m/z$ 50-500 and $^{+}m/z$ 50-300. Five main groups of compound classes were identified: compounds containing carbon, hydrogen, oxygen, and N detected as positive ions (CHON+), compounds containing CHON detected as negative ions (CHON-), compounds containing CHN detected as positive ions (CHN+), and CHON compounds that contain sulfur (S) detected as both positive and negative ions (CHONS+, CHONS-, respectively). The CHON+ compound class has the largest number of compounds detected (i.e., 281), with the majority, i.e., 207, containing only one N atom. The elemental ratios of these compounds and their

detection in the positive ion mode suggest that they are compounds with reduced N functionality. Also detected in this compound class were eight amino acids. It is suggested that the CHON- compound class includes organonitrate compounds. The CHONS- compounds have previously been identified as nitrooxy organosulfates, known contributors to secondary organic aerosol with anthropogenic sources. This molecular level characterization provides important new insights into the complexity and origin of the uncharacterized water soluble organic nitrogen in the atmosphere.

5.2 Introduction

The atmospheric transport and deposition of reactive N are important components of the perturbed global N cycle (Galloway et al., 2003). The cycling of reactive N in the atmosphere is usually measured in terms of inorganic N species (reduced NH_3, NH_4^+, and oxidized NO_x, HNO_3, N_2O, NO_3^-); though it is now recognized that organic nitrogen is also an important component of atmospheric N (Duce et al., 2008;Cornell et al., 1995;Cornell et al., 2003). Atmospheric water soluble organic nitrogen (WSON) is likely a complex mixture of compounds with a wide range of sources. Some sources and components of WSON have been recognized and quantified. For example, organic nitrates exist in both polluted and pristine regions of the atmosphere and form during gas phase reactions of NO_x and volatile organic carbons (VOCs) (Kroll et al., 2006;Jang and Kamens, 2001). Secondary organic aerosol (SOA) formation through gas phase and subsequent aerosol phase reactions has been studied extensively, and identified products include organic nitro- and nitrate compounds (Hung et al., 2005;Alfarra et al., 2006;Dommen et al., 2006;Kroll et al., 2006). Reduced forms of N, including urea and amino acids, exist in the atmosphere and are emitted directly from biomass burning and

agricultural areas (Chan et al., 2005;Dittmar et al., 2001;Matsumoto and Uematsu, 2005;Mopper and Zimmermann, 1987;Sommerville and Preston, 2001). Recently, smog chamber experiments simulating SOA formation in the presence of ammonium sulfate have led to the formation of imidazoles (Galloway, 2008).

Amino acids are one of the few dissolved organic nitrogen (DON) compound classes quantified in rainwater (Gorzelska et al., 1992;Kieber et al., 2005;Mace et al., 2003a;Mace et al., 2003b;Mopper and Zimmermann, 1987), fog water (Zhang and Anastasio, 2001), and aerosols (Zhang et al., 2002). Dissolved free amino nitrogen (DFAN) is typically quantified by an HPLC derivatization technique that is based on a comparison of the retention times of amino acids in a standard mix. Dissolved combined amino nitrogen is quantified by an acid hydrolysis method used to liberate the amino acids in proteins and peptides, then quantified by the same HPLC derivatization technique used for DFAN. Based on these measurements, free and combined amino acids account for 2-25% of the DON in rainwater and fog water, and WSON in aerosols (Cornell et al., 2003). Together, the sum of quantified DON constituents account for less than 50% of atmospheric DON. Thus, attributing the sources and assessing the impacts of DON is difficult.

The coupling of electrospray ionization (ESI) inlet systems to mass spectrometers of various resolutions has greatly improved our ability to chemically characterize polar dissolved organic compounds at the molecular level in aqueous environmental samples (Kujawinski, 2002). The most significant advances have been made with ultra-high resolution ESI Fourier transform ion cyclotron resonance mass spectrometry (FT-ICR MS), which allows the identification and separation of thousands of compounds in a

sample. The FT-ICR MS (7 T magnet) has ultra-high resolution ($m/\Delta m > 1x10^6$ at 400 Da) allowing separation of individual compounds and mass accuracy < 1 ppm allowing exact molecular formula assignments for each compound (Marshall, 2000). For each mass detected, the exact elemental composition ($C_aH_bN_cO_dP_eS_f$), the double bond equivalent (DBE; number of rings plus double bonds), and elemental ratios (H:C, O:C, N:C) can be calculated. Compounds with primarily acidic functional groups (e.g., organonitrate, carboxylic acids) are transferred to the detector as negative ions and those with primarily basic functional groups (e.g., N heterocycles, amines, alcohols) as positive ions, making it an ideal tool for characterizing a complex mixture such as dissolved organic matter (DOM).

Previous studies have attempted to identify the sources and potential importance of rainwater DON by focusing on comparing the bulk concentrations of inorganic and organic nitrogen species across various spatial and temporal scales (Zhang et al., 2008;Cornell et al., 2001;Duce et al., 2008;Spokes and Jickells, 2005;Spokes et al., 2000). Since DON is a subset of the complex dissolved organic carbon (DOC) in the atmosphere, it is likely that DON, like DOC, is a dilute complex mixture of compounds with varying individual sources and concentrations. Analysis of DOM in 11 rainwater samples by unit mass ESI-MS over the mass range 50-500 Da led to the identification of 305 unique masses in the positive and negative ion modes combined (Seitzinger et al., 2003). However, with unit mass ESI-MS it is not possible to discern if there are multiple compounds within a unit mass bin and what elements (e.g., oxygen, nitrogen, sulfur) are present on the compounds that are detected. The goal in this study was to use ultra-high resolution FT-ICR MS to investigate the N containing organic compounds on a molecular

level by identifying the total number of masses that contribute to DON in the rainwater samples and assessing to what extent the N has reduced or oxidized functionalities. By addressing these questions we attempt to link groups of DON compounds to potential primary and secondary sources, and to provide the chemical insight needed to predict the behavior and fate of atmospheric WSON.

5.3 Experimental

Precipitation was collected from two sites in the northeastern USA, as described in detail by Altieri et al. (2008). Briefly, the urban site Camden, NJ (Latitude 39° 56' 57.45" N; Longitude 75° 7' 16.60" W; elevation 11 m) is a city directly across the Delaware River from Philadelphia, PA and is in a heavily urbanized region. The rural site Pinelands, NJ is located 30 miles east of Camden in the Lebanon State Forest (Latitude 39° 56'43.61" N; Longitude 74° 37'1.52" W; elevation 1 m). Though the Pinelands site is located in a state forest it is impacted by urban airflow. Two samples were collected from the Camden, NJ site, one in spring and one in fall. Two summer time samples were collected from the Pinelands, NJ site (Table 5-1). The samples were collected using wet-dry deposition collectors (Aerochem Metrics Model 301, Bushnell, FL). The rain collectors were fitted with stainless steel buckets and opened only during wetfall events. The type of collector used and the placement of the collector at the site adhere to regulations outlined by the National Atmospheric Deposition Program (Bigelow, 2001). Samples were retrieved no more than 12 hours after each rain event to minimize microbial degradation of DOM and consumption of inorganic nutrients. Sample temperature and pH were measured immediately upon retrieval and samples were filtered through glass fiber filters (Whatman GFF; baked for four hours at 500 °C; then

rinsed with deionized water) ensuring analysis of the dissolved constituents only. Rainwater was stored at -20 °C in polypropylene screw-capped tubes until analysis. Contamination due to field sampling and laboratory sample processing was minimal (field and filter blanks < 5 % of sample DOC). Field blanks were prepared by placing E-pure water into the rainwater collector, and then the field blank was sampled, filtered and stored at -20 °C until analysis using the same procedures as for the rainwater samples. The field blanks were analyzed by unit-mass ESI-MS and there were only 18 *m/z*'s detected in the positive and negative ion modes with ion abundances > 500.

Bulk inorganic nutrients (NO_3^- + NO_2^-, NH_4^+, PO_4^{3-}) were measured on the four rainwater samples with an automated nutrient analyzer and standard colorimetric methods (Lachat, Inc). DOC was measured by high-temperature catalytic oxidation with a Shimadzu Total Organic Carbon (TOC) 5000A analyzer (Sharp et al., 1993). Total dissolved nitrogen (TDN) was measured with an Antek 7000 TN Analyzer (Seitzinger and Sanders, 1999). DON was determined as the difference between TDN and dissolved inorganic nitrogen (NO_3^- + NO_2^-, NH_4^+). Calibrations were performed using potassium hydrogen phthalate standards for DOC and urea and nitrate standards for TDN.

Analyses were performed on the four precipitation samples (diluted in methanol 50:50 v/v) with a 7-T ESI FT-ICR MS and operated in both the negative and positive ion mode. The sample was introduced into the ESI source by direct infusion at a flow rate of 5 μL min^{-1}. For the negative ion mode, the needle voltage was 3.02 kV, the capillary voltage was -9.44 V, the capillary temperature was 260 °C, and the tube lens was -57 V. For the positive ion mode, the needle voltage was 4.01 kV, the capillary voltage was 10.47 V, the capillary temperature was 250 °C, and the tube lens was 55 V. The spectra

were mass calibrated with standard ions using an external calibrant (G2421A Agilent "tuning mix") and the residual root mean square error after calibration was 1.1-1.6 ppm. The mass lists were processed and exported using Xcalibur v 2.0 SR2 (ThermoFisher Scientific).

Midas Formula Calculator Software (v1.1) was used to calculate all mathematically possible formulas for all ions with a signal to noise ratio ≥ 10 using a mass tolerance of ±1 ppm. An unlimited number of ^{12}C and ^{1}H, up to fifteen ^{14}N and ^{16}O, and one of each ^{32}S and ^{31}P were allowed in the molecular formula calculations for negative ions. An unlimited number of ^{12}C and ^{1}H, up to fifteen ^{14}N and ^{16}O, and one of each ^{32}S, ^{31}P, and ^{23}Na were allowed in the molecular formula calculations for positive ions. The average mass error for all assignments was 0.1 ppm. Boundary values for molecular elemental ratios were applied as a filtering tool (Koch et al., 2005). The O:C, H:C, and N:C ratios were limited to < 5, ≥ 0.3, and < 2, respectively. Ions were also characterized by the DBE (i.e., number of rings plus double bonds), calculated from equation 5-1 (McLafferty, 1993):

$$DBE = c - \frac{1}{2}h + \frac{1}{2}(n + p) + 1 \quad \text{for elemental composition, } C_cH_hO_oN_nP_pS_s \qquad (5\text{-}1)$$

5.4 Results and Discussion

The four rainwater samples analyzed were collected from two locations over different seasons in New Jersey, USA, yet they are similar in bulk properties and storm trajectories (Table 5-1). The inorganic N concentrations in these samples are consistent with other continental precipitation samples (Avery et al., 2006;Kieber et al., 2005;Kieber et al., 1999;Willey et al., 2000;Cornell et al., 2003). The DON concentration is also consistent with concentrations reported for continental precipitation

collected in the USA (29-38 μM), as is the contribution of DON to TDN (19-30%) (Cornell et al., 2001;Cornell et al., 1995;Cornell and Jickells, 1999;Cornell et al., 2003;Cornell et al., 1998;Mace et al., 2003b).

5.4.1 Sample Comparison

In the discussion that follows, as in Altieri et al. (2008), we have combined the elemental formulas for each of the samples due to the high percentage of overlap in elemental formulas. The similarities in the N containing compounds detected in the positive ion mode were used to compare the rainwater samples. The majority of the N containing elemental formulas detected in the positive ion mode were found in all three rainwater samples (i.e., < 25% unique in each sample), and this similarity across samples was also found for compounds detected as negative ions (Altieri, 2008). As an example, all of the N containing elemental formulas determined in the 20 July, 2002 sample are listed with their corresponding *m/z* (Appendix D1). We consider the combined data representative of N containing organic compounds in rainwater collected from an urban impacted (i.e., downwind of a major city) location in New Jersey, USA.

5.4.2 DON Composition

There were 100 masses detected in the negative ion mode over the mass range 50-500 Da that had elemental formula assignments containing N, and 302 N containing elemental formulas assigned to masses in the positive ion mode over the mass range 50-300 Da (Table 5-2, Figure 5-1). For each elemental composition assigned to a mass there are multiple structural isomers possible, and thus this is likely an underestimate of the total number of compounds contributing to the DON in these rainwater samples. The large number of elemental formulas determined in these mass ranges highlights the

complexity of this mixture of compounds. It should also be noted that the advanced mass spectrometric methods used are non-quantitative, and thus the quantitative contribution of each compound or each compound class is unknown. In order to quantify all of the > 400 DON compounds detected, authentic standards of each compound would be needed, and that is beyond the scope of this study.

The elemental formulas determined fall into five main compound classes: carbon, hydrogen, oxygen, and nitrogen only, detected in the negative ion mode (CHON-), CHON compounds detected in the positive ion mode (CHON+), compounds containing only CHN detected in the positive ion mode (CHN+), sulfur (S) containing CHONS compounds detected in the negative ion mode (CHONS-), and CHONS compounds detected in the positive ion mode (CHONS+).

Though the positive ion mode was scanned over a smaller mass range than the negative ion mode (50-300 Da vs. 50-500 Da, respectively), the CHON+ compound class has the largest number of elemental formulas, representing 70% of the total number of N containing compounds (Figure 5-1). The CHON- group had the second largest number of elemental formulas, contributing 18% to the total. The CHONS- compounds contribute 7% to the total, with the CHONS+ and CHN+ compounds contributing 3% and 2% to the total, respectively. In the following sections, we discuss in detail the compounds found in each compound class focusing on the CHON+ compounds because of their dominance in total number detected.

5.4.3 Amino Acids and Reduced N Compounds

There were eight CHON+ elemental formulas in the rainwater that are consistent with amino acids commonly measured in precipitation as dissolved free amino acids:

valine, leucine (or isoleucine), glutamic acid, phenylalanine, tyrosine, lysine, histidine, and arginine (Gorzelska et al., 1992;Kieber et al., 2005;Mace et al., 2003a;Mace et al., 2003b;Mopper and Zimmermann, 1987). Of the 281 CHON+ elemental formulas, 207 contain only one N atom, 60 have two N atoms, and the remaining 14 compounds have > 3 N atoms. The CHON+ compound class has lower oxygen to carbon (O:C), lower organic molecular weight to organic carbon weight (OM:OC), and lower oxygen to nitrogen (O:N) average (arithmetic mean) ratios than all of the other oxygen containing compound classes (Table 5-2).

In the CHON+ class, there were 184 elemental masses containing one N atom and at least two O atoms on the molecule. This composition is typical for amino acids, but the molecular weights of many of these compounds are higher than known amino acids (up to 240 Da). The oxygen content of these compounds varies from 2-9 O atoms, and the DBE ranges from 0-12. Amino acids can contribute up to 20% of the DON in rain and fog waters (Zhang and Anastasio, 2001;Cornell et al., 2003). They are reactive, and can be oxidized in the atmosphere, and have recently been reported to act as catalysts in atmospheric condensed phase reactions (Noziere, 2009). Given the complexity that can result from atmospheric condensed phase (e.g., in aerosols and clouds) reactions (e.g., oligomerization), it is possible that condensed phase reactions involving amino acids could lead to the formation of many compounds that would not be detected by traditional analytical techniques. For example, ~54 oligomer compounds formed from the aqueous photooxidation of methylglyoxal were detected by FT-ICR MS, but were not detected by traditional HPLC techniques (Altieri et al., 2008). The large number of compounds with 1 N atom on the molecule and varying CHO compositions suggests that whatever

atmospheric reactions are forming these compounds they are not impacting the N functionality of the molecule, and are only altering the carbon and oxygen composition. The amino acids may contribute a fairly small percentage to the total WSON, but their oxidation products and/or oligomerization products might be numerous and would be detected in the CHON+ compound class, thus their quantitative contribution to DON may be higher than an estimate based on amino acids alone.

One way to identify oligomerization products is the van Krevelen diagram, which plots the hydrogen to carbon (H:C) ratio as a function of the O:C ratio. The van Krevelen can be used to display compositional characteristics, to compare the elemental ratios of each compound in a compound class, and to identify groups of compounds related by regular mass differences (Wu et al., 2004). The CHON+ compounds have H:C ratios comparable to the other compound classes, but lower O:C ratios (black circles, Figure 5-2). The low O:C, O:N, and OM:OC average ratios, and the grouping of the compounds on the van Krevelen diagram indicate that the CHON+ compounds do not have organic nitrate functionality, and are likely compounds with reduced N functional groups.

In the traditional van Krevelen diagram (H:C vs. O:C), the CHON+ compounds are grouped very close together and it is difficult to discern patterns. The van Krevelen was modified to focus on the N component of the CHON+ compounds, and the nitrogen to carbon (N:C) ratio was plotted as a function of the O:C ratio (Figure 5-3). In this N based van Krevelen diagram, certain patterns become evident. For example, there is a series of compounds that contain 1 N atom, and differ by CH_2O units (Table 5-3). The DBE does not increase with the addition of CH_2O meaning the number of rings and double bonds does not change on the molecule and the addition of CH_2O is through

single bonds only. The patterns in the van Krevelen and the relationships between series of compounds suggest that some of the CHON+ compounds could be formed through oligomerization reactions in the atmosphere.

5.4.4 Organonitrates

There were 72 CHON- masses in the mass range 50-500 Da. Similar to the CHON+ compounds, the majority (i.e., 59) of the CHON- compounds have only one N atom. Eight compounds have two N atoms, four compounds have 3 N atoms, and one compound has 4 N atoms. The average H:C ratio of the CHON- compound class is comparable to the CHON+ compounds, however, the average O:C, N:C, O:N, and OM:OC ratios are all much higher in the CHON- compound class than in the CHON+ compound class (Table 5-2). The CHON- compounds group to the right of the CHON+ compounds on the van Krevelen diagram (Figure 5-2), indicating a higher degree of oxidation. The higher O:C, O:N, OM:OC ratios, and the placement on the van Krevelen diagram are consistent with the N in these compounds being an organic nitrate (ONO_2) group. The nitrate ion is detected in the negative ion mode, and organonitrates, if present, are also expected to be seen in the negative ion mode. There were 61 CHON- compounds with O:N ratios of 3-9, which allows all 61 compounds to potentially have organic nitrate functionalities.

Elemental formulas consistent with common C_1-C_{15} alkyl nitrates frequently measured in the gas phase (Schneider et al., 1998) were not detected; this is consistent with the low solubility of alkyl nitrates. The CHON- compounds in the rainwater have higher O:C and O:N ratios than simple alkyl nitrates, which might explain why these organonitrate compounds are more water soluble. It is possible that oxidation of alkyl

nitrates and other VOC and NO_x reactions are the sources of these rainwater CHON- compounds.

5.4.5 Sulfur and Nitrogen Containing Compounds

There were 42 elemental formulas assigned that contained CHONS, 14 masses detected in the positive ion mode, and 28 masses detected in the negative ion mode. The 28 CHONS- compounds have been discussed previously (Altieri, 2008). Briefly, 23 of the compounds have enough oxygen in their elemental formula for both a sulfate and nitrate functionality to be present (≥ 7). The elemental ratios, oxygen content, placement on the van Krevelen diagram (Figure 5-2), and comparison with other elemental formulas documented in atmospheric samples, all suggest that these components are nitrooxy organosulfates. Nitrooxy organosulfates are formed in the atmosphere from organic precursors in the presence of high acidity sulfate containing aerosols under high NO_x conditions (Surratt et al., 2008).

The 14 compounds containing CHONS detected in the positive ion mode have comparable average H:C ratios, but lower average O:C, N:C, OM:OC and O:N ratios than the CHONS- compound class (Table 5-2). The molecular weight range (130-257 Da), and the average molecular weight (176 Da) of the CHONS+ compounds is lower than the CHONS- compounds (i.e., 176-493 Da and 271 Da, respectively). The CHONS+ compounds group to the left of the CHONS- compounds on the van Krevelen diagram (Figure 5-2), indicating a lower degree of oxidation. Taken as a whole, this indicates that the CHONS+ compounds do not have a combination of nitrate and sulfate functionalities, and are not nitrooxy organosulfates like the CHONS- compounds. These observations, the low oxygen content of these compounds and their detection in the

positive ion mode suggest that the N and/or S is present in a ring. The DBE values were higher in this group than the others, ranging from 0-8 with an average of 4, which also supports the presence of N and S in a ring structure. However, without further chemical analysis (e.g., tandem MS-MS, LC-MS) it is not possible to positively identify these compounds.

5.4.6 Carbon Hydrogen and Nitrogen Compounds

There were seven masses detected in the positive ion mode that were assigned elemental formulas containing only CHN. There are also other compounds with primary sources that the ESI process would have difficulty ionizing including PAH's, and soot derived material, thus it is possible that the low number of masses detected in this compound class is an underestimate of the actual number of CHN compounds in the rainwater. The average H:C ratio was comparable to the other compound classes, though the average molecular weight and OM:OC ratios were lower than the other compound classes. Because the compounds were detected in the positive ion mode the N functionality is likely as an amine or as a N heterocycle. Similar to the CHONS+ compounds, the DBE values were high in this group and ranged from 0-8 with an average of 4, allowing the compounds to be ring structures or to have multiple double bonds. There are many structures and structural isomers possible for the detected CHN+ formulas including diethylamine ($C_4H_{11}N$), methylimidazole ($C_4H_7N_2$), tetrahydropyridine ($C_5H_{10}N$), aniline (C_6H_8N), and diphenylalamine ($C_{12}H_{12}N$). Though it is not possible to positively identify any of these compounds without further analysis, the likely possibilities are all primary compounds with anthropogenic sources (Graedel et al., 1986).

5.5 Impacts

The large number of elemental formulas with reduced N functionality and the amino acids in the CHON+ compound class likely contribute to the bioavailability of atmospheric DON deposition. There is evidence that atmospheric WSON can be a bioavailable source of N to coastal systems and can be utilized for primary production (Peierls and Paerl, 1997;Seitzinger and Sanders, 1999;Timperley et al., 1985). Though the amino acids are likely from primary emissions, many of the other >200 CHON+ compounds are likely formed through secondary processing in the atmosphere of alkyl amines or amino acids. This is contrary to previous assessments of atmospheric DON which have assumed that reduced N compounds could not be produced *in situ* under the oxidizing conditions of the atmosphere (Neff et al., 2002). In addition to being bioavailable, amino acids, and in theory the amino acid like compounds, can act as efficient ice nuclei and could be surface active (Zhang et al., 2002).

The complexity in the number and type of elemental formulas determined in the rainwater helps explain why traditional analytical techniques have not been able to characterize the full suite of N containing organic compounds. Many of these compounds are multifunctional and some are highly oxygenated, thus they likely contribute to the fraction of atmospheric organic matter that is considered humic like substances (HULIS). Some of these compounds (e.g., nitrooxy organosulfates) are known contributors to SOA, which suggests that SOA formed in the presence of nitrogen could be contributing to the complexity in rainwater DON. This provides motivation for continuing to include nitrogen in experiments on SOA formation mechanisms, but also for detailed product identification in those experiments to identify the formation of

organic N containing compounds (e.g., (Galloway, 2008;Surratt et al., 2008)), especially compounds with reduced nitrogen functionalities.

The majority of the compounds that were detected by the FT-ICR MS are likely to have secondary sources. For example, CHONS- compounds are formed from secondary reactions in the atmosphere in the presence of anthropogenic NO_x, sulfate, and reactive organics. CHON- compounds are likely formed from atmospheric reactions of VOC's and NO_x. As discussed above, the CHON+ compounds could be from secondary processing of amines or amino acids in the atmosphere. Though the reactive organics (e.g., VOCs, amino acids) could potentially be from biogenic sources, the oxidants (e.g., ozone, NO_x) are mostly anthropogenic making them secondary anthropogenic compounds. The bulk of the DON being formed in the atmosphere from secondary reactions is also supported by the similarity in N containing compounds across the different samples. The large contribution of compounds formed through atmospheric reactions that involve anthropogenic oxidants suggests that anthropogenic secondary sources contribute significantly to atmospheric DON. This work provides motivation to expand studies of atmospheric DON to remote locations to determine the potential for deposition of secondary anthropogenic compounds in remote ecosystems. It is important that we continue to improve our understanding of the extent that the perturbed atmospheric N cycle is impacting air quality and receiving ecosystems.

Table 5-1 Rainwater Bulk Properties
Bulk properties of rainwater samples collected in New Jersey, USA.

Date Collected	Storm Trajectory	Rainfall Amount (cm)	Temp °C	pH	NO_3^- (μM)	NH_4^+ (μM)	DON (μM)	DOC (μM)	PO_4^{3-} (μM)
14 May 2002 Camden	SW	3.0	15	4.0	32	44	29	259	0.1
5 October 2002 [a]Camden	W	0.4	21	4.1	44	94	33	263	0.5
20 July 2002 Pinelands	WNW	2.1	22	3.7	59	42	38	224	0.2
10 July 2002 [b]Pinelands	WNW	1.2	22	3.8	53	28	35	253	0.1

[a]Negative ion data only
[b]Positive ion data only

Table 5-2 Elemental Ratios of N Containing Compounds in Rainwater
The number of compounds in each compound class and the average (arithmetic mean ± standard deviation) elemental ratios for each compound class. Compounds that do not contain N in their elemental formulas are not included in this table.

Type	# of compounds	% of Total	H:C	O:C	N:C	O:N	MW	OM:OC
CHON+	281	70	1.8 ±0.4	0.38 ±0.2	0.16 ±0.1	3 ±1.8	204 ±46	1.8 ±0.3
CHON-	72	18	1.9 ±0.9	1.6 ±1.5	0.34 ±0.3	5 ±2.4	191 ±67	3.7 ±2.3
CHN+	7	2	1.4 ±0.7	--	0.26 ±0.2	--	92 ±39	1.4 ±0.2
CHONS+	14	3	1.6 ±1.2	0.8 ±0.5	0.4 ±0.3	2.5 ±2	176 ±39	3.3 ±1.2
CHONS-	28	7	1.8 ±1.6	1.7 ±0.9	2.7 ±1.9	7.5 ±3.3	271 ±60	4.2 ±1.5

Table 5-3 Series of CHON+ Compounds
A series of CHON+ compounds that differ by CH_2O identified in the modified N based van Krevelen (Figure 5-3).

$^{+}m/z$ (measured)	Formula $[M+H]^+$	DBE	H:C	N:C	O:C
162.07607	$C_6H_{12}N_1O_4$	2	1.83	0.17	0.67
192.08666	$C_7H_{14}N_1O_5$	2	1.86	0.14	0.71
222.09721	$C_8H_{16}N_1O_6$	2	1.88	0.13	0.75
252.10777	$C_9H_{18}N_1O_7$	2	1.89	0.11	0.75
282.11832	$C_{10}H_{20}N_1O_8$	2	1.90	0.10	0.80

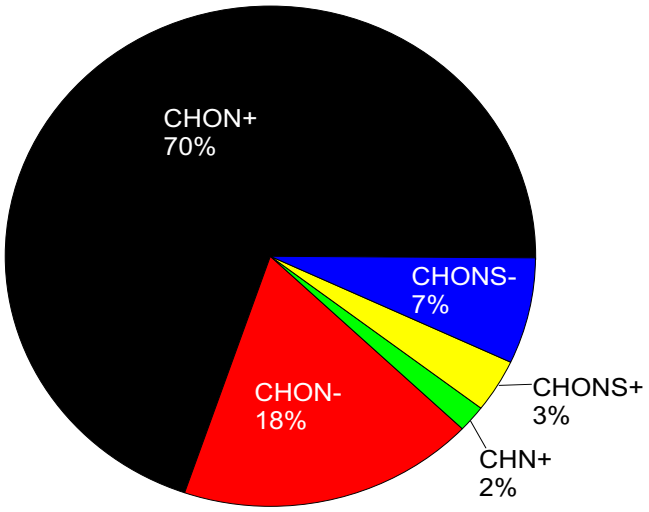

Figure 5-1 Comparison of the Number of Nitrogen Containing Elemental Formulas in Compound Classes

The number of each type of elemental formula detected in the rainwater samples that contained N (positive ion mode $^{+}m/z$ 50-300 and negative ion mode $^{-}m/z$ 50-500). There were 402 N containing compounds detected.

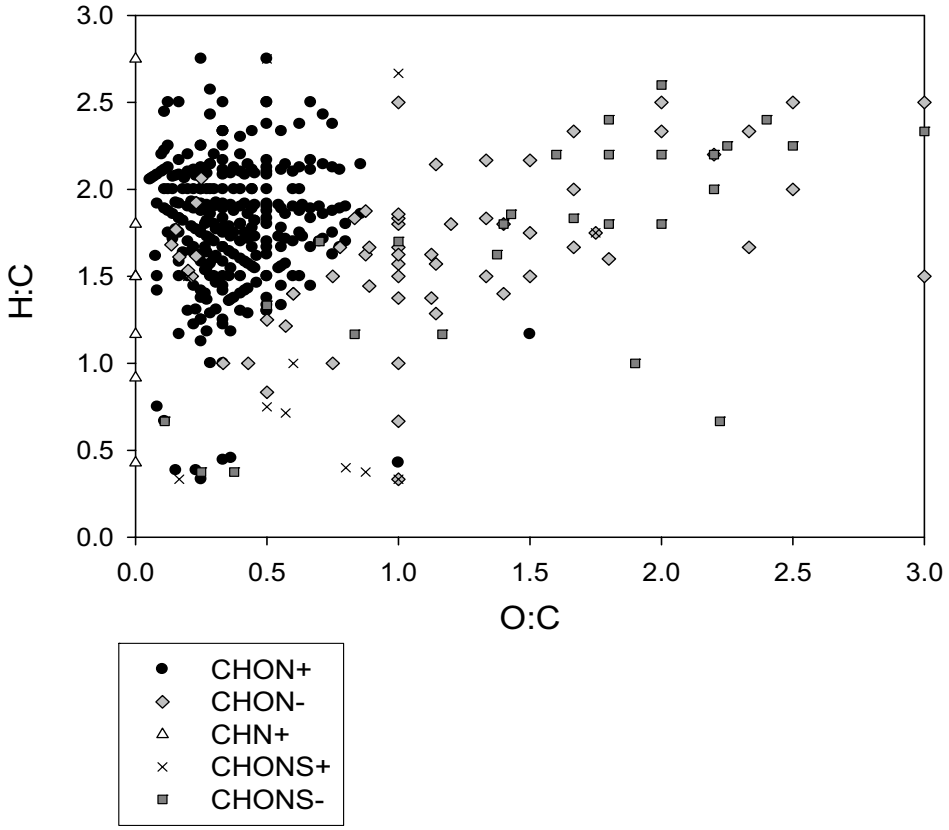

Figure 5-2 Van Krevelen of the N Containing Compounds in Rainwater
The elemental ratios of the N containing compounds (positive and negative ion mode) detected in the rainwater.

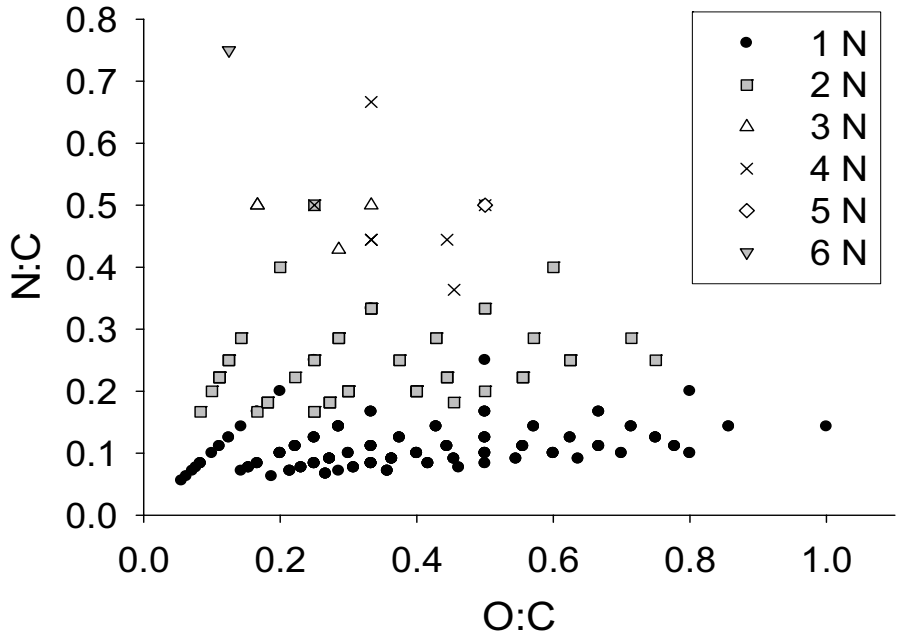

Figure 5-3 Nitrogen Based van Krevelen of the Rainwater DON
The elemental ratios of only the CHON+ compounds detected in the rainwater. The legend denotes the number of N atoms on the molecule.

REFERENCES

Alfarra, M. R., Paulsen, D., Gysel, M., Garforth, A. A., Dommen, J., Prevot, A. S. H., Worsnop, D. R., Baltensperger, U., and Coe, H.: A mass spectrometric study of secondary organic aerosols formed from the photooxidation of anthropogenic and biogenic precursors in a reaction chamber, Atmospheric Chemistry and Physics, 6, 5279-5293, 2006.

Altieri, K. E., Carlton, A. G., Lim, H. J., Turpin, B. J., and Seitzinger, S. P.: Evidence for oligomer formation in clouds: Reactions of isoprene oxidation products, Environmental Science & Technology, 40, 4956-4960, 2006.

Altieri, K. E., Seitzinger, S. P., Carlton, A. G., Turpin, B. J., Klein, G. C., and Marshall, A. G.: Oligomers formed through in-cloud methylglyoxal reactions: Chemical composition, properties, and mechanisms investigated by ultra-high resolution FT-ICR mass spectrometry, Atmos. Environ., 42, 1476-1490, 10.1016/j.atmosenv.2007.11.015|ISSN 1352-2310, 2008.

Altieri, K. E., Turpin, B.J., Seitzinger, S.P.: Oligomers, organosulfates, and nitroxy organosulfates in rainwater identified by ultra-high resolution electrospray ionization FT-ICR mass spectrometry, Atmospheric Chemistry and Physics Discussions, 8, 27, 2008.

Anderson, C., Dibb, J. E., Griffin, R. J., and Bergin, M. H.: Simultaneous measurements of particulate and gas-phase water-soluble organic carbon concentrations at remote and urban-influenced locations, Geophysical Research Letters, 35, L13706 10.1029/2008gl033966, 2008.

Andreae, M. O., Talbot, R. W., Andreae, T. W., and Harriss, R. C.: Formic and acetic acid over the central Amazon region, Brazil 1. Dry season, Journal of Geophysical Research, 93, 1616-1624, 1988.

Atkinson, R.: Atmospheric chemistry of VOCs and NOx, Atmos. Environ., 34, 2063-2101, 2000.

Atkinson, R., and Arey, J.: Gas-phase tropospheric chemistry of biogenic volatile organic compounds: a review, Atmos. Environ., 37, 197-219, 2003.

Avery, G. B., Willey, J. D., and Wilson, C. A.: Formic and acetic acids in coastal north carolina rainwater, Environmental Science & Technology, 25, 1875-1880, 1991.

Avery, G. B., Tang, Y., Kieber, R. J., and Willey, J. D.: Impact of recent urbanization on formic and acetic acid concentrations in coastal North Carolina rainwater, Atmos. Environ., 35, 3353-3359, 2001.

Avery, G. B., Willey, J. D., Kieber, R. J., Shank, G. C., and Whitehead, R. F.: Flux and bioavailability of Cape Fear River and rainwater dissolved organic carbon to Long Bay, southeastern United States, Global Biogeochem. Cycles, 17, 2003.

Avery, G. B., Cooper, W. J., Kieber, R. J., and Willey, J. D.: Hydrogen peroxide at the Bermuda Atlantic Time Series Station: Temporal variability of seawater hydrogen peroxide, Mar. Chem., 97, 236-244, 2005.

Avery, G. B., Kieber, R. J., Witt, M., and Willey, J. D.: Rainwater monocarboxylic and dicarboxylic acid concentrations in southeastern North Carolina, USA, as a function of air-mass back-trajectory, Atmos. Environ., 40, 1683-1693, 2006.

Barsanti, K. C., and Pankow, J. F.: Thermodynamics of the formation of atmospheric organic particulate matter by accretion reactions - Part 3: Carboxylic and dicarboxylic acids, Atmos. Environ., 40, 6676-6686, 2006.

Bigelow, D. S., Dossett, S.R., Bowersox, V.C.: Instruction manual NADP/NTN site selection and installation, National Atmospheric Deposition Program, 2001.

Blando, J. D., and Turpin, B. J.: Secondary organic aerosol formation in cloud and fog droplets: a literature evaluation of plausibility, Atmos. Environ., 34, 1623-1632, 2000.

Carlton, A. G.: Secondary organic aerosol (SOA) formation through cloud processing: Aqueous photooxidation of glyoxal and methylglyoxal PhD, Environmental Science, Rutgers, The State University of New Jersey, New Brunswick, 237 pp., 2006.

Carlton, A. G., Turpin, B. J., Lim, H. J., Altieri, K. E., and Seitzinger, S.: Link between isoprene and secondary organic aerosol (SOA): Pyruvic acid oxidation yields low volatility organic acids in clouds, Geophysical Research Letters, 33, L06822, 2006.

Carlton, A. G., Turpin, B. J., Altieri, K. E., Seitzinger, S., Reff, A., Lim, H.-J., and Ervens, B.: Atmospheric oxalic acid and SOA production from glyoxal: Results of aqueous photooxidation experiments, Atmos. Environ., In Press, Corrected Proof, doi:10.1016/j.atmosenv.2007.05.035, 2007.

Carlton, A. G., Turpin, B. J., Altieri, K. E., Seitzinger, S. P., Mathur, R., Roselle, S. J., and Weber, R. J.: CMAQ Model Performance Enhanced When In-Cloud Secondary Organic Aerosol is Included: Comparisons of Organic Carbon Predictions with Measurements, Environmental Science & Technology, 42, 8798-8802, 10.1021/es801192n, 2008.

Chan, M. N., Choi, M. Y., Ng, N. L., and Chan, C. K.: Hygroscopicity of water-soluble organic compounds in atmospheric aerosols: Amino acids and biomass burning derived organic species, Environmental Science & Technology, 39, 1555-1562, 2005.

Chebbi, A., and Carlier, P.: Carboxylic acids in the troposphere, occurrence, sources, and sinks: A review, Atmos. Environ., 30, 4233-4249, 1996.

Chen, J., Griffin, R. J., Grini, A., and Tulet, P.: Modeling secondary organic aerosol formation through cloud processing of organic compounds, Atmospheric Chemistry and Physics, 7, 5343-5355, 2007.

Claxton, L. D., Matthews, P. P., and Warren, S. H.: The genotoxicity of ambient outdoor air, a review: Salmonella mutagenicity, Mutation Research-Reviews in Mutation Research, 567, 347-399, 2004.

Cornell, S., Rendell, A., and Jickells, T.: Atmospheric Inputs of Dissolved Organic Nitrogen to the Oceans, Nature, 376, 243-246, 1995.

Cornell, S., Mace, K., Coeppicus, S., Duce, R., Huebert, B., Jickells, T., and Zhuang, L. Z.: Organic nitrogen in Hawaiian rain and aerosol, Journal of Geophysical Research-Atmospheres, 106, 7973-7983, 2001.

Cornell, S. E., Jickells, T. D., and Thornton, C. A.: Urea in rainwater and atmospheric aerosol, Atmos. Environ., 32, 1903-1910, 1998.

Cornell, S. E., and Jickells, T. D.: Water-soluble organic nitrogen in atmospheric aerosol: a comparison of UV and persulfate oxidation methods, Atmos. Environ., 33, 833-840, 1999.

Cornell, S. E., Jickells, T. D., Cape, J. N., Rowland, A. P., and Duce, R. A.: Organic nitrogen deposition on land and coastal environments: a review of methods and data, Atmos. Environ., 37, 2173-2191, 2003.

Cox, F. J., Johnston, M. V., Qian, K., and Peiffer, D. G.: Compositional analysis of isobutylene/p-methylstyrene copolymers by matrix-assisted laser desorption/ionization mass spectrometry, J. Am. Soc. Mass. Spectrom., 15, 681-688, 10.1016/j.jasms.2003.12.017, 2004.

Crahan, K. K., Hegg, D., Covert, D. S., and Jonsson, H.: An exploration of aqueous oxalic acid production in the coastal marine atmosphere, Atmos. Environ., 38, 3757-3764, 2004.

de Gouw, J. A., Middlebrook, A. M., Warneke, C., Goldan, P. D., Kuster, W. C., Roberts, J. M., Fehsenfeld, F. C., Worsnop, D. R., Canagaratna, M. R., Pszenny, A. A. P., Keene, W. C., Marchewka, M., Bertman, S. B., and Bates, T. S.: Budget of organic carbon in a polluted atmosphere: Results from the New England Air Quality Study in 2002, Journal of Geophysical Research-Atmospheres, 110, D16305 10.1029/2004jd005623, 2005.

Decesari, S., Facchini, M. C., Fuzzi, S., and Tagliavini, E.: Characterization of water-soluble organic compounds in atmospheric aerosol: A new approach, Journal of Geophysical Research-Atmospheres, 105, 1481-1489, 2000.

Decesari, S., Facchini, M. C., Mircea, M., Cavalli, F., and Fuzzi, S.: Solubility properties of surfactants in atmospheric aerosol and cloud/fog water samples, Journal of Geophysical Research-Atmospheres, 108, 2003.

Denkenberger, K. A., Moffet, R. C., Holecek, J. C., Rebotier, T. P., and Prather, K. A.: Real-Time, Single-Particle Measurements of Oligomers in Aged Ambient Aerosol Particles, Environ. Sci. Technol., 41, 5439-5446, 2007.

Dinar, E., Taraniuk, I., Graber, E. R., Katsman, S., Moise, T., Anttila, T., Mentel, T. F., and Rudich, Y.: Cloud Condensation Nuclei properties of model and atmospheric HULIS, Atmospheric Chemistry and Physics, 6, 2465-2481, 2006.

Dinar, E., Riziq, A. A., Spindler, C., Erlick, C., Kiss, G., and Rudich, Y.: The complex refractive index of atmospheric and model humic-like substances (HULIS) retrieved by a cavity ring down aerosol spectrometer (CRD-AS), Faraday Discuss., 137, 279-295, 10.1039/b703111d, 2008.

Dittmar, T., Fitznar, H. P., and Kattner, G.: Origin and biogeochemical cycling of organic nitrogen in the eastern Arctic Ocean as evident from D- and L-amino acids, Geochim. Cosmochim. Acta, 65, 4103-4114, 2001.

Dommen, J., Metzger, A., Duplissy, J., Kalberer, M., Alfarra, M. R., Gascho, A., Weingartner, E., Prevot, A. S. H., Verheggen, B., and Baltensperger, U.: Laboratory observation of oligomers in the aerosol from isoprene/NOx photooxidation, Geophysical Research Letters, 33, L13805
Artn l13805, 2006.

Duce, R. A., LaRoche, J., Altieri, K., Arrigo, K. R., Baker, A. R., Capone, D. G., Cornell, S., Dentener, F., Galloway, J., Ganeshram, R. S., Geider, R. J., Jickells, T., Kuypers, M. M., Langlois, R., Liss, P. S., Liu, S. M., Middelburg, J. J., Moore, C. M., Nickovic, S., Oschlies, A., Pedersen, T., Prospero, J., Schlitzer, R., Seitzinger, S., Sorensen, L. L., Uematsu, M., Ulloa, O., Voss, M., Ward, B., and Zamora, L.: Impacts of atmospheric anthropogenic nitrogen on the open ocean, Science, 320, 893-897, 10.1126/science.1150369|ISSN 0036-8075, 2008.

El-Zanan, H. S., Lowenthal, D. H., Zielinska, B., Chow, J. C., and Kumar, N.: Determination of the organic aerosol mass to organic carbon ratio in IMPROVE samples, Chemosphere, 60, 485-496, 2005.

EPA: Air quality criteria for particulate matter, U.S. Government Printing Office, Washington D.C.1, 2004.

Ervens, B., George, C., Williams, J. E., Buxton, G. V., Salmon, G. A., Bydder, M., Wilkinson, F., Dentener, F., Mirabel, P., Wolke, R., and Herrmann, H.: CAPRAM 2.4 (MODAC mechanism): An extended and condensed tropospheric aqueous phase mechanism and its application, Journal of Geophysical Research-Atmospheres, 108, 4426 Artn 4426, 2003.

Ervens, B., Feingold, G., Frost, G. J., and Kreidenweis, S. M.: A modeling study of aqueous production of dicarboxylic acids: Chemical pathways and speciated organic mass production, Journal of Geophysical Research-Atmospheres, 109, D15205, 2004.

Ervens, B., Carlton, A. G., Turpin, B. J., Altieri, K. E., Kreidenweis, S. M., and Feingold, G.: Secondary organic aerosol yields from cloud-processing of isoprene oxidation products, Geophysical Research Letters, 35, L02816
10.1029/2007gl031828, 2008.

Feng, J., and Moller, D.: Characterization of water-soluble macromolecular substances in cloud water, Journal of Atmospheric Chemistry, 48, 217-233, 2004a.

Feng, J. S., and Moller, D.: Characterization of water-soluble macromolecular substances in cloud water, Journal of Atmospheric Chemistry, 48, 217-233, 2004b.

Fu, T. M., Jacob, D. J., Wittrock, F., Burrows, J. P., Vrekoussis, M., and Henze, D. K.: Global budgets of atmospheric glyoxal and methylglyoxal, and implications for formation of secondary organic aerosols, Journal of Geophysical Research-Atmospheres, 113, D15303
10.1029/2007jd009505, 2008.

Galloway, J. N., Aber, J. D., Erisman, J. W., Seitzinger, S. P., Howarth, R. W., Cowling, E. B., and Cosby, B. J.: The nitrogen cascade, Bioscience, 53, 341-356, 2003.

Galloway, J. N., Dentener, F. J., Capone, D. G., Boyer, E. W., Howarth, R. W., Seitzinger, S. P., Asner, G. P., Cleveland, C. C., Green, P. A., Holland, E. A., Karl, D. M., Michaels, A. F., Porter, J. H., Townsend, A. R., and Vorosmarty, C. J.: Nitrogen cycles: past, present, and future, Biogeochemistry, 70, 153-226, 2004.

Galloway, M. M., Chhabra, P.S., Chan, A.W.H., Surratt, J.D., Flagan, R.C., Seinfeld, J.H., Keutsch, F.N.: Glyoxal uptake on ammonium sulphate seed aerosol: reaction products and reversibility of uptake under dark and irradiated conditions, Atmospheric Chemistry and Physics Discussions, 8, 39, 2008.

Gao, S., Keywood, M., Ng, N. L., Surratt, J., Varutbangkul, V., Bahreini, R., Flagan, R. C., and Seinfeld, J. H.: Low-molecular-weight and oligomeric components in secondary organic aerosol from the ozonolysis of cycloalkenes and alpha-pinene, J. Phys. Chem. A, 108, 10147-10164, 2004a.

Gao, S., Ng, N. L., Keywood, M., Varutbangkul, V., Bahreini, R., Nenes, A., He, J. W., Yoo, K. Y., Beauchamp, J. L., Hodyss, R. P., Flagan, R. C., and Seinfeld, J. H.: Particle phase acidity and oligomer formation in secondary organic aerosol, Environmental Science & Technology, 38, 6582-6589, 2004b.

Gao, S., Surratt, J. D., Knipping, E. M., Edgerton, E. S., Shahgholi, M., and Seinfeld, J. H.: Characterization of polar organic components in fine aerosols in the southeastern United States: Identity, origin, and evolution, Journal of Geophysical Research-Atmospheres, 111, 2006.

Gelencser, A., Meszaros, T., Blazso, M., Kiss, G., Krivacsy, Z., Molnar, A., and Meszaros, E.: Structural characterisation of organic matter in fine tropospheric aerosol by pyrolysis-gas chromatography-mass spectrometry, Journal of Atmospheric Chemistry, 37, 173-183, 2000a.

Gelencser, A., Sallai, M., Krivacsy, Z., Kiss, G., and Meszaros, E.: Voltammetric evidence for the presence of humic-like substances in fog water, Atmospheric Research, 54, 157-165, 2000b.

Gelencser, A., Hoffer, A., Kiss, G., Tombacz, E., Kurdi, R., and Bencze, L.: In-situ formation of light-absorbing organic matter in cloud water, Journal of Atmospheric Chemistry, 45, 25-33, 2003.

Gelencser, A., and Varga, Z.: Evaluation of the atmospheric significance of multiphase reactions in atmospheric secondary organic aerosol formation, Atmospheric Chemistry and Physics, 5, 2823-2831, 2005.

Gors, S., Rentsch, D., Schiewer, U., Karsten, U., and Schumann, R.: Dissolved organic matter along the eutrophication gradient of the Dar beta-Zingst Bodden Chain, Southern Baltic Sea: I. Chemical characterisation and composition, Mar. Chem., 104, 125-142, 2007.

Gorzelska, K., Galloway, J. N., Watterson, K., and Keene, W. C.: Water-soluble primary amine compounds in rural continental precipitation, Atmos. Environ., 26A, 1005-1018, 1992.

Graber, E. R., and Rudich, Y.: Atmospheric HULIS: How humic-like are they? A comprehensive and critical review, Atmospheric Chemistry and Physics, 6, 729-753, 2006.

Graedel, T. E., Hawkins, D. T., and Claxton, L. D.: Atmospheric chemical compounds: Sources, occurrence, and bioassay, Academic Press, Inc., Orlando, 1986.

Guzman, M. I., Colussi, A. I., and Hoffmann, M. R.: Photoinduced oligomerization of aqueous pyruvic acid, J. Phys. Chem. A, 110, 3619-3626, 2006.

Hallquist, M., Wenger, J.C., Baltensperger, U., Rudich, Y., Simpson, D., Claeys, M., Dommen, J., Donahue, N.M., George, C., Goldstein, A.H., Hamilton, J.F., Herrmann, H., Hoffmann, T., Iinuma, Y., Jang, M., Jenkin, M., Jimenez, J.L., Kiendler-Scharr, A., Maenhaut, W., McFiggans, G., Mentel, Th.F., Monod, A., Prevot, A.S.H., Seinfeld, J.H., Surratt, J.D., Szmigielski, R., Wildt, J.: The formation, properties and impact of secondary organic aerosol: current and emerging issues, Atmospheric Chemistry and Physics Discussions, 9, 207, 2009.

Ham, J. E., Proper, S. P., and Wells, J. R.: Gas-phase chemistry of citronellol with ozone and OH radical: Rate constants and products, Atmos. Environ., 40, 726-735, 2006.

Hastings, W. P., Koehler, C. A., Bailey, E. L., and DeHaan, D. O.: Secondary Organic Aerosol Formation by Glyoxal Hydration and Oligomer Formation: Humidity Effects and Equilibrium Shifts during Analysis, Environmental Science & Technology, 39, 8728-8735, 2005.

Heald, C. L., Jacob, D. J., Turquety, S., Hudman, R. C., Weber, R. J., Sullivan, A. P., Peltier, R. E., Atlas, E. L., de Gouw, J. A., Warneke, C., Holloway, J. S., Neuman, J. A., Flocke, F. M., and Seinfeld, J. H.: Concentrations and sources of organic carbon aerosols in the free troposphere over North America, Journal of Geophysical Research-Atmospheres, 111, D23S47, D23s47
Artn d23s47, 2006.

Henze, D. K., and Seinfeld, J. H.: Global secondary organic aerosol from isoprene oxidation, Geophysical Research Letters, 33, L09812, L09812
Artn l09812, 2006.

Hoffer, A., Gelencser, A., Guyon, P., Kiss, G., Schmid, O., Frank, G. P., Artaxo, P., and Andreae, M. O.: Optical properties of humic-like substances (HULIS) in biomass-burning aerosols, Atmospheric Chemistry and Physics, 6, 3563-3570, 2006.

Holmes, B. J., and Petrucci, G. A.: Water-Soluble Oligomer Formation from Acid-Catalyzed Reactions of Levoglucosan in Proxies of Atmospheric Aqueous Aerosols, Environmental Science & Technology, 40, 4983-4989, 2006.

Howarth, R. W., Swaney, D. P., Butler, T. J., and Marino, R.: Climatic control on eutrophication of the Hudson River estuary, Ecosystems, 3, 210-215, 2000.

Hung, H. M., Katrib, Y., and Martin, S. T.: Products and Mechanisms of the Reaction of Oleic Acid with Ozone and Nitrate Radical, J. Phys. Chem. A, 109, 4517-4530, 2005.

Iinuma, Y., Muller, C., Boge, O., Gnauk, T., and Herrmann, H.: The formation of organic sulfate esters in the limonene ozonolysis secondary organic aerosol (SOA) under acidic conditions, Atmos. Environ., 41, 5571-5583, 10.1016/j.atmosenv.2007.03.007|ISSN 1352-2310, 2007.

IPCC: Climate Change: The scientific basis, Cambridge University Press, UK, 2001.

IPCC: Climate Change: The scientific basis, Cambridge University Press, UK, 2007.

Jang, M., and Kamens, R. M.: Characterization of secondary aerosol from the photooxidation of toluene in the presence of NOx and 1-Propene, Environmental Science & Technology, 35, 3626-3639, 2001.

Jang, M., Czoschke, N. M., Lee, S., and Kamens, R. M.: Heterogeneous Atmospheric Aerosol Production by Acid-Catalyzed Particle-Phase Reactions, Science, 298, 814-817, 2002.

Jickells, T.: The role of air-sea exchange in the marine nitrogen cycle, Biogeosciences, 3, 271-280, 2006.

Kalberer, M., Paulsen, D., Sax, M., Steinbacher, M., Dommen, J., Prevot, A. S. H., Fisseha, R., Weingartner, E., Frankevich, V., Zenobi, R., and Baltensperger, U.: Identification of polymers as major components of atmospheric organic aerosols, Science, 303, 1659-1662, 2004.

Kanakidou, M., Seinfeld, J. H., Pandis, S. N., Barnes, I., Dentener, F. J., Facchini, M. C., van Dingenen, R., Ervens, B., Nenes, A., Nielsen, C. J., Swietlicki, E., Putaud, J. P., Balkanski, Y., Fuzzi, S., Horth, J., Moortgat, G. K., Winterhalter, R., Myhre, C. E. L., Tsigaridis, K., Vignati, E., Stephanou, E. G., and Wilson, J.: Organic aerosol and global climate modelling: a review, Atmospheric Chemistry and Physics Discussions, 4, 5855-6024, 2004.

Kanakidou, M., Seinfeld, J. H., Pandis, S. N., Barnes, I., Dentener, F. J., Facchini, M. C., Van Dingenen, R., Ervens, B., Nenes, A., Nielsen, C. J., Swietlicki, E., Putaud, J. P., Balkanski, Y., Fuzzi, S., Horth, J., Moortgat, G. K., Winterhalter, R., Myhre, C. E. L., Tsigaridis, K., Vignati, E., Stephanou, E. G., and Wilson, J.: Organic aerosol and global climate modelling: a review, Atmospheric Chemistry and Physics, 5, 1053-1123, 2005.

Kawahata, H., and Ishizuka, T.: Amino acids in interstitial waters from ODP Sites 689 and 690 on the Maud Rise, Antarctic Ocean, Geochem. J., 34, 247-261, 2000.

Kawamura, K., Kasukabe, H., and Barrie, L. A.: Source and reaction pathways of dicarboxylic acids, ketoacids and dicarbonyls in arctic aerosols: One year of observations, Atmos. Environ., 30, 1709-1722, 1996a.

Kawamura, K., Steinberg, S., and Kaplan, I. R.: Concentrations of monocarboxylic and dicarboxylic acids and aldehydes in southern California wet precipitations: Comparison

of urban and nonurban samples and compositional changes during scavenging, Atmos. Environ., 30, 1035-1052, 1996b.

Kawamura, K., and Yasui, O.: Diurnal changes in the distribution of dicarboxylic acids, ketocarboxylic acids and dicarbonyls in the urban Tokyo atmosphere, Atmos. Environ., 39, 1945-1960, 2005.

Kieber, R. J., Rhines, M. F., Willey, J. D., and Avery, G. B.: Nitrite variability in coastal North Carolina rainwater and its impact on the nitrogen cycle in rain, Environmental Science & Technology, 33, 373-377, 1999.

Kieber, R. J., Peake, B., Willey, J. D., and Avery, G. B.: Dissolved organic carbon and organic acids in coastal New Zealand rainwater, Atmos. Environ., 36, 3557-3563, 2002.

Kieber, R. J., Long, M. S., and Willey, J. D.: Factors influencing nitrogen speciation in coastal rainwater, Journal of Atmospheric Chemistry, 52, 81-99, 2005.

Kim, S., Kaplan, L.A., Hatcher, P.G. : Biodegradable dissolved organic matter in a temperate and a tropical stream determined from ultra-high resolution mass spectrometry, Limnol. Oceanogr., 51, 1054-1063, 2006.

Kiss, G., Varga, B., Galambos, I., and Ganszky, I.: Characterization of water-soluble organic matter isolated from atmospheric fine aerosol, Journal of Geophysical Research-Atmospheres, 107, 8339, 2002.

Kiss, G., Tombacz, E., and Hansson, H. C.: Surface tension effects of humic-like substances in the aqueous extract of tropospheric fine aerosol, Journal of Atmospheric Chemistry, 50, 279-294, 10.1007/s10874-005-5079-5, 2005.

Koch, B. P., Witt, M. R., Engbrodt, R., Dittmar, T., and Kattner, G.: Molecular formulae of marine and terrigenous dissolved organic matter detected by electrospray ionization Fourier transform ion cyclotron resonance mass spectrometry, Geochim. Cosmochim. Acta, 69, 3299-3308, 2005.

Krivacsy, Z., Kiss, G., Varga, B., Galambos, I., Sarvari, Z., Gelencser, A., Molnar, A., Fuzzi, S., Facchini, M. C., Zappoli, S., Andracchio, A., Alsberg, T., Hansson, H. C., and Persson, L.: Study of humic-like substances in fog and interstitial aerosol by size-exclusion chromatography and capillary electrophoresis, Atmos. Environ., 34, 4273-4281, 2000.

Kroll, J. H., Ng, N. L., Murphy, S. M., Flagan, R. C., and Seinfeld, J. H.: Secondary organic aerosol formation from isoprene photooxidation, Environmental Science & Technology, 40, 1869-1877, 2006.

Kujawinski, E. B.: Electrospray ionization Fourier transform ion cyclotron resonance mass spectrometry (ESI FT-ICR MS): characterization of complex environmental mixtures, Environmental Forensics, 3, 207-216, 2002.

Kujawinski, E. B., Hatcher, P. G., and Freitas, M. A.: High-resolution Fourier transform ion cyclotron resonance mass spectrometry of humic and fulvic acids: Improvements and comparisons, Anal. Chem., 74, 413-419, 2002.

Lamb, D., and Bowersox, V.: The national atmospheric deposition program: an overview, Atmos. Environ., 34, 1661-1663, 2000.

Liggio, J., Li, S. M., and McLaren, R.: Heterogeneous reactions of glyoxal on particulate matter: Identification of acetals and sulfate esters, Environmental Science & Technology, 39, 1532-1541, 2005.

Likens, G. E., E.S. Edgerton, Galloway, J.N.: The composition and deposition of organic carbon in precipitation, Tellus, 35B, 16-24, 1983.

Lim, H. J., and Turpin, B. J.: Origins of primary and secondary organic aerosol in Atlanta: Results' of time-resolved measurements during the Atlanta supersite experiment, Environmental Science & Technology, 36, 4489-4496, 10.1021/es0206487, 2002.

Lim, H. J., Carlton, A. G., and Turpin, B. J.: Isoprene Forms Secondary Organic Aerosol through Cloud Processing: Model Simulations, Environmental Science & Technology, 39, 4441-4446, 2005.

Loeffler, K. W., Koehler, C. A., Paul, N. M., and De Haan, D. O.: Oligomer formation in evaporating aqueous glyoxal and methyl glyoxal solutions, Environmental Science & Technology, 40, 6318-6323, 2006.

Mace, K. A., Artaxo, P., and Duce, R. A.: Water-soluble organic nitrogen in Amazon Basin aerosols during the dry (biomass burning) and wet seasons, Journal of Geophysical Research-Atmospheres, 108, 2003a.

Mace, K. A., Duce, R. A., and Tindale, N. W.: Organic nitrogen in rain and aerosol at Cape Grim, Tasmania, Australia, Journal of Geophysical Research-Atmospheres, 108, 2003b.

Marshall, A. G.: Fourier-Transform Ion-Cyclotron Resonance Mass-Spectrometry Retrospect and Prospects, Abstracts of Papers of the American Chemical Society, 209, 78-ANYL, 1995.

Marshall, A. G., and Guan, S. H.: Advantages of high magnetic field for Fourier transform ion cyclotron resonance mass spectrometry, Rapid Commun. Mass Spectrom., 10, 1819-1823, 1996.

Marshall, A. G.: FT-ICR mass spectrometry at high magnetic field, Abstracts of Papers of the American Chemical Society, 213, 195-ANYL, 1997.

Marshall, A. G., Hendrickson, C. L., and Jackson, G. S.: Fourier transform ion cyclotron resonance mass spectrometry: A primer, Mass Spectrom. Rev., 17, 1-35, 1998.

Marshall, A. G.: Milestones in Fourier transform ion cyclotron resonance mass spectrometry technique development, Int. J. Mass spectrom., 200, 331-356, 2000.

Martinelango, P. K., Dasgupta, P. K., and Al-Horr, R. S.: Atmospheric production of oxalic acid/oxalate and nitric acid/nitrate in the Tampa Bay airshed: Parallel pathways, Atmos. Environ., 41, 4258-4269, 2007.

Matsumoto, K., Kawai, S., and Igawa, M.: Dominant factors controlling concentrations of aldehydes in rain, fog, dew water, and in the gas phase, Atmos. Environ., 39, 7321-7329, 2005.

Matsumoto, K., and Uematsu, M.: Free amino acids in marine aerosols over the western North Pacific Ocean, Atmos. Environ., 39, 2163-2170, 2005.

McFiggans, G., Artaxo, P., Baltensperger, U., Coe, H., Facchini, M. C., Feingold, G., Fuzzi, S., Gysel, M., Laaksonen, A., Lohmann, U., Mentel, T. F., Murphy, D. M., O'Dowd, C. D., Snider, J. R., and Weingartner, E.: The effect of physical and chemical aerosol properties on warm cloud droplet activation, Atmospheric Chemistry and Physics, 6, 2593-2649, 2006.

McLafferty, F. W., Turecek, F.: Interpretation of Mass Spectra, 4 ed., University Science Books, Mill Valley, 1993.

Mopper, K., and Zimmermann, F.: Free amino acids in marine rains: evidence for oxidation and potential role in nitrogen cycling, Nature, 325, 246-249, 1987.

Munger, J. W., Jacob, D. J., Daube, B. C., Horowitz, L. W., Keene, W. C., and Heikes, B. G.: Formaldehyde, glyoxal, and methylglyoxal in air and cloud water at a rural mountain site in central Virginia, Journal of Geophysical Research-Atmospheres, 100, 9325-9333, 1995.

Neff, J. C., Holland, E. A., Dentener, F. J., McDowell, W. H., and Russell, K. M.: The origin, composition and rates of organic nitrogen deposition: A missing piece of the nitrogen cycle?, Biogeochemistry, 57, 99-136, 2002.

Nielen, M. W. F.: Maldi time-of-flight mass spectrometry of synthetic polymers, Mass Spectrom. Rev., 18, 309-344, 1999.

Noziere, B., Dziedzic, P., Cordova, A.: Common inorganic ions are efficient catalysts for organic reactions in atmospheric aerosols and other natural environments, Atmospheric Chemistry and Physics Discussions, 9, 21, 2009.

Paerl, H. W., Willey, J. D., Go, M., Peierls, B. L., Pinckney, J. L., and Fogel, M. L.: Rainfall stimulation of primary production in western Atlantic Ocean waters: roles of different nitrogen sources and co-limiting nutrients, Marine Ecology-Progress Series, 176, 205-214, 1999.

Pang, Y., Turpin, B. J., and Gundel, L. A.: On the importance of organic oxygen for understanding organic aerosol particles, Aerosol Sci. Technol., 40, 128-133, 2006.

Peierls, B. L., and Paerl, H. W.: Bioavailability of atmospheric organic nitrogen deposition to coastal phytoplankton, Limnology and Oceanography, 42, 1819-1823, 1997.

Pena, R. M., Garcia, S., Herrero, C., Losada, M., Vazquez, A., and Lucas, T.: Organic acids and aldehydes in rainwater in a northwest region of Spain, Atmos. Environ., 36, 5277-5288, 2002.

Pettine, M., Patrolecco, L., Manganelli, M., Capri, S., and Farrace, M. G.: Seasonal variations of dissolved organic matter in the northern Adriatic Sea, Mar. Chem., 64, 153-169, 1999.

Polidori, A., Turpin, B. J., Lim, H. J., Cabada, J. C., Subramanian, R., Robinson, A. L., and Pandis, S. N.: Local and regional secondary organic aerosol: Insights from a year of semi-continuous carbon measurements at Pittsburgh, Aerosol Sci. Technol., 2005.

Poulain, L., Monod, A., Worthham, H.: Development of a new on-line mass spectrometer to study the reactivity of soluble organic compounds in the aqueous phase under tropospheric conditions: Application to OH-oxidation of N-methylpyrrolidone, J. Photochemistry and Photobiology A: Chemistry, doi:10.1016/j.jphotochem.2006.1009.1006, 2006.

Raymond, P. A.: The composition and transport of organic carbon in rainfall: Insights from the natural (C-13 and C-14) isotopes of carbon, Geophysical Research Letters, 32, 2005.

Reemtsma, T., These, A., Springer, A., and Linscheid, M.: Fulvic acids as transition state of organic matter: Indications from high resolution mass spectrometry, Environmental Science & Technology, 40, 5839-5845, 2006a.

Reemtsma, T., These, A., Venkatachari, P., Xia, X. Y., Hopke, P. K., Springer, A., and Linscheid, M.: Identification of fulvic acids and sulfated and nitrated analogues in atmospheric aerosol by electrospray ionization Fourier transform ion cyclotron resonance mass spectrometry, Anal. Chem., 78, 8299-8304, 2006b.

Reinhardt, A., Emmenegger, C., Gerrits, B., Panse, C., Dommen, J., Baltensperger, U., Zenobi, R., and Kalberer, M.: Ultrahigh Mass Resolution and Accurate Mass Measurements as a Tool To Characterize Oligomers in Secondary Organic Aerosols, Anal. Chem., 2007.

Rogge, W. F., Hildemann, L. M., Mazurek, M. A., Cass, G. R., and Simoneit, B. R. T.: Sources of Fine Organic Aerosol .4. Particulate Abrasion Products from Leaf Surfaces of Urban Plants, Environmental Science & Technology, 27, 2700-2711, 1993.

Saxena, P., and Hildemann, L. M.: Water-soluble organics in atmospheric particles: A critical review of the literature and application of thermodynamics to identify candidate compounds, Journal of Atmospheric Chemistry, 24, 57-109, 1996.

Schneider, M., Luxenhofer, O., Deissler, A., and Ballschmiter, K.: C1-C15 Alkyl Nitrates, Benzyl Nitrate, and Bifunctional Nitrates: Measurements in California and South Atlantic Air and Global Comparison Using C2Cl4 and CHBr3 as Marker Molecules, Environmental Science & Technology, 32, 3055-3062, doi:10.1021/es980132g, 1998.

Seinfeld, J. H., and Pankow, J. F.: Organic atmospheric particulate material, Annu. Rev. Phys. Chem., 54, 121-140, 2003.

Seitzinger, S. P., and Sanders, R. W.: Atmospheric inputs of dissolved organic nitrogen stimulate estuarine bacteria and phytoplankton, Limnology and Oceanography, 44, 721-730, 1999.

Seitzinger, S. P., Styles, R. M., Lauck, R., and Mazurek, M. A.: Atmospheric pressure mass spectrometry: A new analytical chemical characterization method for dissolved organic matter in rainwater, Environmental Science & Technology, 37, 131-137, 2003.

Seitzinger, S. P., Hartnett, H., Lauck, R., Mazurek, M., Minegishi, T., Spyres, G., and Styles, R.: Molecular-Level Chemical Characterization and Bioavailability of Dissolved Organic Matter in Stream Water Using Electrospray-Ionization Mass Spectrometry, Limnology and Oceanography, 50, 1-12, 2005.

Senko, M. W., Hendrickson, C. L., PasaTolic, L., Marto, J. A., White, F. M., Guan, S. H., and Marshall, A. G.: Electrospray ionization Fourier transform ion cyclotron resonance at 9.4 T, Rapid Commun. Mass Spectrom., 10, 1824-1828, 1996.

Senko, M. W., Hendrickson, C. L., Emmett, M. R., Shi, S. D. H., and Marshall, A. G.: External accumulation of ions for enhanced electrospray ionization Fourier transform ion cyclotron resonance mass spectrometry, J. Am. Soc. Mass. Spectrom., 8, 970-976, 1997.

Sharp, J. H., Benner, R., Bennett, L., Carlson, C. A., Dow, R., and Fitzwater, S. E.: Re-Evaluation of High Temperature Combustion and Chemical Oxidation Measurements of Dissolved Organic Carbon in Seawater, Limnology and Oceanography, 38, 1774-1782, 1993.

Smith, D. F., Kleindienst, T. E., and McIver, C. D.: Primary product distributions from the reaction of OH with m-, p-xylene, 1,2,4- and 1,3,5-trimethylbenzene, Journal of Atmospheric Chemistry, 34, 339-364, 1999.

Sokal, R. R., Rohlf, F.J.: Biometry, in, 2 ed., Freeman, 1981.

Sommerville, K., and Preston, T.: Characterisation of dissolved combined amino acids in marine waters, Rapid Commun. Mass Spectrom., 15, 1287-1290, 2001.

Sorooshian, A., Ng, L., Chan, A. W. H., Feingold, G., Flagan, R. C., and Seinfeld, J. H.: Particulate organic acids and overall water-soluble aerosol composition measurements from the 2006 Gulf of Mexico Atmospheric Composition and Climate Study (GoMACCS), Journal of Geophysical Research-Atmospheres, 112, 2007.

Spokes, L. J., Yeatman, S. G., Cornell, S. E., and Jickells, T. D.: Nitrogen deposition to the eastern Atlantic Ocean. The importance of south-easterly flow, Tellus Series B-Chemical and Physical Meteorology, 52, 37-49, 2000.

Spokes, L. J., and Jickells, T. D.: Is the atmosphere really an important source of reactive nitrogen to coastal waters?, Continental Shelf Research, 25, 2022-2035, 2005.

Stefan, M. I., Hoy, A. R., and Bolton, J. R.: Kinetics and mechanism of the degradation and mineralization of acetone in dilute aqueous solution sensitized by the UV photolysis of hydrogen peroxide, Environmental Science & Technology, 30, 2382-2390, 1996.

Stefan, M. I., and Bolton, J. R.: Reinvestigation of the acetone degradation mechanism in dilute aqueous solution by the UV/H2O2 process, Environmental Science & Technology, 33, 870-873, 1999.

Surratt, J. D., Murphy, S. M., Kroll, J. H., Ng, N. L., Hildebrandt, L., Sorooshian, A., Szmigielski, R., Vermeylen, R., Maenhaut, W., Claeys, M., Flagan, R. C., and Seinfeld, J. H.: Chemical composition of secondary organic aerosol formed from the photooxidation of isoprene, J. Phys. Chem. A, 110, 9665-9690, 2006.

Surratt, J. D., Kroll, J. H., Kleindienst, T. E., Edney, E. O., Claeys, M., Sorooshian, A., Ng, N. L., Offenberg, J. H., Lewandowski, M., Jaoui, M., Flagan, R. C., and Seinfeld, J. H.: Evidence for organosulfates in secondary organic aerosol, Environmental Science & Technology, 41, 517-527, 2007.

Surratt, J. D., Gomez-Gonzalez, Y., Chan, A. W. H., Vermeylen, R., Shahgholi, M., Kleindienst, T. E., Edney, E. O., Offenberg, J. H., Lewandowski, M., Jaoui, M., Maenhaut, W., Claeys, M., Flagan, R. C., and Seinfeld, J. H.: Organosulfate Formation in Biogenic Secondary Organic Aerosol, J. Phys. Chem. A, 112, 8345-8378, 2008.

Talaska, G., Underwood, P., Maier, A., Lewtas, J., Rothman, N., and Jaeger, M.: Polycyclic aromatic hydrocarbons (PAHs), nitro-PAHs and related environmental

compounds: Biological markers of exposure and effects, 1996, ISI:A1996VU00500008, 901-906,

Timperley, M. H., Vigor-Brown, R. J., Kawashima, M., and Jickells, T.: Organic nitrogen compounds in atmospheric precipitation: Their chemistry and availability to phytoplankton, Continental Shelf Research, 42, 1171-1177, 1985.

Tolocka, M. P., Myoseon, J., Joy, M. G., Frederick, J. C., Richard, M. K., and Murray, V. J.: Formation of oligomers in secondary organic aerosol, Environmental Science & Technology, 38, 1428-1434, 2004.

Turpin, B. J., and Huntzicker, J. J.: Identification of Secondary Organic Aerosol Episodes and Quantitation of Primary and Secondary Organic Aerosol Concentrations During Scaqs, Atmos. Environ., 29, 3527-3544, 1995.

Turpin, B. J., Saxena, P., and Andrews, E.: Measuring and simulating particulate organics in the atmosphere: problems and prospects, Atmos. Environ., 34, 2983-3013, 2000.

Turpin, B. J., and Lim, H. J.: Species contributions to PM2.5 mass concentrations: Revisiting common assumptions for estimating organic mass, Aerosol Sci. Technol., 35, 602-610, 2001.

Vitousek, P. M., Aber, J. D., Howarth, R. W., Likens, G. E., Matson, P. A., Schindler, D. W., Schlesinger, W. H., and Tilman, D. G.: Human alteration of the global nitrogen cycle: Sources and consequences, Ecological Applications, 7, 737-750, 1997.

Wang, W. F., Schuchmann, M. N., Schuchmann, H. P., and von Sonntag, C.: The importance of mesomerism in the termination of alpha-carboxymethyl radicals from aqueous malonic and acetic acids, Chemistry-a European Journal, 7, 791-795, 2001.

Warneck, P.: In-cloud chemistry opens pathway to the formation of oxalic acid in the marine atmosphere, Atmos. Environ., 37, 2423-2427, 2003.

Wilcox, B. E., Hendrickson, C. L., and Marshall, A. G.: Improved ion extraction from a linear octopole ion trap: SIMION analysis and experimental demonstration, J. Am. Soc. Mass. Spectrom., 13, 1304-1312, 2002.

Willey, J. D., Kieber, R. J., Eyman, M. S., and Avery, G. B.: Rainwater dissolved organic carbon: Concentrations and global flux, Global Biogeochem. Cycles, 14, 139-148, 2000.

Wu, Z. G., Rodgers, R. P., and Marshall, A. G.: Two- and three-dimensional van Krevelen diagrams: A graphical analysis complementary to the Kendrick mass plot for sorting elemental compositions of complex organic mixtures based on ultrahigh-resolution broadband Fourier transform ion cyclotron resonance mass measurements, Anal. Chem., 76, 2511-2516, 2004.

Yu, J. Z., Huang, X. F., Xu, J. H., and Hu, M.: When aerosol sulfate goes up, so does oxalate: Implication for the formation mechanisms of oxalate, Environmental Science & Technology, 39, 128-133, 2005.

Zappoli, S., Andracchio, A., Fuzzi, S., Facchini, M. C., Gelencser, A., Kiss, G., Krivacsy, Z., Molnar, A., Meszaros, E., Hansson, H. C., Rosman, K., and Zebuhr, Y.: Inorganic, organic and macromolecular components of fine aerosol in different areas of Europe in relation to their water solubility, Atmos. Environ., 33, 2733-2743, 1999.

Zhang, Q., and Anastasio, C.: Chemistry of fog waters in California's Central Valley - Part 3: concentrations and speciation of organic and inorganic nitrogen, Atmos. Environ., 35, 5629-5643, 2001.

Zhang, Q., Anastasio, C., and Jimemez-Cruz, M.: Water-soluble organic nitrogen in atmospheric fine particles (PM2.5) from northern California, Journal of Geophysical Research-Atmospheres, 107, 2002.

Zhang, Y., Zheng, L. X., Liu, X. J., Jickells, T., Cape, J. N., Goulding, K., Fangmeier, A., and Zhang, F. S.: Evidence for organic N deposition and its anthropogenic sources in China, Atmos. Environ., 42, 1035-1041, 10.1016/j.atmosenv.2007.12.015|ISSN 1352-2310, 2008.

Zoller, D. L., and Johnston, M. V.: Microstructures of butadiene copolymers determined by ozonolysis/MALDI mass spectrometry, Macromolecules, 33, 1664-1670, 2000.

Appendix A: Supplemental Information for Chapter 2

Appendix A1
Pyruvic Acid Response to Varying Fragmentor Voltages

Pyruvic acid response measured as the change in ion abundance of *m/z* 87 to varying fragmentor voltages in standards and samples (1:10 dilution).

Fragmentor Voltage (V)	Standard 0.5 mM	Standard 1.0 mM	Sample t_3	Sample t_6
40	314329	458855	6084	2542
60	170588	283055	23754	10819
80	35641	61496	39973	23502
100	8459	17541	27002	23874
120	6400	11223	14723	11858
150	4094	6458	6679	5267
200	1547	2181	4054	2810

Appendix A2
Glyoxylic Acid Response to Varying Fragmentor Voltages

Glyoxylic acid response measured as the change in ion abundance of *m/z* 73 to varying fragmentor voltages in standards and samples.

Fragmentor Voltage (V)	Standard 0.5 mM	Standard 1.0 mM	Sample tg1*	Sample tg2*
40	408172	234078	7284	4494
60	338578	205205	10448	9550
80	134717	82688	11755	12550
100	42981	29981	7998	8268
120	23470	15074	5309	4295
150	12495	6256	2592	2784
200	5782	3273	2092	1270

* 21 and 59 minute samples from replicate experiment due to insufficient sample volume

Appendix A3
Oxalic Acid Response to Varying Fragmentor Voltages

Oxalic acid response measured as the change in ion abundance of *m/z* 89 to varying fragmentor voltages in standards and samples (1:10 dilution).

Fragmentor Voltage (V)	Standard 0.5 mM	Standard 1.0 mM	Sample t_3	Sample t_6
40	442274	619061	15225	30021
60	144558	240837	8947	17555
80	9519	15514	3443	5596
100	2476	2949	1394	1992
120	952	2145	1311	1138
150	0	0	1107	1202
200	0	0	0	0

Appendix A4
Estimates of Monomer Concentrations

Concentrations of monomers based on ESI-MS ion abundance calculated using standard curves (Table 2-1) from authentic standards in the same matrix as the samples. Units of concentration are mM. Standard deviations are below 0.01 mM based on standard deviations of ion abundances and linear regression analysis (Table 2-1).

Time (min)		Pyruvic acid	Glyoxylic acid	Oxalic acid
Experimental Samples		[a]ESI-MS	ESI-MS	ESI-MS
t_1	0	N/A	N/A	N/A
t_2	10	0.46	0.07	0.06
t_3	27	0.20	0.08	0.04
t_4	43	0.27	0.04	0.18
t_5	59	0.27	0.03	0.19
t_6	86	0.23	0.02	0.30
t_7	138	0.26	0.01	0.39
t_8	202	0.22	N/D	0.38

N/A=not analyzed
N/D=below 0.0046 mM
[a]$[M-H]^-$ and $[2M-H]^-$

Appendix B: Supplemental Information for Chapter 3

Appendix B1
Comparison of ESI-MS and FT-ICR MS spectra

Comparison of t=69 minute negative ion ESI-MS and FT-ICR MS methylglyoxal UV/H_2O_2 oxidation sample. Note the break in the y-axis scale.

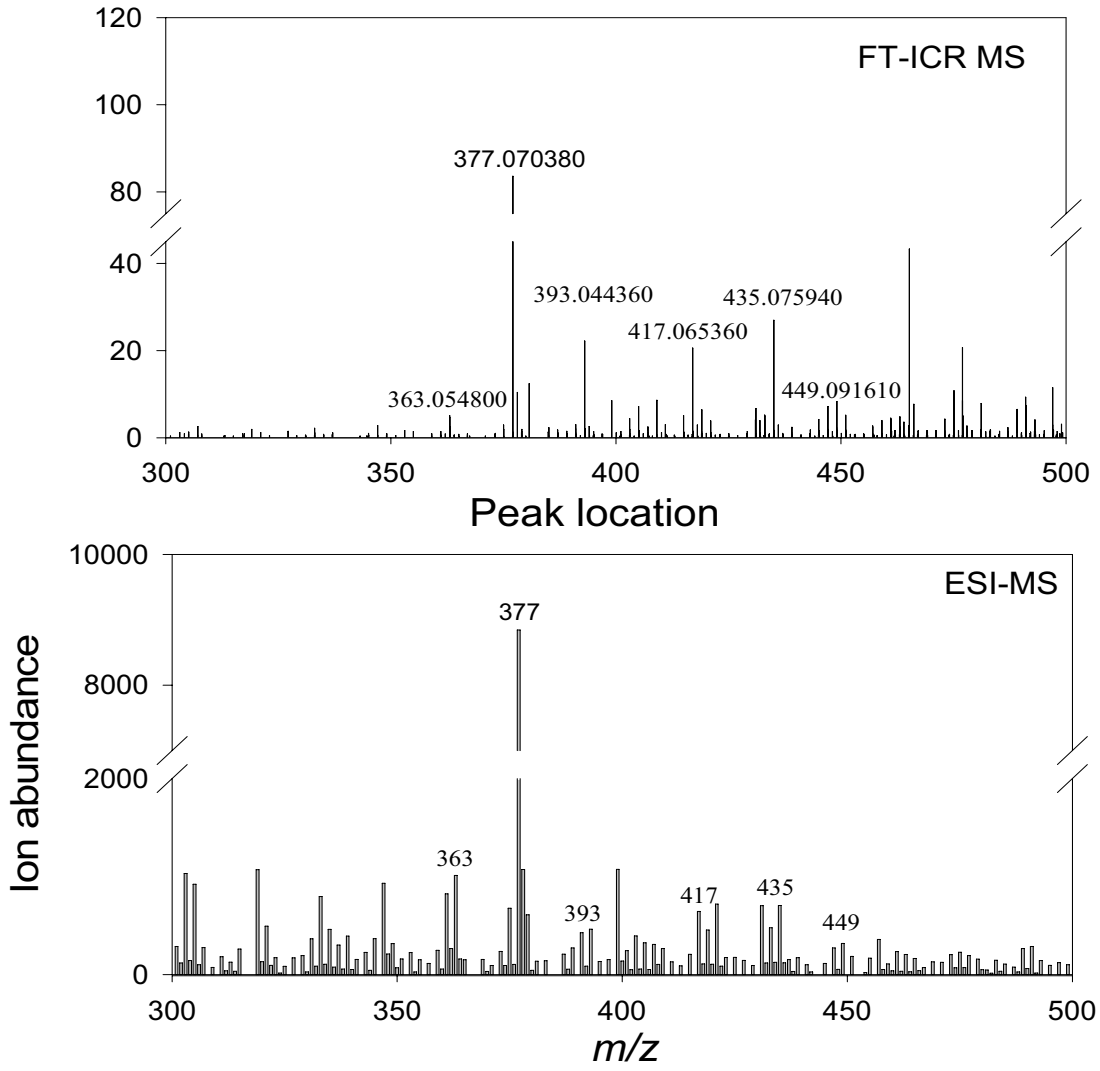

Appendix B2
Methylglyoxal Control Spectra

ESI-MS spectra from control experiments of methylglyoxal plus UV only (no H_2O_2) left panels, and methylglyoxal plus H_2O_2 only (no UV) right panels.

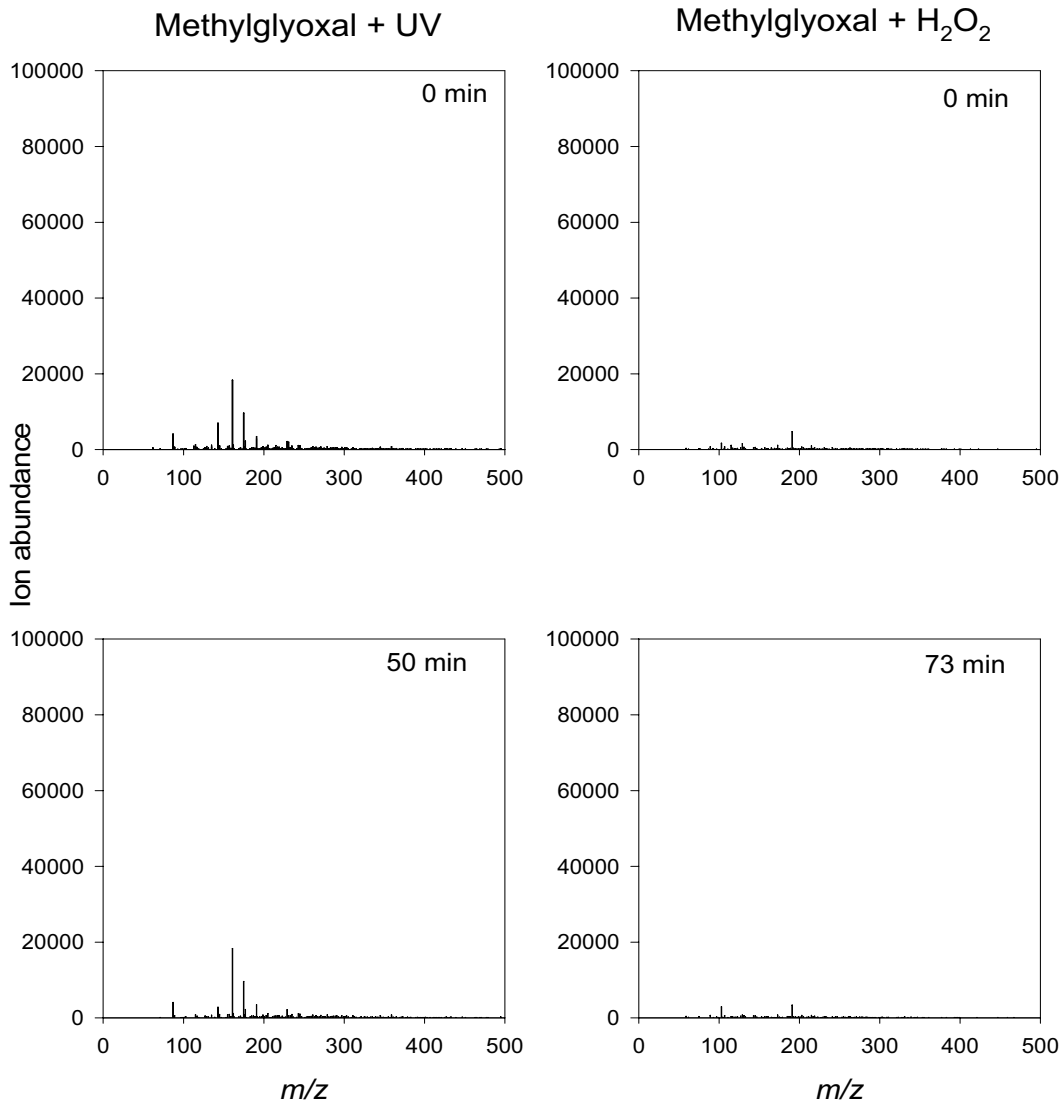

Appendix B3
Tandem ESI-MS^n Spectrum of *m/z* 131

ESI-MS-MS (negative ion) of *m/z* 131 from t=129 minute methylglyoxal hydroxyl radical photooxidation experiments. Losses of CO_2 (-44), H_2O (-18), CO_2+H_2O (-62) indicative of carboxylic acid functionality are indicated. Loss of one subunit (-72) leaving acetic acid (*m/z* 59) is indicated and the two proposed structures based on esterification with either (A) hydracrylic acid or (B) lactic acid are in the upper right hand corner with the red line indicating the site of fragmentation.

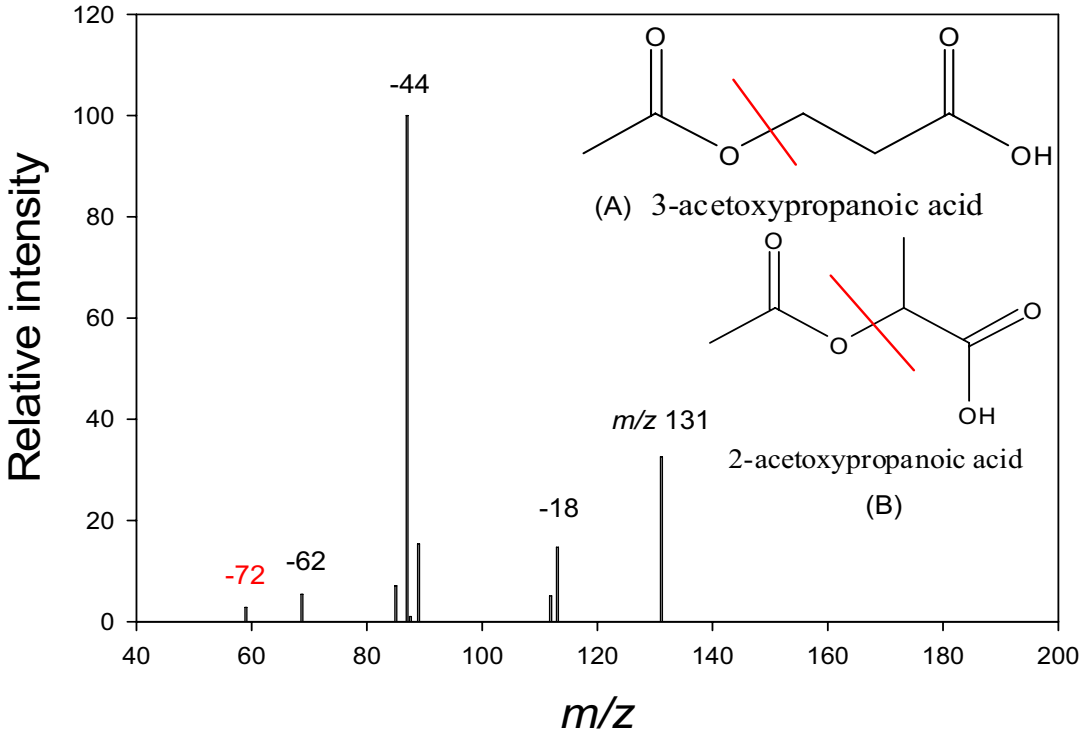

Appendix B4
Nine Oligomer Series

The nine series of compounds starting with the parent organic acid and differing in mass by 72.02113, which is equivalent to $C_3H_4O_2$, are grouped to show the regular increase in mass, DBE, and elemental composition within the series. The series of formulas starting with oxalic acid (*m/z* 89), and *m/z* 177 are distinguished by the labels numeral (1-9), and letter (a-h), respectively, here and in Figure 3-3. nl indicates the mass is not labeled on Figure 3-3. -- indicates the mass was detected using the ESI-MS and the elemental formula was assigned based on the "subunit" series. [a]Double bond equivalents (number of rings plus double bonds) for neutral compound.

Label	*m/z* (Measured)	Formula $[M-H]^-$	DBE[a]	Mass Error (ppm)
1	89	$C_2H_1O_4$	2	--
2	161	$C_5H_5O_6$	3	--
3	233	$C_8H_9O_8$	4	--
4	305.05163	$C_{11}H_{13}O_{10}$	5	0.7
5	377.07274	$C_{14}H_{17}O_{12}$	6	0.5
6	449.09398	$C_{17}H_{21}O_{14}$	7	0.7
7	521.11503	$C_{20}H_{25}O_{16}$	8	0.4
8	593.13631	$C_{23}H_{29}O_{18}$	9	0.6
a	177	$C_6H_9O_6$	2	--
b	249.06175	$C_9H_{13}O_8$	3	0.6
c	321.08295	$C_{12}H_{17}O_{10}$	4	0.7
d	393.10417	$C_{15}H_{21}O_{12}$	5	0.8
e	465.12534	$C_{18}H_{25}O_{14}$	6	0.8
f	537.14629	$C_{21}H_{29}O_{16}$	7	0.3
g	609.16781	$C_{24}H_{33}O_{18}$	8	0.9

nl	73	$C_2H_1O_3$	2	--
nl	145	$C_5H_5O_5$	3	--
nl	217	$C_8H_9O_7$	4	--
nl	289.05671	$C_{11}H_{13}O_9$	5	0.7
nl	361.07786	$C_{14}H_{17}O_{11}$	6	0.6
nl	433.09909	$C_{17}H_{21}O_{13}$	7	0.8
nl	505.12027	$C_{20}H_{25}O_{15}$	8	0.7
nl	577.14153	$C_{23}H_{29}O_{17}$	9	0.9
nl	87	$C_3H_3O_3$	2	--
nl	159	$C_6H_7O_5$	3	--
nl	231	$C_9H_{11}O_7$	4	--
nl	303.07240	$C_{12}H_{15}O_9$	5	0.8
nl	375.09360	$C_{15}H_{19}O_{11}$	6	0.8
nl	447.11486	$C_{18}H_{23}O_{13}$	7	1.0
nl	519.13597	$C_{21}H_{27}O_{15}$	8	0.8
nl	75	$C_2H_3O_3$	1	--
nl	147	$C_5H_7O_5$	2	--
nl	219	$C_8H_{11}O_7$	3	--
nl	291.07238	$C_{11}H_{15}O_9$	4	0.8
nl	363.09359	$C_{14}H_{19}O_{11}$	5	0.8
nl	435.11472	$C_{17}H_{23}O_{13}$	6	0.7
nl	507.13597	$C_{20}H_{27}O_{15}$	7	0.8
nl	579.15727	$C_{23}H_{31}O_{17}$	8	1.0

nl	103	$C_3H_3O_4$	2	--
nl	175	$C_6H_7O_6$	3	--
nl	247.04607	$C_9H_{11}O_8$	4	0.5
nl	319.06735	$C_{12}H_{15}O_{10}$	5	0.9
nl	391.08856	$C_{15}H_{19}O_{12}$	6	0.9
nl	463.10966	$C_{18}H_{23}O_{14}$	7	0.7
nl	535.13088	$C_{21}H_{27}O_{16}$	8	0.8
nl	607.15204	$C_{24}H_{31}O_{18}$	9	0.7
nl	117	$C_4H_5O_4$	2	--
nl	189	$C_7H_9O_6$	3	--
nl	261	$C_{10}H_{13}O_8$	4	--
nl	333.08298	$C_{13}H_{17}O_{10}$	5	0.8
nl	405.10409	$C_{16}H_{21}O_{12}$	6	0.6
nl	477.12539	$C_{19}H_{25}O_{14}$	7	0.9
nl	133	$C_4H_5O_5$	2	--
nl	205	$C_7H_9O_7$	3	--
nl	277	$C_{10}H_{13}O_9$	4	--
nl	349.07787	$C_{13}H_{17}O_{11}$	5	0.7
nl	421.09915	$C_{16}H_{21}O_{13}$	6	0.9
nl	493.12037	$C_{19}H_{25}O_{15}$	7	1.0
nl	565.14160	$C_{22}H_{29}O_{17}$	8	1.0
nl	131	$C_5H_7O_4$	2	--
nl	203	$C_8H_{11}O_6$	3	--

nl	275.07744	$C_{11}H_{15}O_8$	4	0.7
nl	347.09862	$C_{14}H_{19}O_{10}$	5	0.7
nl	419.11989	$C_{17}H_{23}O_{12}$	6	0.7
nl	491.14098	$C_{20}H_{27}O_{14}$	7	0.6

Appendix C: Supplemental Information for Chapter 4

Appendix C1
All Measured *m/z*'s and Elemental Formulas in the Rainwater

The measured *m/z*'s and assigned elemental formulas for the rainwater sample collected in the Pinelands, NJ on July 20, 2002. The sample was analyzed in the negative ion mode over the mass range *m/z* 50-400 using the instrument conditions described in Section 4.3.3.

CHO	$^{-}$*m/z* measured	Elemental Formula $[M-H]^{-}$
	59.01384	C2 H3 O2
	69.03457	C4 H5 O1
	71.01383	C3 H3 O2
	72.9931	C2 H1 O3
	73.02948	C3 H5 O2
	75.00875	C2 H3 O3
	103.00368	C3 H3 O4
	115.04009	C5 H7 O3
	117.01935	C4 H5 O4
	119.03502	C4 H7 O4
	121.02954	C7 H5 O2
	125.02445	C6 H5 O3
	125.06083	C7 H9 O2
	127.00373	C5 H3 O4
	127.04011	C6 H7 O3
	129.01937	C5 H5 O4
	129.05576	C6 H9 O3
	130.99861	C4 H3 O5
	131.03501	C5 H7 O4
	131.0714	C6 H11 O3
	133.01427	C4 H5 O5
	133.05067	C5 H9 O4
	134.9935	C3 H3 O6
	135.0299	C4 H7 O5
	135.04519	C8 H7 O2
	137.00916	C3 H5 O6
	137.02446	C7 H5 O3
	137.06085	C8 H9 O2
	139.00373	C6 H3 O4
	139.04011	C7 H7 O3
	139.07649	C8 H11 O2
	141.01936	C6 H5 O4
	141.05575	C7 H9 O3
	143.03501	C6 H7 O4

	143.07141	C7 H11 O3
	145.01426	C5 H5 O5
	145.05067	C6 H9 O4
	147.02991	C5 H7 O5
	149.00917	C4 H5 O6
	149.04555	C5 H9 O5
	149.06085	C9 H9 O2
	151.04012	C8 H7 O3
	153.01938	C7 H5 O4
	153.09214	C9 H13 O2
	155.03503	C7 H7 O4
	155.07141	C8 H11 O3
	157.01428	C6 H5 O5
	157.05064	C7 H9 O4
	157.08706	C8 H13 O3
	159.0299	C6 H7 O5
	159.0663	C7 H11 O4
	161.00917	C5 H5 O6
	161.04556	C6 H9 O5
	163.00377	C8 H3 O4
	163.02481	C5 H7 O6
	165.01934	C8 H5 O4
	169.05069	C8 H9 O4
	171.02993	C7 H7 O5
	171.06632	C8 H11 O4
	171.10273	C9 H15 O3
	173.04557	C7 H9 O5
	173.082	C8 H13 O4
	175.02483	C6 H7 O6
	175.06122	C7 H11 O5
	177.04047	C6 H9 O6
	179.03503	C9 H7 O4
	181.0143	C8 H5 O5
	181.07176	C6 H13 O6
	185.0456	C8 H9 O5
	185.082	C9 H13 O4
	187.02485	C7 H7 O6
	187.06126	C8 H11 O5
	187.09766	C9 H15 O4
	189.04051	C7 H9 O6
	191.01975	C6 H7 O7
	197.08203	C10 H13 O4
	199.06131	C9 H11 O5
	199.09768	C10 H15 O4
	201.04056	C8 H9 O6
	201.07694	C9 H13 O5

	201.1133	C10 H17 O4
	203.01985	C7 H7 O7
	203.0562	C8 H11 O6
	205.03546	C7 H9 O7
	207.03	C10 H7 O5
	207.05107	C7 H11 O7
	209.00926	C9 H5 O6
	209.04568	C10 H9 O5
	211.0613	C10 H11 O5
	211.13402	C12 H19 O3
	213.04056	C9 H9 O6
	213.07695	C10 H13 O5
	213.11333	C11 H17 O4
	213.14967	C12 H21 O3
	215.01991	C8 H7 O7
	215.05621	C9 H11 O6
	215.09259	C10 H15 O5
	215.12895	C11 H19 O4
	217.03546	C8 H9 O7
	217.07186	C9 H13 O6
	217.10819	C10 H17 O5
	219.01468	C7 H7 O8
	219.05107	C8 H11 O7
	219.08746	C9 H15 O6
	219.1755	C15 H23 O1
	221.03033	C7 H9 O8
	221.04564	C11 H9 O5
	221.06674	C8 H13 O7
	221.08199	C12 H13 O4
	223.02489	C10 H7 O6
	223.04594	C7 H11 O8
	223.06126	C11 H11 O5
	223.08233	C8 H15 O7
	223.09765	C12 H15 O4
	223.13404	C13 H19 O3
	225.00415	C9 H5 O7
	225.04048	C10 H9 O6
	225.06157	C7 H13 O8
	225.0769	C11 H13 O5
	225.1133	C12 H17 O4
	225.1497	C13 H21 O3
	227.0562	C10 H11 O6
	227.09257	C11 H15 O5
	227.12895	C12 H19 O4
	227.16531	C13 H23 O3
	227.20169	C14 H27 O2

	229.03545	C9 H9 O7
	229.07184	C10 H13 O6
	229.10821	C11 H17 O5
	229.14457	C12 H21 O4
	231.01473	C8 H7 O8
	231.05109	C9 H11 O7
	231.08746	C10 H15 O6
	231.12383	C11 H19 O5
	233.03034	C8 H9 O8
	233.06672	C9 H13 O7
	233.1031	C10 H17 O6
	233.15473	C15 H21 O2
	235.04596	C8 H11 O8
	235.08236	C9 H15 O7
	235.17041	C15 H23 O2
	237.0405	C11 H9 O6
	237.06161	C8 H13 O8
	237.07694	C12 H13 O5
	239.05619	C11 H11 O6
	239.07731	C8 H15 O8
	239.09259	C12 H15 O5
	239.12894	C13 H19 O4
	241.07181	C11 H13 O6
	241.10821	C12 H17 O5
	241.18101	C14 H25 O3
	241.21736	C15 H29 O2
	243.05109	C10 H11 O7
	243.08744	C11 H15 O6
	243.12384	C12 H19 O5
	243.16027	C13 H23 O4
	245.03029	C9 H9 O8
	245.06671	C10 H13 O7
	245.10308	C11 H17 O6
	247.04596	C9 H11 O8
	247.08236	C10 H15 O7
	249.0616	C9 H13 O8
	253.07181	C12 H13 O6
	253.14461	C14 H21 O4
	255.05105	C11 H11 O7
	255.08744	C12 H15 O6
	255.23303	C16 H31 O2
	257.06669	C11 H13 O7
	257.10314	C12 H17 O6
	259.04596	C10 H11 O8
	259.08235	C11 H15 O7
	259.11868	C12 H19 O6

	261.02522	C9 H9 O9
	261.06157	C10 H13 O8
	261.09798	C11 H17 O7
	263.04082	C9 H11 O9
	263.07722	C10 H15 O8
	269.06665	C12 H13 O7
	269.21227	C16 H29 O3
	271.0459	C11 H11 O8
	271.08227	C12 H15 O7
	273.06155	C11 H13 O8
	273.09802	C12 H17 O7
	275.04083	C10 H11 O9
	275.07719	C11 H15 O8
	277.05647	C10 H13 O9
	277.09279	C11 H17 O8
	277.1446	C16 H21 O4
	283.26421	C18 H35 O2
	285.06157	C12 H13 O8
	285.09789	C13 H17 O7
	287.07721	C12 H15 O8
CHOS	$^{-}m/z$ measured	Elemental Formula $[M-H]^{-}$
	110.97577	C1 H3 O4 S1
	124.99144	C2 H5 O4 S1
	136.99144	C3 H5 O4 S1
	138.97073	C2 H3 O5 S1
	139.00711	C3 H7 O4 S1
	140.98638	C2 H5 O5 S1
	142.96558	C1 H3 O6 S1
	152.98638	C3 H5 O5 S1
	153.02277	C4 H9 O4 S1
	154.96565	C2 H3 O6 S1
	155.00205	C3 H7 O5 S1
	167.00202	C4 H7 O5 S1
	167.03842	C5 H11 O4 S1
	168.98125	C3 H5 O6 S1
	170.99693	C3 H7 O6 S1
	181.0177	C5 H9 O5 S1
	181.05408	C6 H13 O4 S1
	182.99693	C4 H7 O6 S1
	184.9762	C3 H5 O7 S1
	194.99696	C5 H7 O6 S1
	197.01265	C5 H9 O6 S1
	198.99188	C4 H7 O7 S1
	199.02827	C5 H11 O6 S1
	200.97104	C3 H5 O8 S1
	209.01264	C6 H9 O6 S1

	209.04898	C7 H13 O5 S1
	209.08534	C8 H17 O4 S1
	210.9919	C5 H7 O7 S1
	211.02828	C6 H11 O6 S1
	211.06462	C7 H15 O5 S1
	212.97116	C4 H5 O8 S1
	213.00754	C5 H9 O7 S1
	214.98676	C4 H7 O8 S1
	215.02317	C5 H11 O7 S1
	216.95712	C4 H9 O8 S1
	221.08535	C9 H17 O4 S1
	222.99183	C6 H7 O7 S1
	223.02828	C7 H11 O6 S1
	223.06462	C8 H15 O5 S1
	223.10103	C9 H19 O4 S1
	225.00751	C6 H9 O7 S1
	225.04387	C7 H13 O6 S1
	225.0803	C8 H17 O5 S1
	226.98677	C5 H7 O8 S1
	227.02316	C6 H11 O7 S1
	228.96605	C4 H5 O9 S1
	229.00243	C5 H9 O8 S1
	230.98163	C4 H7 O9 S1
	231.01805	C5 H11 O8 S1
	237.00751	C7 H9 O7 S1
	237.04388	C8 H13 O6 S1
	237.11667	C10 H21 O4 S1
	238.98677	C6 H7 O8 S1
	239.02317	C7 H11 O7 S1
	239.05956	C8 H15 O6 S1
	241.00243	C6 H9 O8 S1
	241.03882	C7 H13 O7 S1
	242.98168	C5 H7 O9 S1
	243.01805	C6 H11 O8 S1
	244.99727	C5 H9 O9 S1
	246.9765	C4 H7 O10 S1
	247.01289	C5 H11 O9 S1
	251.02315	C8 H11 O7 S1
	251.05953	C9 H15 O6 S1
	253.00243	C7 H9 O8 S1
	253.03884	C8 H13 O7 S1
	254.98166	C6 H7 O9 S1
	255.01808	C7 H11 O8 S1
	255.05446	C8 H15 O7 S1
	256.99729	C6 H9 O9 S1
	257.03371	C7 H13 O8 S1

	258.97654	C5 H7 O10 S1
	259.01292	C6 H11 O9 S1
	260.99212	C5 H9 O10 S1
	262.98665	C8 H7 O8 S1
	265.0388	C9 H13 O7 S1
	265.14796	C12 H25 O4 S1
	267.01806	C8 H11 O8 S1
	267.05446	C9 H15 O7 S1
	268.99727	C7 H9 O9 S1
	269.03366	C8 H13 O8 S1
	269.07007	C9 H17 O7 S1
	270.97649	C6 H7 O10 S1
	271.01288	C7 H11 O9 S1
	271.0493	C8 H15 O8 S1
	272.99216	C6 H9 O10 S1
	273.02857	C7 H13 O9 S1
	275.00776	C6 H11 O10 S1
	277.01156	C20 H5 S1
	277.0234	C6 H13 O10 S1
	279.05435	C10 H15 O7 S1
	279.16357	C13 H27 O4 S1
	281.03366	C9 H13 O8 S1
	281.07002	C10 H17 O7 S1
	283.01288	C8 H11 O9 S1
	283.04927	C9 H15 O8 S1
	283.08568	C10 H19 O7 S1
	284.99211	C7 H9 O10 S1
	285.0285	C8 H13 O9 S1
	285.06489	C9 H17 O8 S1
	287.00774	C7 H11 O10 S1
	287.04419	C8 H15 O9 S1
	289.02334	C7 H13 O10 S1
	293.17924	C14 H29 O4 S1
	295.04925	C10 H15 O8 S1
	297.02848	C9 H13 O9 S1
	297.06488	C10 H17 O8 S1
	297.15295	C16 H25 O3 S1
	299.00775	C8 H11 O10 S1
	299.04413	C9 H15 O9 S1
	300.98708	C7 H9 O11 S1
	301.02341	C8 H13 O10 S1
	309.17405	C14 H29 O5 S1
	311.00772	C9 H11 O10 S1
	311.04407	C10 H15 O9 S1
	311.08053	C11 H19 O8 S1
	311.16856	C17 H27 O3 S1

	313.02342	C9 H13 O10 S1
	313.05979	C10 H17 O9 S1
	315.00268	C8 H11 O11 S1
	315.03909	C9 H15 O10 S1
	317.01832	C8 H13 O11 S1
	325.02345	C10 H13 O10 S1
	325.18422	C18 H29 O3 S1
	327.03902	C10 H15 O10 S1
	329.01832	C9 H13 O11 S1
	329.0546	C10 H17 O10 S1
	331.0339	C9 H15 O11 S1
	339.19986	C19 H31 O3 S1
	343.03398	C10 H15 O11 S1
CHONS	$^{-}m/z$ measured	Elemental Formula $[M-H]^{-}$
	217.01897	C9 H5 N4 O1 S1
	217.96123	C2 H4 N1 O9 S1
	226.00272	C5 H8 N1 O7 S1
	231.97693	C3 H6 N1 O9 S1
	235.98708	C6 H6 N1 O7 S1
	244.0133	C5 H10 N1 O8 S1
	245.99251	C4 H8 N1 O9 S1
	257.99251	C5 H8 N1 O9 S1
	260.00817	C5 H10 N1 O9 S1
	261.98736	C4 H8 N1 O10 S1
	273.98743	C5 H8 N1 O10 S1
	275.019	C5 H11 N2 O9 S1
	276.00297	C5 H10 N1 O10 S1
	278.01865	C5 H12 N1 O10 S1
	288.00303	C6 H10 N1 O10 S1
	291.99794	C5 H10 N1 O11 S1
	302.01864	C7 H12 N1 O10 S1
	304.99317	C5 H9 N2 O11 S1
	323.00371	C5 H11 N2 O12 S1
Other	$^{-}m/z$ measured	Elemental Formula $[M-H]^{-}$
	142.9751	C1 H4 O6 P1
	231.00626	C8 H8 O6 P1
	244.98545	C8 H6 O7 P1
	294.98216	C3 H8 N2 O12 P1
	304.99317	C7 H6 N4 O8 P1
	323.00371	C7 H8 N4 O9 P1
	333.01709	C15 H10 O7 P1

Appendix D: Supplemental Information for Chapter 5

Appendix D1
All Measured *m/z*'s and Elemental Formulas of Nitrogen Containing Compounds in the Rainwater

The measured *m/z*'s and elemental formulas that contain nitrogen for the rainwater sample collected in the Pinelands, NJ on July 20, 2002. The sample was analyzed in both the positive and negative ion modes using the instrument conditions described in the Experimental Section 5-3.

CHON+	$^{+}m/z$ measured	Elemental Formula $[M+H]^{+}$, $[M+Na]^{+}$
	74.06003	C3 H8 N1 O1
	82.02633	C2 H5 N1 O1 Na1
	88.07568	C4 H10 N1 O1
	90.09133	C4 H12 N1 O1
	101.07094	C4 H9 N2 O1
	102.09134	C5 H12 N1 O1
	114.09134	C6 H12 N1 O1
	115.08657	C5 H11 N2 O1
	116.0706	C5 H10 N1 O2
	116.10699	C6 H14 N1 O1
	118.08625	C5 H12 N1 O2
	118.12263	C6 H16 N1 O1
	128.10697	C7 H14 N1 O1
	130.08625	C6 H12 N1 O2
	132.10188	C6 H14 N1 O2
	134.11753	C6 H16 N1 O2
	138.05492	C7 H8 N1 O2
	138.06616	C6 H8 N3 O1
	139.05018	C6 H7 N2 O2
	140.07059	C7 H10 N1 O2
	140.08182	C6 H10 N3 O1
	141.10221	C7 H13 N2 O1
	142.08623	C7 H12 N1 O2
	142.12262	C8 H16 N1 O1
	143.08148	C6 H11 N2 O2
	143.11787	C7 H15 N2 O1
	144.0655	C6 H10 N1 O3
	144.10188	C7 H14 N1 O2
	144.13827	C8 H18 N1 O1
	145.09712	C6 H13 N2 O2
	146.08115	C6 H12 N1 O3
	146.11753	C7 H16 N1 O2
	147.07639	C5 H11 N2 O3

147.11278	C6 H15 N2 O2
148.06041	C5 H10 N1 O4
148.0968	C6 H14 N1 O3
148.13319	C7 H18 N1 O2
150.11244	C6 H16 N1 O3
152.07055	C8 H10 N1 O2
154.08622	C8 H12 N1 O2
155.11786	C8 H15 N2 O1
156.06549	C7 H10 N1 O3
156.07673	C6 H10 N3 O2
156.10188	C8 H14 N1 O2
156.13827	C9 H18 N1 O1
157.06072	C6 H9 N2 O3
157.09713	C7 H13 N2 O2
157.13352	C8 H17 N2 O1
158.08115	C7 H12 N1 O3
158.11753	C8 H16 N1 O2
158.15391	C9 H20 N1 O1
159.0764	C6 H11 N2 O3
159.11279	C7 H15 N2 O2
159.14917	C8 H19 N2 O1
160.0968	C7 H14 N1 O3
160.13318	C8 H18 N1 O2
162.07607	C6 H12 N1 O4
162.11245	C7 H16 N1 O3
163.14408	C7 H19 N2 O2
164.09171	C6 H14 N1 O4
166.08623	C9 H12 N1 O2
166.10736	C6 H16 N1 O4
168.10187	C9 H14 N1 O2
170.08117	C8 H12 N1 O3
170.11752	C9 H16 N1 O2
171.07643	C7 H11 N2 O3
171.11281	C8 H15 N2 O2
171.14917	C9 H19 N2 O1
172.09679	C8 H14 N1 O3
172.13319	C9 H18 N1 O2
172.16957	C10 H22 N1 O1
173.09206	C7 H13 N2 O3
173.12844	C8 H17 N2 O2
173.16484	C9 H21 N2 O1
174.07606	C7 H12 N1 O4
174.11244	C8 H16 N1 O3
174.12366	C7 H16 N3 O2
174.14883	C9 H20 N1 O2
175.11893	C6 H15 N4 O2

175.18046	C9 H23 N2 O1
176.09171	C7 H14 N1 O4
176.12809	C8 H18 N1 O3
178.10737	C7 H16 N1 O4
180.10187	C10 H14 N1 O2
182.08113	C9 H12 N1 O3
182.11754	C10 H16 N1 O2
184.07567	C12 H10 N1 O1
184.09685	C9 H14 N1 O3
184.13321	C10 H18 N1 O2
186.07609	C8 H12 N1 O4
186.11248	C9 H16 N1 O3
186.14886	C10 H20 N1 O2
187.10772	C8 H15 N2 O3
187.14413	C9 H19 N2 O2
187.18051	C10 H23 N2 O1
188.09175	C8 H14 N1 O4
188.12814	C9 H18 N1 O3
188.16451	C10 H22 N1 O2
189.08699	C7 H13 N2 O4
189.12341	C8 H17 N2 O3
190.10741	C8 H16 N1 O4
190.14379	C9 H20 N1 O3
192.08666	C7 H14 N1 O5
192.12304	C8 H18 N1 O4
192.1383	C12 H18 N1 O1
194.10233	C7 H16 N1 O5
194.1387	C8 H20 N1 O4
195.08766	C8 H11 N4 O2
196.11798	C7 H18 N1 O5
198.11246	C10 H16 N1 O3
198.18525	C12 H24 N1 O1
200.12813	C10 H18 N1 O3
200.20089	C12 H26 N1 O1
202.10739	C9 H16 N1 O4
202.14376	C10 H20 N1 O3
204.12305	C9 H18 N1 O4
206.10232	C8 H16 N1 O5
206.13869	C9 H20 N1 O4
207.14922	C12 H19 N2 O1
208.03935	C13 H6 N1 O2
208.08157	C7 H14 N1 O6
208.09684	C11 H14 N1 O3
208.11796	C8 H18 N1 O5
208.1543	C9 H22 N1 O4
208.16958	C13 H22 N1 O1

210.09725	C7 H16 N1 O6
210.11246	C11 H16 N1 O3
210.13361	C8 H20 N1 O5
210.14887	C12 H20 N1 O2
211.14409	C11 H19 N2 O2
212.09175	C10 H14 N1 O4
212.12811	C11 H18 N1 O3
212.16451	C12 H22 N1 O2
213.1234	C10 H17 N2 O3
213.15975	C11 H21 N2 O2
213.99844	C7 H4 N1 O7
214.10737	C10 H16 N1 O4
214.14377	C11 H20 N1 O3
214.18015	C12 H24 N1 O2
215.10262	C9 H15 N2 O4
215.13902	C10 H19 N2 O3
215.1754	C11 H23 N2 O2
216.02917	C11 H6 N1 O4
216.08666	C9 H14 N1 O5
216.12303	C10 H18 N1 O4
216.15943	C11 H22 N1 O3
216.1958	C12 H26 N1 O2
217.0819	C8 H13 N2 O5
217.11828	C9 H17 N2 O4
217.15466	C10 H21 N2 O3
217.17701	C8 H21 N6 O1
218.1023	C9 H16 N1 O5
218.13868	C10 H20 N1 O4
218.17507	C11 H24 N1 O3
219.09755	C8 H15 N2 O5
219.13393	C9 H19 N2 O4
219.17031	C10 H23 N2 O3
220.08156	C8 H14 N1 O6
220.11795	C9 H18 N1 O5
220.15432	C10 H22 N1 O4
221.11327	C8 H17 N2 O5
222.09721	C8 H16 N1 O6
222.11249	C12 H16 N1 O3
222.13361	C9 H20 N1 O5
222.17001	C10 H24 N1 O4
224.03415	C13 H6 N1 O3
224.09172	C11 H14 N1 O4
224.11285	C8 H18 N1 O6
224.12812	C12 H18 N1 O3
224.14926	C9 H22 N1 O5
225.02951	C12 H5 N2 O3

226.10739	C11 H16 N1 O4	
226.12853	C8 H20 N1 O6	
226.14379	C12 H20 N1 O3	
226.18016	C13 H24 N1 O2	
227.06385	C7 H12 N2 O5	Na1
227.10265	C10 H15 N2 O4	
227.13899	C11 H19 N2 O3	
227.17541	C12 H23 N2 O2	
228.08664	C10 H14 N1 O5	
228.12303	C11 H18 N1 O4	
228.15944	C12 H22 N1 O3	
228.19581	C13 H26 N1 O2	
228.23219	C14 H30 N1 O1	
229.08194	C9 H13 N2 O5	
229.11831	C10 H17 N2 O4	
229.12954	C9 H17 N4 O3	
229.15468	C11 H21 N2 O3	
230.10232	C10 H16 N1 O5	
230.13869	C11 H20 N1 O4	
230.17508	C12 H24 N1 O3	
230.21147	C13 H28 N1 O2	
231.09756	C9 H15 N2 O5	
231.1339	C10 H19 N2 O4	
231.17031	C11 H23 N2 O3	
232.08156	C9 H14 N1 O6	
232.11796	C10 H18 N1 O5	
232.15435	C11 H22 N1 O4	
232.19072	C12 H26 N1 O3	
233.11323	C9 H17 N2 O5	
233.12446	C8 H17 N4 O4	
233.14961	C10 H21 N2 O4	
234.09723	C9 H16 N1 O6	
234.1336	C10 H20 N1 O5	
234.16999	C11 H24 N1 O4	
234.20635	C12 H28 N1 O3	
235.09254	C8 H15 N2 O6	
236.11288	C9 H18 N1 O6	
236.12809	C13 H18 N1 O3	
236.14927	C10 H22 N1 O5	
238.10743	C12 H16 N1 O4	
238.1286	C9 H20 N1 O6	
239.01766	C9 H4 N4 O3	Na1
240.12306	C12 H18 N1 O4	
242.13873	C12 H20 N1 O4	
242.17514	C13 H24 N1 O3	
244.11799	C11 H18 N1 O5	

244.15437	C12 H22 N1 O4	
244.19077	C13 H26 N1 O3	
244.22716	C14 H30 N1 O2	
245.18598	C12 H25 N2 O3	
246.09724	C10 H16 N1 O6	
246.13362	C11 H20 N1 O5	
246.17	C12 H24 N1 O4	
246.20642	C13 H28 N1 O3	
247.12887	C10 H19 N2 O5	
247.14008	C9 H19 N4 O4	
247.96148	C4 H3 N1 O10	Na1
248.11288	C10 H18 N1 O6	
248.14927	C11 H22 N1 O5	
248.18565	C12 H26 N1 O4	
250.09213	C9 H16 N1 O7	
250.12848	C10 H20 N1 O6	
250.16488	C11 H24 N1 O5	
250.20125	C12 H28 N1 O4	
252.10777	C9 H18 N1 O7	
252.12304	C13 H18 N1 O4	
252.14414	C10 H22 N1 O6	
254.12338	C9 H20 N1 O7	
254.13865	C13 H20 N1 O4	
254.17506	C14 H24 N1 O3	
256.11795	C12 H18 N1 O5	
256.15436	C13 H22 N1 O4	
256.19071	C14 H26 N1 O3	
256.26352	C16 H34 N1 O1	
258.1336	C12 H20 N1 O5	
258.16999	C13 H24 N1 O4	
258.20639	C14 H28 N1 O3	
260.00126	C6 H7 N1 O9	Na1
260.11287	C11 H18 N1 O6	
260.14928	C12 H22 N1 O5	
260.18565	C13 H26 N1 O4	
261.14452	C11 H21 N2 O5	
262.12854	C11 H20 N1 O6	
262.16491	C12 H24 N1 O5	
264.10781	C10 H18 N1 O7	
264.14418	C11 H22 N1 O6	
264.18053	C12 H26 N1 O5	
266.12343	C10 H20 N1 O7	
268.15428	C14 H22 N1 O4	
278.12341	C11 H20 N1 O7	
278.15982	C12 H24 N1 O6	
280.10268	C10 H18 N1 O8	

	280.13907	C11 H22 N1 O7
	280.1543	C15 H22 N1 O4
	280.17544	C12 H26 N1 O6
	282.11832	C10 H20 N1 O8
	282.13365	C14 H20 N1 O5
	282.17001	C15 H24 N1 O4
	284.09901	C10 H14 N5 O5
	284.14927	C14 H22 N1 O5
	284.18562	C15 H26 N1 O4
	284.29477	C18 H38 N1 O1
	286.12851	C13 H20 N1 O6
	286.16484	C14 H24 N1 O5
	286.2013	C15 H28 N1 O4
	288.14416	C13 H22 N1 O6
	288.18051	C14 H26 N1 O5
	288.25326	C16 H34 N1 O3
	289.15067	C11 H21 N4 O5
CHON-	$^{-}m/z$ measured	Elemental Formula $[M-H]^{-}$
	68.01417	C3 H2 N1 O1
	72.00908	C2 H2 N1 O2
	74.02474	C2 H4 N1 O2
	107.99384	C1 H2 N1 O5
	123.98876	C1 H2 N1 O6
	128.03536	C5 H6 N1 O3
	134.0095	C3 H4 N1 O5
	135.98877	C2 H2 N1 O6
	138.00441	C2 H4 N1 O6
	138.0197	C6 H4 N1 O3
	141.99934	C1 H4 N1 O7
	151.98368	C2 H2 N1 O7
	152.02007	C3 H6 N1 O6
	152.03535	C7 H6 N1 O3
	165.99932	C3 H4 N1 O7
	220.04626	C7 H10 N1 O7
	222.02558	C6 H8 N1 O8
	222.06199	C7 H12 N1 O7
	224.0412	C6 H10 N1 O8
	226.05684	C6 H12 N1 O8
	234.02555	C7 H8 N1 O8
	234.06195	C8 H12 N1 O7
	236.04118	C7 H10 N1 O8
	236.07758	C8 H14 N1 O7
	242.05178	C6 H12 N1 O9
	242.17625	C13 H24 N1 O3
	248.04116	C8 H10 N1 O8
	248.07757	C9 H14 N1 O7

	250.05682	C8 H12 N1 O8	
	250.14494	C14 H20 N1 O3	
	262.05679	C9 H12 N1 O8	
	264.03607	C8 H10 N1 O9	
	264.07237	C9 H14 N1 O8	
	264.16054	C15 H22 N1 O3	
	266.05171	C8 H12 N1 O9	
	266.15128	C13 H20 N3 O3	
	271.04181	C6 H11 N2 O10	
	288.03203	C5 H10 N3 O11	
	306.20742	C18 H28 N1 O3	
	333.01709	C5 H9 N4 O13	
CHONS	$^{+}m/z$ measured	Elemental Formula $[M+H]^{+}$, $[M+Na]^{+}$	
	138.0583	C4 H12 N1 O2 S1	
	139.05355	C3 H11 N2 O2 S1	
	153.03275	C3 H9 N2 O3 S1	
	153.95705	C3 H1 N1 O3 S1	Na1
	158.00186	C4 H4 N3 O2 S1	
	172.97799	C6 H2 N2 O1 S1	Na1
	179.0097	C2 H8 N2 O4 S1	Na1
	181.98821	C5 H5 N1 O3 S1	Na1
	185.98889	C5 H3 N2 O4 S1	
	192.10529	C8 H18 N1 O2 S1	
	214.00181	C4 H8 N1 O7 S1	
	214.08961	C10 H16 N1 O2 S1	
	228.00755	C7 H6 N3 O4 S1	
	257.97035	C8 H4 N1 O7 S1	
CHONS	$^{-}m/z$ measured	Elemental Formula $[M-H]^{-}$	
	217.01897	C9 H5 N4 O1 S1	
	217.96123	C2 H4 N1 O9 S1	
	226.00272	C5 H8 N1 O7 S1	
	231.97693	C3 H6 N1 O9 S1	
	235.98708	C6 H6 N1 O7 S1	
	244.0133	C5 H10 N1 O8 S1	
	245.99251	C4 H8 N1 O9 S1	
	257.99251	C5 H8 N1 O9 S1	
	260.00817	C5 H10 N1 O9 S1	
	261.98736	C4 H8 N1 O10 S1	
	273.98743	C5 H8 N1 O10 S1	
	275.019	C5 H11 N2 O9 S1	
	276.00297	C5 H10 N1 O10 S1	
	278.01865	C5 H12 N1 O10 S1	
	288.00303	C6 H10 N1 O10 S1	
	291.99794	C5 H10 N1 O11 S1	
	302.01864	C7 H12 N1 O10 S1	
	304.99317	C5 H9 N2 O11 S1	

	323.00371	C5 H11 N2 O12 S1
CHN	$^{+}m/z$ measured	Elemental Formula [M+H]+
	74.09642	C4 H12 N1
	83.06037	C4 H7 N2
	84.08077	C5 H10 N1
	94.06512	C6 H8 N1
	102.03385	C7 H4 N1
	170.0964	C12 H12 N1

CURRICULUM VITAE

KATYE E. ALTIERI

EDUCATION

Rutgers, The State University of New Jersey — New Brunswick, NJ
Ph.D., Oceanography, May 2009

The College of New Jersey — Ewing, NJ
B.S., Chemistry, May 2004

TEACHING EXPERIENCE

Teaching Assistant, Oceanographic Methods and Data Analysis, Spring 2007
Guest Lecturer, History of Earth Systems, Fall 2008
Guest Lecturer, Chemical Oceanography, Fall 2008
Assistant Instructor, Ocean Science Inquiry, Spring 2009

PUBLICATIONS

Carlton A.G., Lim, H.J., **Altieri, K.E.**, Seitzinger, S.P., Turpin, B.J. Link between isoprene and SOA: Fate of pyruvic acid during photochemical oxidation in cloud droplets. *Geophysical Research Letters*, 2006, vol.33, L06822

Altieri, K.E., Carlton, A.G., Turpin, B.J., Seitzinger, S.P. Evidence for oligomer formation in clouds: Reactions of isoprene oxidation products. *Environmental Science and Technology*, 2006, vol. 40, 4956-4960

Carlton, A.G., Turpin, B.J., **Altieri, K.E.**, Reff, A., Lim, H.J., Seitzinger, S.P., Atmospheric oxalic acid and SOA production from glyoxal: Results from aqueous photo-oxidation experiments. *Atmospheric Environment*, 2007, vol. 41 (35), 7588-7602

Ervens, B., Carlton, A.G., Turpin, B.J., **Altieri, K.E.**, Kreidenweis, S., Feingold, G. Secondary organic aerosol yields from cloud-processing of isoprene oxidation products. *Geophysical Research Letters*, 2008, vol. 35, L02816

***Altieri, K.E.**, Seitzinger, S.P., Carlton, A.G., Turpin, B.J., Klein, G.C., Marshall, A.G. Oligomers formed through in-cloud methylglyoxal reactions: Chemical composition, properties, and mechanisms investigated by ultra-high resolution FT-ICR Mass Spectrometry. *Atmospheric Environment*, 2008, vol. 42 (7), 1476-1490

R.A. Duce, J. LaRoche, **K. Altieri**, K. Arrigo, A. Baker, D. Capone, S. Cornell, F. Dentener, J. Galloway, R. Ganeshram, R.Geider, T. Jickells, M. Kuypers, R. Langlois, P. S. Liss, S. M. Liu, J.Middelburg, C.M. Moore, S. Nickovic, A. Oschlies, T. Pedersen, J. Prospero, S. Seitzinger, L.L. Sorensen, M. Uematsu, O. Ulloa, M. Voss, B. Ward, L.

Zamora, Impacts of atmospheric anthropogenic nitrogen on the open ocean. *Science*, May 16, 2008, vol. 320, no. 5878, 893-897

Altieri, K.E., Turpin, B.J., Seitzinger, S.P. Oligomers, organosulfates, and nitroxy organosulfates in rainwater identified by ultra-high resolution FT-ICR mass spectrometry. *Atmospheric Chemistry and Physics*, 2009, vol.9, 2533-2542

Carlton, A.G., B.J. Turpin, **K.E. Altieri**, S.P. Seitzinger, R. Mathur, S. Roselle, R.J. Weber CMAQ model performance enhanced when in-cloud SOA is included: Comparisons of OC predictions with measurements. *Environmental Science & Technology,* 2008, vol. 42, 8798-8802